This is to certify that the
dissertation entitled

ENDOTHELIN-1 ACTIONS ON NOREPINEPHRINE TRANSPORTER AND SUPEROXIDE ANION IN SYMPATHETIC NEURONS: ROLES IN DEOXYCORTICOSTERONE ACETATE-SALT HYPERTENSION

presented by

Xiaoling Dai

has been accepted towards fulfillment
of the requirements for the

Ph.D. degree in Neuroscience Program

Major Professor's Signature

August 28, 2004

Date

ENDOTHELIN-1 ACTIONS ON NOREPINEPHRINE TRANSPORTER AND SUPEROXIDE ANION IN SYMPATHETIC NEURONS: ROLES IN DEOXYCORTICOSTERONE ACETATE-SALT HYPERTENSION

By

Xiaoling Dai

A DISSERTATION

Submitted to
Michigan State University
In partial fulfillment of the requirements
for the degree of

DOCTOR OF PHILOSOPHY

Neuroscience Program

2004

ABSTRACT

ENDOTHELIN-1 ACTIONS ON NOREPINEPHRINE TRANSPORTER AND SUPEROXIDE ANION IN SYMPATHETIC NEURONS: ROLES IN DEOXYCORTICOSTERONE ACETATE-SALT HYPERTENSION

By

Xiaoling Dai

Hypertensive humans exhibit an elevated sympathetic nerve activity. This also has been observed in several animal models of hypertension, particularly the salt-sensitive forms. Many factors are potentially responsible for the changes that occur in the sympathetic nervous system in hypertension. Increased production of the humoral factor endothelin-1 (ET-1) may be an important factor in the development of salt-sensitive hypertension, and the sympathetic nervous system may be a target for ET-1 actions. Defective neuronal uptake of norepinephrine by norepinephrine transporter (NET), and oxidative stress, especially elevated $O_2^{\cdot-}$, play critical roles in the pathogenesis of hypertension. Therefore, the aim of my research project was to test the overall hypothesis that ET-1 contributes to the maintenance of salt-sensitive hypertension by reducing reuptake of norepinephrine into sympathetic neurons and increasing $O_2^{\cdot-}$ generation in sympathetic ganglia. To test this hypothesis, I devised a series of specific aims to evaluate ET-1 actions on NET and $O_2^{\cdot-}$ generation in

sympathetic neurons in deoxycorticosterone acetate-salt (DOCA-salt) model of experimental hypertension in the rat. Based on the key findings in studies conducted, I propose that increased endothelin level in DOCA-salt hypertension in the rat produces several significant effects on the sympathetic nervous system, which may affect hypertension development. First, NET mRNA and protein are present in tissue extracts of rat mesenteric arteries, mesenteric veins, celiac ganglia and dorsal root ganglia (DRG) and both NET mRNA and protein levels are elevated in mesenteric blood vessels and sympathetic celiac ganglia, but not in DRG, from DOCA-salt hypertensive rats compared to Sham rats. Second, ET-1 produces both acute and long-term changes in NET mRNA and protein levels in differentiated PC-12 cells, with persistently reduced uptake through 7 days of study. Third, $O_2^{\cdot-}$ levels are elevated in prevertebral sympathetic ganglia in DOCA-salt hypertensive rats, an effect that may be stimulated by ET-1 and mediated by the upregulated ET_B receptor pathway. Fourth, NAD(P)H oxidase is present in sympathetic neurons and NAD(P)H oxidase activation in sympathetic neurons results in elevated $O_2^{\cdot-}$ production. Increased sympathetic $O_2^{\cdot-}$ production in DOCA-salt hypertensive rats may rise from upregulated NAD(P)H oxidase activity. Finally, ET-1 acts on ET_B receptors coupled to a PKC-dependent pathway, and activates NAD(P)H oxidase to generate $O_2^{\cdot-}$ in sympathetic neurons. Based on these findings, I conclude that ET-1 contributes to the maintenance of DOCA-salt hypertension in the rat, in part, by impairing norepinephrine uptake and increasing $O_2^{\cdot-}$ generation in neurons in sympathetic ganglia.

DEDICATION

To my parents Wei Dai and Li Shu, my husband Jianjun Bai and my daughter Daisy Bai,

who have always been there for me.

ACKNOWLEDGEMENTS

I would like to thank my mentor Dr. David L. Kreulen. Thank you for your precious time and seemingly endless supply of patience, guidance and assistance. You have been helping me grow as a scientist as well as a person. Thanks a lot!!!

Furthermore, I would like to thank the members of my dissertation committee, Drs. Williams Atchison, Gregory Fink, James Galligan and Karl Olson. Thank you for your interest in my project, valuable time and many suggestions.

I would like to thank to the director of Neuroscience program, Dr. Cheryl Sisk. Thank you for recruiting me to the program, and continuously supporting my research and study along these years.

I wish to thank to the crew of Kreulen's laboratory for their help and support: Jake Manteuffel, Jill Larson, Jolene Zheng, Erica Wehrwein, Xiaohong Wang, and Xian Cao.

I would like to express my gratitude and thanks to my friends in neighborhood laboratories for their help, support and friendship, Diana Ye, Katrina Linning, Tracy Walker, Wen-hsin Ku, Carrie Northcott, Hong Wang, Alex Perez-Rivera, Andy Shin, Jinghua Xu, Weiqin Chen, Yun Wang, Xiaochun Bian, and Wei Ni. I really cherish the great times we have.

I would also like to express my never-ending gratitude to my parents, Wei Dai and Li Shu. Thank you for teaching me and encouraging me never giving up.

Finally, I would like to thank to my husband, Jianjun Bai, for your endless

love, and support along the past fifteen years, especially last five years in the states, and my dear daughter, Daisy Bai, for your accompanying with me along my dissertation writing and always warming my heart.

TABLE OF CONTENTS

LIST OF TABLES

LIST OF FIGURES

LIST OF ABBREVIATIONS

Ang II	angiotensin II
ASP^+	(4-(4-(dimethylamino)styryl)-*N*-methylpyridinium iodide (4-Di-1-ASP))
ATCC	american type culture collection
BP	blood pressure
BQ610	ET_A receptor antagonist
BQ788	ET_B receptor antagonist
Ca^{2+}	calcium
cDNA	complementary dna
CG	celiac ganglia
CNS	central nervous system
CO	cardiac output
DAG	diacylglycerol
dATP	deoxyadenosine 5'-triphosphate
dCTP	deoxycytidine 5'-triphosphate
DEPC	diethylpyrocarbonate
dGTP	deoxyguanosine 5'-triphosphate
DHE	dihydroethidine
$DMPH_4$	6,7-dimethyl-5,6,7,8-tetrahydropteridine
DMSO	dimethylsulfoxide

DNA	deoxyribonucleic acid
DOCA	deoxycorticosterone acetate
DRG	dorsal root ganglia
DTT	dithiothreitol
dTTP	deoxythymidine 5'-triphosphate
EDTA	ethylenediaminetetraacetic acid
ET-1	endothelin-1
ET_A receptor	endothelin receptor subtype a
ET_B receptor	endothelin receptor subtype a
GAPDH	glyceraldehyde phosphate dehydrogenase
GTSF	genomic technology support facility
HCl	hydrochloric acid
HEPES	4-(2-hydroxyethyl) piperazine-1 ethanesulfonic acid
HR	heart rate
IMG	inferior mesenteric ganglia
IP_3	inositol trisphosphate
KCl	potassium chloride
MA	mesenteric artery
MAP	mean blood pressure
MEM	minimal essential medium
Mg^{2+}	magnesium

MV	mesenteric vein
NaCl	sodium chloride
NADH	β-Nicotinamide-adenine dinucleotide, reduced
NADPH	β-Nicotinamide-adenine dinucleotide phosphate, reduced
NCBI	national center for biotechnology information
NE	norepinephrine
NET	norepinephrine transporter
NGF	nerve growth factor
NO	nitric oxide
NOLA	N-nitro- L-arginine
NOX	non-phagocytic oxidase
$O_2^{\bullet-}$	superoxide anion
PAGE	polyacrylamide gel electrophoresis
PBS	phosphate-buffered saline
PC-12 cells	rat pheochromocytoma cell line cells
PCR	polymerase chain reaction
PI	phosphoinositol
PIP_2	phosphatidilinositol-4,5 biphosphate
PKA	protein kinase A
PKC	protein kinase C

PLC	phospholipase C
PMA	phorbol 12-myristate 13-acetate
PMSF	phenol methane sulfanyl fluoride
PVDF	polyvinylidene Fluoride
Rac	small ras related g protein
Ras	rat sarcoma viral oncogene homolog
RNA	ribonucleic acid
ROS	reactive oxygen species
RPMI-1640	developed at roswell park memorial institute
RT-PCR	reverse transcription polymerase chain reaction
S6c	sarafotoxin 6c
SDS	sodium dodecyl sulfate
SHR	spontaneously hypertensive rat
SHR	spontaneously hypertensive rat
SV	stroke volume
TAE buffer	tris-glacial acetic acid-EDTA buffer
TEMED	tetramethylethylenediamine
TPR	total peripheral resistance

LIST OF SOURCES OF CHEMICALS AND SUPPLIES

Chemical name	Vendor	Location
allopurinol	Sigma-Aldrich Co.	St. Louis, MO
apocynin	Sigma-Aldrich Co.	St. Louis, MO
aprotinin	Sigma-Aldrich Co.	St. Louis, MO
ascorbic acid	Sigma-Aldrich Co.	St. Louis, MO
ASP^+	Molecular Probes	Eugene, OR
BQ610	Peninsula Laboratories Inc. Member of the Bachem group.	San Carlos, CA
BQ788	Peninsula Laboratories Inc. Member of the Bachem group.	San Carlos, CA
chloroform	J.T.Baker	Phillipsburg NJ
collagenase	Worthington Biochemical Corporation	Lakewood, NJ
coomassie blue	Invitrogen Corporation	Carlsbad, CA
Costar® 24-well tissue culture plate	Corning	Corning, NY
cytosine arabinoside	Sigma-Aldrich Co.	St. Louis, MO
dATP	Roche Applied Sciences	Indianapolis, IN
dCTP	Roche Applied Sciences	Indianapolis, IN
DEPC	Sigma-Aldrich Co.	St. Louis, MO

dGTP	Roche Applied Sciences	Indianapolis, IN
DHE	Molecular Probes	Eugene, OR
$DMPH_4$	Sigma-Aldrich Co.	St. Louis, MO
DMSO	Sigma-Aldrich Co.	St. Louis, MO
DNA ladder	New England Biolabs Inc.	Beverly, MA
DOCA	Sigma-Aldrich Co.	St. Louis, MO
dispase	Roche Applied Sciences	Indianapolis, IN
DTT	Sigma-Aldrich Co.	St. Louis, MO
DTTP	Roche Applied Sciences	Indianapolis, IN
EDTA	Sigma-Aldrich Co.	St. Louis, MO
ET-1	Peninsula Laboratories Inc. Member of the Bachem group.	San Carlos, CA
ET-1 QuantiGlo Chemiluminescent Assay Kit	R&D systems	Minneapolis, MN
ET_B receptor antibody	Alomone labs	
ethidium bromide	Sigma-Aldrich Co.	St. Louis, MO
fat-free dry milk	Meijer	Grand Rapids, MI
fetal bovine serum	Invitrogen Corporation	Carlsbad, CA
fluorodeoxyuridine	Sigma-Aldrich Co.	St. Louis, MO
Fungizone®	Invitrogen Corporation	Carlsbad, CA
GAPDH primers	Applied Biosystems	Foster City, CA
glacial acetic acid	Sigma-Aldrich Co.	St. Louis, MO

glucose	J.T.Baker	Phillipsburg NJ
glutathione	Sigma-Aldrich Co.	St. Louis, MO
goat anti-mouse IgG HRP conjugated secondary antibody	Santa Cruz Biotech	Santa Cruz, CA
goat anti-rabbit IgG HRP conjugated secondary antibody	Santa Cruz Biotech	Santa Cruz, CA
HCl	J.T.Baker	Phillipsburg NJ
heat inactivated horse serum	Invitrogen Corporation	Carlsbad, CA
HEPES	Sigma-Aldrich Co.	St. Louis, MO
ImagePro® Plus	Media Cybernetics, Inc.	Silver Spring, MD
isopropanol	J.T.Baker	Phillipsburg NJ
KCl	J.T.Baker	Phillipsburg NJ
Kodak Biomax Light scientific imaging film	Kodak	Rochester, NY
leupeptin	Sigma-Aldrich Co.	St. Louis, MO
L-glutamine	Invitrogen Corporation	Carlsbad, CA
MEMBRANE	Invitrogen Corporation	Carlsbad, CA
NaCl	J.T.Baker	Phillipsburg NJ
$NaHCO_3$	J.T.Baker	Phillipsburg NJ
NGF 2.5S	Chemicon International, Inc.	Temecula, CA

NOLA	Sigma-Aldrich Co.	St. Louis, MO
Oligo(dT)$_{12-18}$ primers	Invitrogen Corporation	Carlsbad, CA
papain	Worthington Biochemical Corporation	Lakewood, NJ
PC-12 cells	ATCC	Manassas, VA
penicillin-streptomycin	Invitrogen Corporation	Carlsbad, CA
PMA	Sigma-Aldrich Co.	St. Louis, MO
PMSF	Sigma-Aldrich Co.	St. Louis, MO
polyacrilamide	Bio-Rad Laboratories	Hercules, CA
polyinosinic acid	Sigma-Aldrich Co.	St. Louis, MO
poly-L-lysine	Sigma-Aldrich Co.	St. Louis, MO
poly-L-lysine	Sigma-Aldrich Co.	St. Louis, MO
protein assay Kit	Bio-Rad Laboratories	Hercules, CA
PVDF	Bio-Rad Laboratories	Hercules, CA
QIAquick Gel Extraction Kit	Qiagen	Valencia, CA
QIAquick PCR Purification Kit	Qiagen	Valencia, CA
rabbit anti-rat NET	Chemicon International, Inc.	Temecula, CA
rat serum	Harlan Bioproducts for Science, Inc.	Indianapolis, Indiana
RNase inhibitor	Roche Applied Sciences	Indianapolis, IN
RO-31-8425	LC Laboratories	Woburn, MA

RPMI-1640	Invitrogen Corporation	Carlsbad, CA
S6c	Peninsula Laboratories Inc.	San Carlos, CA
	Member of the Bachem group.	
salmon testes DNA	Stratagene	La Jolla, CA
SDS	Sigma Chemical Co.	
sodium pentobarbital	Abbott Laboratories	North Chicago, IL
Superscript II® RNase H^- reverse transcriptase	Invitrogen Corporation	Carlsbad, CA
SuperSignal® West Pico chemiluminescence kit	Pierce	Rockford, IL
SYBR® Green Master Mix	Applied Biosystems	Foster City, CA
Taq DNA polymerase	Invitrogen Corporation	Carlsbad, CA
TEMED	Invitrogen Corporation	Carlsbad, CA
TRIzol®	Invitrogen Corporation	Carlsbad, CA
uridine	Sigma-Aldrich Co.	St. Louis, MO
β-NADH	Sigma-Aldrich Co.	St. Louis, MO
β-NADPH	Sigma-Aldrich Co.	St. Louis, MO

CHAPTER 1: INTRODUCTION

1 Hypertension

Cardiovascular diseases claim forty percent of all deaths in the United States. Twenty percent of Americans have one or more types of cardiovascular diseases, with hypertension being the dominant form of these diseases (American Heart Association, 2004). According to recent estimates, one in four U.S. adults are hypertensive. However, nearly one-third of these people don't even know they have it, because there are no symptoms. This is why hypertension is often called the "silent killer". Uncontrolled high blood pressure is a risk factor for stroke, heart attack, congestive heart failure and kidney failure. With 50 million adults in the United States afflicted with hypertension and with only 27% of those with their blood pressure properly controlled, alerting the public about the dangers of untreated hypertension is critical (American Heart Association, 2004). Thus, it is important to understand the mechanisms underlying hypertension in order to develop an effective approach to alleviate or treat the people who suffer from cardiovascular diseases, especially hypertension.

High blood pressure (HBP) is defined as a systolic pressure of 140 mm Hg or higher, and/or a diastolic pressure of 90 mm Hg or higher. "Prehypertension" is a systolic pressure of 120-139 mm Hg, or a diastolic pressure of 80-89 mm Hg, or both, which needs to be watched carefully (American Heart Association, 2004).

1.1 Types of hypertension: essential hypertension and

secondary hypertension

There are two types of hypertension: essential or primary hypertension and secondary hypertension (American Heart Association, 2004).

Approximately 90 percent of hypertensives are said to have essential hypertension. In essential hypertension, patients do not experience any specific symptoms and/or identifiable causes. Although the etiology of essential hypertension is currently unknown, it is thought that essential hypertension is the result of multiple abnormalities, such as stress, emotional disturbance, heredity, race, geographical location and climatic condition of place of stay or obesity, and appears to involve a genetic component as well. Support for this comes from evidence showing that essential hypertension tends to cluster in families and is represented by a collection of genetically based diseases or syndromes with several resultant inherited biochemical abnormalities. Blood pressure is determined by several genetically-controlled factors interacting with various environmental factors, thereby altering the severity of blood pressure elevation and the timing of hypertension onset (Oparil et al., 2003). Many pathophysiological factors have been implicated in the genesis of hypertension: increased sympathetic nervous system activity, long-term high salt intake, overproduction of sodium-retaining hormones and vasoconstrictors; increased or inappropriate renin secretion with resultant increased production of Angiotensin II (Ang II) and aldosterone; deficiencies of vasodilators, such as nitric oxide (NO) and the natriuretic peptides; abnormalities of blood vessels; alterations in adrenergic receptors that influence heart rate and vascular tone (Oparil et al.,

2003). Since blood pressure regulation is under several levels of control in the body; defects in any of them, including abnormalities of the central and peripheral nervous systems, baroreceptors, adrenal glands, kidneys, blood vessels and hearts, either individually or collectively, could account for the development of essential hypertension.

On the other hand, secondary hypertension has recognized causes and occurs secondarily to some physical causes, such as endocrine disorders (excess hormone secretion from the adrenal gland or malfunctioning of endocrine glands), renal diseases (infection or damage to kidney), mechanical vascular abnormalities (narrowing or loss of elasticity of arteries/veins, arteriosclerosis, or blocks in blood vessels) or pregnancy.

Treatments for these two types of hypertension are different. The secondary hypertension can be healed or alleviated by targeting the principal causes. The difficulty with treatments of essential hypertension lies in the facts of unknown causes of this disease. For now, the therapeutic approach to essential hypertension and its cardiovascular complications remains generic in order to control the elevation of blood pressure.

1.2 Salt-sensitive hypertension

Human essential hypertension appears to be a salt-related disease. Low salt intake populations have no hypertension at all (Carvalho et al., 1989). Yet, if such people migrate to a high salt society, about 30% will show a significant rise in blood pressure (Tobian, 1991). Blood pressure in around 60 percent of essential hypertensive patients is sensitive to salt intake (Gonzalez-Albarran et

al., 1998;Luft and Weinberger, 1982;Preuss, 1997;Somova et al., 1999;Williams and Hollenberg, 1989). Dietary salt is one of the key risk factors for essential hypertension (Borgman, 1985). Similarly, there are certain strains of animals that develop a significant rise in blood pressure when placed on a high salt diet (Tobian, 1991).

The concept of salt sensitivity originated in population surveys conducted in various parts of the world, demonstrating that the prevalence of hypertension rises with habitual dietary sodium intake or urinary sodium excretion (Dahl, 1972). The incidence of hypertension in individuals challenged with high salt intake also depends upon if the individuals are salt-sensitive. The most widely applied definition comes from a National Institutes of Health protocol. It is defined as a 10% or greater rise in mean arterial blood pressure (MAP) from the seventh day of 10 mM sodium intake to the seventh day of a 240 mM sodium intake (Dustan, 1991).

No identified mechanisms has been put forth to explain the changes in blood pressure due to salt-sensitivity. This suggests that there are complex, multifactorial and probably interrelated mechanisms. The compelling evidence supports that salt-sensitivity is genetically transmitted in laboratory animals (Dahl et al., 1962;Rapp, 1982). Various abnormalities of the autonomic nervous system and renal system have also been described to come into play in development of salt-sensitivity (Rapp, 1982;Sullivan, 1991). The difficulties in studying salt-sensitivity mechanisms in humans are due to the fact of lack of uniformity of techniques, criteria, and magnitude of blood pressure change required to identify

an individual as salt-sensitive, although the reported prevalence of salt-sensitivity is similar, especially among hypertensive patients (Dustan, 1991;Sullivan, 1991). Salt-sensitive animals might be good models to study the mechanisms underlying salt-sensitivity and some of the mechanisms that have been observed in salt-sensitive animals have also been observed in humans who appear to be salt-sensitive.

1.3 Hemodynamics of blood pressure

Blood pressure is generally thought of as being determined by cardiac output (CO) and total peripheral resistance (TPR). Mean arterial blood pressure (MAP) can be calculated by the following formula: MAP=TPR x CO. TPR is determined by the arterial tone, whereas CO is determined by stroke volume (SV) and heart rate (HR): CO=SV x HR. While the heart provides the pumping pressure and rate, venous return determines end-diastolic filling pressure and stroke volume (Guyton, 1991a). Venous return is determined by mean circulatory filling pressure (MCFP), which represents the pressure that drives venous return and is determined by the vascular capacitance, an index of venous vascular tone and blood volume (Guyton, 1991a).

Hypertensive animals and humans exhibit abnormal hemodynamics by presenting altered CO and/or TPR. Hemodynamic studies performed in young mild and borderline human essential hypertensive patients have shown an elevated CO in the presence of a normal TPR in the initial stages of hypertension development (Lund-Johansen, 1994). This is in agreement with findings animal studies (Ledingham and Pelling, 1970). However, both human and animal

studies show a reduced CO and an elevated TPR in the established phase of hypertension (Lund-Johansen, 1994).

1.4 Sympathetic innervation in hypertension

The sympathetic nervous system is an important regulator of the cardiovascular system (Sved, 2000). Sympathetic nerves have vasoconstrictor effects both on arteries and arterioles to increase the peripheral resistance and on veins to increase the venous return to the heart that will increase cardiac output. By affecting the two determinants of blood pressure, peripheral resistance and cardiac output, increased sympathetic activity elevates blood pressure (Guyton, 1991b).

Considerable evidence favors an important role for the sympathetic nervous system in the development of hypertension in various experimental models, as well as the established phase in a significant proportion of hypertensive population (de Champlain et al., 1977).

1.4.1 Increased sympathetic activity in hypertension

A significant amount of data points to increased sympathetic activity in hypertensive humans and animals. In the past 30 years, several techniques designed to quantify sympathetic cardiovascular influences in humans have shown sympathetic activity to be increased in essential hypertension (Mancia et al., 1999). Julius and coworkers showed that the elevated resting heart rate values of borderline-hypertensive subjects were reduced by intravenous administration of a ß-blocking drug (propranolol) to a more marked degree than the lower heart rate of normotensive controls, suggesting that in the early

hypertensive stage, cardiac sympathetic drive is enhanced (Julius et al., 1971). Further information has come from the greater plasma levels of the adrenergic neurotransmitter norepinephrine (NE) in essential-hypertensive patients compared to normotensive individuals (Goldstein, 1983). Microneurographic recording of efferent postganglionic sympathetic nerve activity provides further evidence of sympathetic overactivity in human hypertension (Vallbo and Hagbarth, 1968). An increase in norepinephrine synthesis in various peripheral organs and circulating catecholamine levels is found in experimentally manipulated hypertensive animal models (de Champlain et al., 1977). In view of the demonstration of an elevated sympathetic drive coupled with an enhancement of vasomotor sympathetic modulation, sympathetic neurohumoral disturbances play a special role in essential hypertension (Pagani and Lucini, 2001). However, the exact pathophysiology of sympathetic dysfunction in hypertension remains to be elucidated.

1.4.2 Salt and sympathetic nervous system interaction

Salt sensitive hypertension, which comprises around 60 percent of people with essential hypertension (Luft et al., 1982;Somova et al., 1999), is considered to depend on the existence of abnormalities in regulation of the sympathetic nervous system (Gonzalez-Albarran et al., 1998).

Numerous studies have shown that high sodium diets can alter sympathetic nervous system activity in animals and humans (Ely, 1997). The physiological discharge rates of mesenteric resistance blood vessels from high sodium diet rats are about twice of those from low sodium diet, whereas the

median effective dose and the dose response curves for exogenous norepinephrine are the same, suggesting that norepinephrine release from sympathetic postganglionic nerve terminals is modulated by dietary sodium (Nilsson et al., 1984;Nilsson et al., 1985). In addition, the quantal transmitter release per sympathetic nerve impulse may be directly related to sodium intake in chronic studies. Neurotransmitter release is increased when dietary sodium intake is high, whereas it is decreased when sodium intact is low (Ely, 1997;Gradin et al., 1986;Luft et al., 1982;Sjoblom-Widfeldt et al., 1989).

1.5 Animal models of experimental hypertension

The etiology and pathogenesis of hypertension are heterogeneous, in which hypertensives vary according to salt-sensitivity, sympathetic nervous system function, renal function etc. A number of experimental hypertensive animal models have been developed to target subsets or subpopulations of hypertensives with diverse dysfunctional systems during the development of hypertension. Several interventions are used to induce hypertension in experimental animals. The most used interventions are renal ischemia, mineralcorticoid excess, genetic manipulation and neural denervation or deafferentation.

1.5.1 Experimental renal hypertension

Hypertension of renal etiology is the most common form of human secondary hypertension (Lilly, 1993). Therefore, renal models of experimental hypertension may best represent animal counterparts to secondary forms of hypertension in humans. In 1934, Goldblatt and colleagues showed that partial

constriction of the renal artery and removal of the opposite kidney produced persistent hypertension (one kidney, one clip hypertension [1K1C]) in dogs. In contrast, the constriction of one renal artery in rats results in hypertension regardless of the presence or absence of the contralateral kidney (2K1C or 1K1C) (Bohr and Dominiczak, 1991). In the 2K1C model of hypertension, an elevation of blood pressure depends on an increased TPR with a reduction in CO while the 1K1C model involves an increase in TPR with a small increase in CO (Thurston, 1994). Both models show decreased total venous capacity and elevations in mean circulatory filling pressure (MCFP) (Yamamoto et al., 1981).

1.5.2 Genetic hypertension

Genetic hypertensive animal models are produced by selectively inbreeding normotensive strains of animals. In 1958, Smirk and Hall developed the first colony of hypertensive rats by breeding rats with above-average tail blood pressure, now known as New Zealand strain. In 1962, Dahl introduced a rat model that invariably developed hypertension when given a high sodium diet. This model was produced by selective inbreeding of animals showing a hypertensive response to sodium (Dahl et al., 1962). By 1969, Okamoto and Aoki successfully developed an inbred strain of spontaneously hypertensive rats (SHR), which develops hypertension spontaneously as early as several months after birth and iss homozygous in more than 99% of all genetic loci (Bohr and Dominiczak, 1991). Blood pressure is a variable determined by both genetic and nongenetic factors. The absence of genetic variation among the individuals of an inbred strain makes this strain a powerful tool for a study of the determinants of

blood pressure. The effects of specific nongenetic interventions on the variables of blood pressure are much more readily defined in the inbred strain than in a nonhomogeneous colony of rats, because of the lack of genetic variation in an inbred strain (Bohr and Dominiczak, 1991).

1.5.3 Neural models of hypertension

The central nervous system (CNS) and peripheral nervous system play critical roles in the maintenance of blood pressure and hence are implicated in the pathophysiology of hypertension. The CNS responds to peripheral pathological conditions associated with hypertension via humoral and afferent inputs. Several specifically neural animal models of experimental hypertension have been developed although the nervous systems are also involved in the development of hypertension of other experimental hypertensive animal models. Some of the animal models are achieved by the surgical and pharmacological manipulations of critical CNS centers for blood pressure regulation, such as the nucleus tractus solitairus (NTS), rostral ventral lateral medulla (RVLS) and paraventricular nucleus (PVN) (Reis et al., 1981). Models focusing on the role of the peripheral nervous system can be induced by baroreceptor denervation (Osborn, 1997;Sved et al., 1997).

1.5.4 Mineralcorticoid excess hypertension

Excess production of mineralcorticoids, also known as primary aldosteronism, is a well-known form of secondary hypertension in humans. In 1939, Kuhlman observed that daily subcutaneous injections of deoxycorticosterone acetate (DOCA) produced an increase in blood pressure in

unilaterally nephrectomized dogs (Kuhlman et al., 1939). The major impetus for the study of DOCA-induced hypertension came in 1943, when Selye et al introduced this model of hypertension in the rat (Selye et al., 1943). Typically, this experimental model is produced by surgical uniphrectomy followed by administration (implants or injections) of excess minerocorticoids (deoxycorticosterone acetate salt) and salt (in diet or drinking water). By binding to the renal type 1 adrenocorticosteroid receptor in the collecting tubule of the nephron, mineralcorticoids enhance permeation of renal tubules to sodium ions via an amiloride-sensitive Na^+-H^+ exchanger and activation of a serosal sodium pump (Garty, 1986). This model is therefore a renin-independent (low-renin) and salt-sensitive form of experimental hypertension. The animals will develop hypertension even after one week of uniphrectomy, DOCA implants and salt intake treatment, and will become malignant due to weight loss and end-organ damage.

The mechanism by which this treatment increases blood pressure is not fully understood and there is no clear indication which factors are most important in the pathogenesis of mineralcorticoid-induced hypertension. Initiation of hypertension may involve sodium retention and a subsequent volume expansion; however, it is not likely that sodium retention causes hypertension by means of plasma expansion and increased extracellular fluid volume alone. Rather, it appears that increased sodium levels can alter neurohormonal pressor baroreflexes (Ferrario et al., 1987), which then contribute to the initiation and/or maintenance of hypertension. Salt-depletion may inhibit the pressor responses

mediated by carotid occlusion in dogs, which can be enhanced by the salt-loading (Schenk and McNeill, 1992;Szilagyi et al., 1981). This indicates that hypertensive states involving a sodium imbalance may be related to alterations in the central and peripheral control of autonomic nervous system function.

1.5.4.1 Cardiovascular dynamics of DOCA-salt hypertension

DOCA-salt hypertension is associated with an increased cardiac output. Cardiac output and stroke volume are significantly elevated without concomitant increases in heart rate and total peripheral resistance in DOCA-salt hypertensive dogs, likely due to an augmented venous return and an expanded blood volume (Ueno et al., 1988a). Other studies of DOCA-salt hypertensive dogs attribute the elevation in arterial pressure to an increase in TPR and CO (Schenk and McNeill, 1992). Moreover, the vascular structure is altered during the development of hypertension to contribute further to the overall pathophysiology of DOCA-salt hypertension; this change is due to the increased pressure and not the result of a direct of DOCA treatment. However, it does not appear that this change in cardiac output is required for the initiation or maintenance of DOCA-salt hypertension (Schenk and McNeill, 1992), as evidence shows that the use of a β-blocking agent manages the cardiac output to control levels yet doesn't inhibit the development of DOCA-salt hypertension (Schenk and McNeill, 1992).

1.5.4.2 Hormonal mechanisms

Hormonal mechanisms, including Ang II, vasopressin, catecholamines and endothlins, are implicated in the development of DOCA-salt hypertension and are

involved in the regulatory control of autonomic function via central or peripheral actions. Ang II, a critical component of brain pressor regulatory pathways, is linked to DOCA-salt hypertension (Itaya et al., 1986). Vasopressin contributes to the initiation and maintenance of DOCA-salt hypertension in rats (Crofton et al., 1979). Central catecholamine depletion prevents or reverses DOCA-salt hypertension in rats (Lamprecht et al., 1977). Intravenous bolus injection of the endothelin receptor blocker FR139317 produced a more pronounced hypotensive effect in DOCA-salt hypertensive rats than in control rats (Fujita et al., 1995).

1.5.4.3 Neurogenic mechanisms

Altered neural mechanisms in the development of DOCA-salt hypertension include increased peripheral sympathetic discharge, distorted baroreflex response to various stimuli (Schenk and McNeill, 1992), altered local adrenergic modulatory mechanisms, and modified cardiovascular effector cell responses to sympathetic activation. Basal plasma norepinephrine levels are significantly higher in DOCA-salt hypertensive rats than in normotensive rats (Drolet et al., 1989), pointing to a generalized increase in sympathetic tone in DOCA-salt treated animals. Sympathetic nerve fiber activity is also elevated in DOCA-salt treated rats as reflected in an enhanced splanchnic sympathetic nerve output in response to electrical stimulation of the hypothalamus (Takeda et al., 1988a). The baroreflex responses to aortic depressor nerve stimulation are attenuated in DOCA-salt treated animals (Takeda et al., 1988b). An attenuated α_2-presynaptic inhibition in isolated mesenteric vascular sympathetic fibers

implies the existence of an impaired sympathetic local modulation in DOCA-salt hypertension (Luo et al., 2003). The enhanced α_1 adrenergic receptor mediated activation of the phosphoinositol (PI) pathway is present in the atria, ventricles and mesenteric artery of DOCA-salt hypertensive animals, suggesting cardiovascular adrenergic receptor hyperactivity occurred in close association with the development of hypertension in this model (Eid and de Champlain, 1988b;Eid and de Champlain, 1988a).

In conclusion, this model of induced DOCA-salt hypertension is important because it allows an examination of the salt, neural, and hormonal contribution to hypertension secondary to adrenal steroid excess, which is relevant to the understanding of certain states of essential hypertension (Schenk and McNeill, 1992).

2 Endothelin

2.1 Endothelins family

The endothelins (ETs) are a family of 21-amino-acid peptides. Initially, Yanagisawa et al isolated and described a new peptide, endothelin (ET)-1, derived from the supernatant of cultured porcine aortic endothelial cells (Yanagisawa et al., 1988c). ET-1 was soon joined by two additional isoforms, ET-2 and ET-3, as well as four highly homologous cardiotoxic peptides, sarafotoxins (S6a, S6b, S6c and S6d), which can be isolated from snake venom (Lee and Chiappinelli, 1989). Endothelin family members share a relatively high peptide sequence homology. Each has a common structure of a hydrophobic C terminal end and two disulfide bonds that form a hairpin structure and confer ETs receptor

binding and biological activity (Yanagisawa et al., 1988a).

2.2 Secretion, biosynthesis and regulation of ET-1

ETs are produced in many tissues and cell types. ET-1 is produced primarily by endothelial cells, but is also found in a variety of other cell types in heart (epicardium), lung (bronchial epithelial cells), kidney (tubular cells), and central and peripheral nervous systems (astrocytes and neurons) (Goddard and Webb, 2000).

ETs are formed through enzymatic processing of a precursor molecule. ET-1 is generated from a two-step procedure beginning with proteolytic cleavage of a 212 amino acid precursor polypeptide, prepro-ET-1 to a relatively inactive 38 amino acid precursor, big ET-1. Big ET-1 is then catalyzed by ET-converting enzyme (ECE) to its mature 21 amino acid active form (Goddard and Webb, 2000). A group of ECEs for ET-1 have been identified, each with a different tissue distribution (Goddard and Webb, 2000).

Production of ET-1 is regulated at the level of gene transcription. The stimulant factors include hormones (insulin, catecholamine, angiotensin II, vasopressin), cytokines (platelet-derived growth factor and transforming growth factor-β), hypoxia, blood flow sheer stress, as well as ET-1 itself (Benatti et al., 1994). Some of these factors may stimulate ET-1 gene transcription through an activation of protein kinase C (PKC) pathway (Yanagisawa et al., 1989).

2.3 Endothelin receptor subtypes and their localization

Two receptors for ETs have been identified, endothelin receptor subtype A (ET_A receptor) and endothelin receptor subtype B (ET_B receptor). Both of them

are rhodopsin-like G-protein-coupled receptors incorporating seven membrane-spanning domains and a relatively long extracellular N terminal (Arai et al., 1990;Sakamoto et al., 1991). These receptors differ in their affinities for the various ET peptides. The ET_A receptor has high affinity and specificity for both ET-1 and ET-2, whereas two orders of magnitude less affinity for ET-3. The ET_B receptor is relatively non-selective and exhibits equal high binding affinities to all ETs peptides (Mateo and de Artinano, 1997).

The two receptors were believed to exist only in vasculature tissues at first. Now they are found on adrenal medulla chromaffin cells (Wilkes and Boarder, 1991a), and in the sympathetic (Damon, 1999), central (Sullivan and Morton, 1996) and enteric (Nataf et al., 1996) nervous systems (Mateo and de Artinano, 1997). Messenger RNA and protein for the ET_A receptor is found predominantly in aorta, heart and kidney smooth muscle cells of but not endothelial cells. Messenger RNA and protein of the ET_B receptor is mostly expressed in endothelial cells, and they are also shown to be present in vascular smooth muscle cells (Mateo and de Artinano, 1997). Specific binding sites for synthetic endothelin (ET) isoforms, ET-1 and ET-3, are found in the bovine adrenomedullary chromaffin cell preparation (Wilkes and Boarder, 1991a). Radioligand binding assay indicates that sympathetic postganglionic neurons bind ET-1, and the intracellular Ca^{++} increase activated by ET-1 further confirms the presence of functional ET receptors in those neurons (Damon, 1999). Northern blotting analysis reveals that mRNA of ET_A and ET_B receptors is present on cerebellar neurons (Lysko et al., 1995), whereas binding assay

experiments revealed that the ET_B receptor is located on enteric cholinergic neurons (Yoshimura et al., 1996).

2.4 ET receptors signal transduction

Binding of endothelins to ET_A or ET_B receptors produces G-protein dependent activation of phospholipase C (PLC) (Kodama et al., 1989). In vascular cells, this leads to hydrolysis of phosphatidylinositol-4,5 biphosphate (PIP_2) and generation of cytosolic inositol trisphosphate (IP_3) and membrane-bound diacylglycerol (DAG) (Griendling et al., 1989). IP_3 causes a rapid increase in intracellular concentration of calcium ($[Ca^{2+}]_i$), to trigger smooth muscle cell contraction. In addition, DAG activates protein kinase C (PKC), producing a maintained contraction in vascular smooth muscles (Kodama et al., 1989). However, the intracellular events after ET receptor activation in neurons are not clear. So far only one research article has reported on the intracellular events occurring after ET receptor activation in a neuronal cell line (the mouse neuroblastoma and rat glioma hybrid NG108-15 cells). This report shows that endothelin receptors are present on NG108-15 cells, the G protein coupled to endothelin receptors induces activation of phospholipase C and increases the free intracellular Ca^{2+}, and the PKC is involved in the regulation of endothelin-induced responses (Yue et al., 1991).

2.5 Actions of endothelins

ETs exert a wide range of biological effects on both cardiovascular and noncardiovascular tissues.

2.5.1 Actions on the vascular system

ET-1 plays a critical role in blood pressure maintenance. ET-1 produces a potent and sustained contraction of vascular smooth muscle cells. Bolus injection of ET-1 produces dose-dependent increases in blood pressure (Mortensen and Fink, 1990;Mortensen et al., 1990) and endothelin-induced increase in mean arterial pressure in conscious rats is salt-sensitive (Mortensen and Fink, 1992). Applications of ET receptor antagonists to hypertensive patients (Krum et al., 1998) and various hypertensive animal models (Matsumura et al., 1995) dramatically lowers arterial blood pressure to normotensive levels, suggesting a role of ETs in hypertension pathogenesis.

Reports regarding plasma concentrations of circulating ET-1 are not consistent, either in experimental animal models or in clinical hypertensives. There exists much controversy with regard to the significance of circulating concentrations of ET-1 and its correlation with hypertension development and maintenance (Goddard and Webb, 2000). A significant correlation between the level of hypertension and aortic tissue ET-1 immunoreactivity is noted in DOCA-salt hypertensive rats (Fujita et al., 1995;Matsumura et al., 1995), even though changes in plasma levels of ET-1 are insignificant (Suzuki et al., 1990). The locally increased ET-1 generation occurring in the blood vessels of hypertensive subjects, not being clearly reflected in the plasma concentration, may have crucial effects on vascular function.

2.5.2 Actions on the central nervous system

ET-1 is generated within the CNS neurons or non-neuronal cells because it does not appear to cross through the blood-brain-barrier from the peripheral

circulation into the CNS. ET-1 messenger RNA and immunoreactivity are detected widely in neurons and endothelial cells of cerebellum, cerebral cortex, striatum, pituitary, supraoptic and paraventricular hypothalamic nuclei (SON and PVN), hippocampus, and spinal cord (Giaid et al., 1991;Mortensen, 1999). This extensive distribution suggests extensive roles for ET-1 in CNS regulation of multiple physiological functions.

ET-1 may act as a neuropeptide and regulate CNS functions, including cardiovascular functions. This is supported by evidence showing that ET-1 binding sites are widely dispersed throughout the CNS; especially dense concentrations of receptors are found within the brainstem and cerebellum (Koseki et al., 1989). Additional evidence shows that intracisternal ET-1 administration elicits a transient increase in renal sympathetic nerve activity, phrenic nerve activity, arterial blood pressure and heart rate (Kuwaki et al., 1995). Ganglionic blockade pretreatment is able to prevent these ET-1 induced blood pressure increases, further suggesting a sympathetically mediated effect (Kuwaki et al., 1995).

2.5.3 Actions on the peripheral sympathetic nervous systems

ET-1 is synthesized and released from post-ganglionic sympathetic neurons. Northern analysis and in situ hybridization analysis reveal that ET-1 messenger RNA is expressed in whole mount and dissociated sympathetic ganglia (superior cervical ganglia, SCG) (Damon, 1998;Milner et al., 2000a). Immunoreactivity of ET-1 is localized on the postganglionic neurons (Dai et al.,

2004b;Damon, 1998;Milner et al., 2000a). Radioimmunoassay indicates that ET-1 is present in the culture medium of SCG neurons and in the extract of SCG (Damon, 1998). The site of ET-1 release from postganglionic sympathetic neurons is not defined yet. If ET-1 is released from nerve terminals, it could modulate neurotransmission or the innervated end-organ function, such as vasoconstriction. If ET-1 is released from the cell body, it could act on adjacent postganglionic sympathetic neurons or glial cells as a paracrine modulator (Damon, 1999).

ET-1 has effects on release of neurotransmitters from postganglionic sympathetic neurons and modulation of the functions of sympathetic target organs. ET-1 superfused in isolated canine mesenteric veins enhances contractile responses to the selective α2-adrenergic agonist UK-14304, an effect which is blocked by the selective α2-adrenergic antagonist rauwolscine, but is not sensitive to the selective α1-adrenergic antagonist prazosin (Shimamoto et al., 1992). The authors conclude that ET-1 potentiates responses to UK-14304 through the amplification of postjunctional α2-adrenergic receptor-mediated responses. ET-1 superfusion significantly reduces norepinephrine and ATP overflow in response to electric field stimulation, an effect that is blocked by the selective ET_B receptor antagonist BQ-788 (Mutafova-Yambolieva and Westfall, 1998), suggesting that ET_B receptor is involved in the ET-1 effects on the presynaptic neuromodulation of sympathetic tone to the blood vessels.

2.6 Endothelin-1 and hypertension

2.6.1 Endothelin-1 and essential human hypertension

ETs are implicated in several cardiovascular diseases, including essential hypertension (Rubanyi and Polokoff, 1994). Endothelin receptor antagonists reduce blood pressure and peripheral vascular resistance in both normotensive persons and patients with mild to moderate essential hypertension (Krum et al., 1998), supporting the interpretation that endothelin plays a role in the pathogenesis of hypertension. Enhanced endothelial expression of the ET-1 gene is seen using in situ hybridization in small arteries from some patients with moderate-to-severe essential hypertension. This is the first demonstration that overexpression of the ET-1 gene may occur in the vascular wall in a small sample of this subset of hypertensive patients (Schiffrin et al., 1997). Circulating endothelin levels are increased in some hypertensive patients, particularly African Americans (Ergul et al., 1996). This pathophysiological phenomenon could play a role in blood pressure elevation and perhaps in the pathogenesis of vascular hypertrophy. In addition, salt-sensitive patients often have low plasma renin activity and demonstrate an exaggerated rise in plasma ET-1 levels in association with elevated plasma catecholamines following sodium depletion. This suggests a relationship between the sympathetic system, sodium sensitivity, and the reactivity of the endothelin system that may contribute to blood pressure elevation in these subjects (Schiffrin, 1999).

2.6.2 Endothelin-1 and DOCA-salt hypertension

ET-1 plays a critical role in the development and maintenance of DOCA-salt hypertension. This opinion is supported by the observation that there is more endothelial ET-1 mRNA and higher basal release of endogenous endothelin in

DOCA-salt hypertensive rats (Millette et al., 2003;Yu et al., 2002) and that chronic endothelin receptor blockade treatment decreases blood pressure to normal range (Doucet et al., 1996).

The fundamental mechanisms of blood pressure elevation by ET-1 in DOCA-salt hypertension are under investigation. The first possible mechanism is the direct vasoconstrictive effect provided by ET-1, considering the high level of endothelial ET-1 released in DOCA-salt hypertension. Second, ET-1 possesses mitogenic and hypertrophic properties (Hirata et al., 1989). Hypertrophy of the vascular media of arteries of DOCA-salt hypertensive rats in prominent (Schiffrin, 1999). Third, ET-1 has the ability to modulate sympathetic transmission. In the rabbit saphenous artery ET-1 potentiates the purinergic component of the contractile responses to both exogenous ATP and electrical stimulation postjunctionally (Mutafova-Yambolieva and Radomirov, 1994). Last, a significant amount of evidence supports the notion that vascular cells generate reactive oxygen species (ROS), such as superoxide ($O_2^{\bullet-}$), which play critical roles in hypertension (Lassegue and Clempus, 2003). In DOCA-salt hypertension, there is a profound increase in vascular $O_2^{\bullet-}$ (Li et al., 2003). The increased $O_2^{\bullet-}$ quenches the potent endogenous vasodilator nitric oxide (NO) to impair the endothelium-dependent relaxation and result in hypertension.

Therefore, elevations in systemic blood pressure in the DOCA-salt hypertension model could be due to the combination of vasoconstriction, vascular hypertrophy, modulation of sympathetic activity and oxidative stress.

3 Mesenteric circulation

The splanchnic circulation is the circulation of blood through the vessels supplying the abdominal viscera, including the gastrointestinal tract, liver, spleen, and pancreas. It is the largest single blood reservoir and stores 38 percent of the total blood volume (Greenway, 1983a). The splanchnic circulation is important for its contribution to peripheral resistance and its reflex capacitance control to secure the cardiac filling (Greenway, 1983a).

3.1 Sympathetic innervation to mesenteric arteries and veins

The splanchnic circulation is richly innervated by the sympathetic nervous system (Pang, 2001) and up to 64 percent of it can be mobilized by direct stimulation of sympathetic nerves (Greenway, 1983a). Sympathetic innervation to the splanchnic circulation contributes significantly to the regulation of systemic blood pressure by increasing the resistance and decreasing the capacitance (Kreulen and Keef, 1989). The resistance and capacitance vessels of the splanchnic circulation have different sensitivities to sympathetic nerve stimulation (Karim and Hainsworth, 1976). Specific alterations in venous control may contribute to some vascular disorders. For example, orthostatic hypotension associated with autonomic insufficiency can be countered by drugs that cause splanchnic venoconstriction (Lamarre-Cliche and Cusson, 1999). Also, patients with salt-sensitive hypertension show a greater decrease in venous capacitance during salt-loading than do subjects with salt-resistant hypertension (Sullivan and Ratts, 1988;Takeshita et al., 1984).

Sympathetic innervation pathways to arteries and veins differ. Studies on the responses to sympathetic nerve stimulation demonstrate a frequency-

dependent activation of capacitance and resistance vessels, which results in predominant venoconstriction at lower frequencies and arterial constrictions at higher frequencies (Hottenstein and Kreulen, 1987). Moreover, a single stimulus to postganglionic nerves elicits an excitatory junction potential (EJP) in arterial smooth muscle, but not in venous smooth muscle. Veins depolarize proportionally more at low frequency stimuli (1-5 Hz) than do arteries, which require higher frequency (10-20 Hz) to depolarize maximally (Hottenstein and Kreulen, 1987). Studies using retrograde tracing and electrophysiology show that arteries and veins in the mesenteric circulation are innervated by different sympathetic neurons, which have different neurochemical and functional properties (Browning et al., 1999). This differential neurotransmission and distinct anatomical pathways of sympathetic innervation to arteries and veins provides a template for separate sympathetic control of vascular resistance and capacitance.

4 Sympathetic neurotransmission in vasculature

The sympathetic nervous system innervates mesenteric vasculature to cause vasoconstriction by releasing vasoconstrictive neurotransmitters, such as ATP and norepinephrine, from nerve terminals to act on postjunctional receptors. Action potentials travel along sympathetic nerves to their endings on smooth muscle cells and voltage-sensitive calcium channels are activated to permit calcium entry and initiate a cascade of events leading to the exocytosis of neurotransmitters from synaptic vesicles. The sympathetic tone is determined by the number of action potentials traveling to nerve terminals per unit time, namely

the impulse frequency. The higher the frequency, the more the neurotransmitters released from nerve terminals. Upon released neurotransmitters, sympathetic control of vascular tone is further decided by the reactivity of postjunctional receptors for neurotransmitters, such as the density or the binding ability of receptors.

4.1 Noradrenergic neurotransmission

4.1.1 Norepinephrine synthesis, release, uptake and metabolism (Figure 1)

Through the action of dopamine-β-hydroxylase (DβH) localized within synaptic vesicles, where norepinephrine is stored and released via exocytosis, norepinephrine is synthesized from dopamine (DA), which is hydrolyzed and decarboxylated from tyrosine via the rate-limiting enzyme tyrosine hydroxylase (TH) and aromatic amino acid decarboxylase (AAAD). The released norepinephrine from nerve terminals into neuromuscular junctions is subjected to three possible fates (Eisenhofer, 1994;Eisenhofer, 2001): 1) Around 90% of it is reuptaken back into nerve terminals via norepinephrine transporter (NET) and transported into synaptic vesicles, which is released into neuromuscular junctions again or leaked out of synaptic vesicles to be metabolized to dihydroxyphenylglycol (DHPG) by monoamine oxidase (MAO) and diffused into plasma. 2) Some of it is spilled over into blood circulation. 3) Some of it is transported into vascular cells via extraneuronal norepinephrine transporter, organic cation transporter 3 (OCT3).

Figure 1: Schematic diagram summarizing norepinephrine synthesis, release, uptake and metabolism. The first step in the synthesis of norepinephrine is the conversion of tyrosine to dihydroxyphenylalanine (DOPA) by tyrosine hydroxylase (TH), which is the rate-limiting enzyme in norepinephrine synthesis. DOPA is then decarboxylated to form dopamine (DA) by aromatic amino acid decarboxylase (AAAD). After taken up into the synaptic vesicles by monoamine transporter, DA is converted to norepinephrine through the action of dopamine- - hydroxylase (DβH). Norepinephrine is released from nerve terminals into neuromuscular junctions and subjected to three possible fates: 1) Around 90% of it is reuptaken back into nerve terminals to be transported into synaptic vesicles via norepinephrine transporter (NET), which is released into neuromuscular junctions again or leaked out of synaptic vesicles to be metabolized to dihydroxyphenylglycol (DHPG) by monoamine oxidase (MAO) and diffused into plasma. 2) Some of it is spilled over into blood circulation. 3) Some of it is transported into vascular cells via extraneuronal norepinephrine transporter, oorganic cation transporter 3 (OCT3).

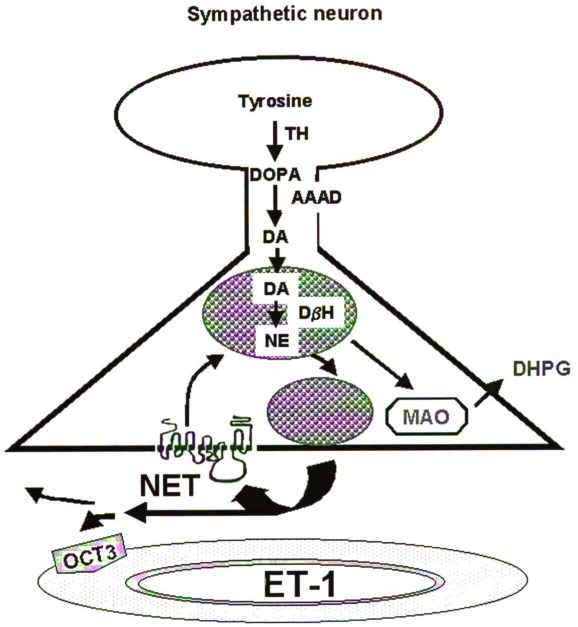
Sympathetic neuron
Tyrosine
TH
DOPA
AAAD
DA
DA
DβH
NE
DHPG
MAO
NET
OCT3
ET-1
Blood Vessel

Norepinephrine acts on the G-protein coupled metabotropic α- adrenergic receptors on vascular smooth muscle cells to cause vasoconstriction, which is slowly developing and long lasting (Guimaraes and Moura, 2001). Upon norepinephrine binding to α- adrenergic receptors, the G protein is activated to stimulate phospholipase C activity and that this enzyme promotes the hydrolysis of phosphatidylinositol bisphosphate (PIP_2) producing IP_3 and DAG, which act as second messengers mediating intracellular calcium release from nonmitochondrial pools and contract smooth muscle cells (Guimaraes and Moura, 2001).

4.1.2 Postjunctional effects of norepinephrine

Two types of α- adrenergic receptors, α1 adrenergic receptors and α2 adrenergic receptors, are both present on vascular smooth muscle cells and mediate vasoconstriction (Guimaraes and Moura, 2001). Binding affinities of norepinephrine for α1 adrenergic receptors are much higher than α2 adrenergic receptors (Docherty, 1998). Arterial vasoconstriction is mainly mediated through postjunctional α1 adrenergic receptors, whereas venous vasoconstriction is mainly mediated through postjunctional α2 adrenergic receptors (Docherty, 1998). In mesenteric arteries, only α1 adrenergic receptors mediate norepinephrine induced vasoconstriction, in which prazosin, an α1 adrenergic receptor antagonist, completely inhibits norepinephrine vasoconstriction (Hottenstein and Kreulen, 1987;Luo et al., 2003). In contrast, α2 adrenergic receptors mediate norepinephrine induced vasoconstriction in mesenteric veins (Shi et al., 1990). Alterations in binding characteristics and/or intracellular signal

transduction of postjunctional vascular adrenergic receptors seem to contribute to high blood pressure in spontaneously hypertensive rats (Takata and Kato, 1996) and DOCA-salt hypertensive rats (Perry and Webb, 1988).

4.1.3 Prejunctional effects of norepinephrine

The α2 adrenergic receptors are also located on sympathetic nerve terminals as prejunctional autoreceptors. The activation of α2 adrenergic receptors leads to the dissociation of β and γ subunits from G-protein, which interact directly with pore-forming α1 subunits of N- and P/Q- type calcium channels and thus reduce the channel's open probability and inhibit calcium entry into the cytoplasm and, eventually, norepinephrine release from nerve terminals (Starke, 2001). However, some observations on presynaptic α2 adrenergic inhibition could not be explained on basis of any inhibition of calcium entry through voltage sensitive calcium channels (Starke, 2001). Inhibition of transmitter release may occur by mechanisms other than modulation of calcium-entry through N-type calcium channels in postganglionic sympathetic nerves (Smith and Cunnane, 1998), such as regulation of intracellular calcium homeostasis (Jackisch et al., 1992;Schwartz, 1997). Inhibition of norepinephrine release by α2 adrenergic receptors is frequency dependent (Scheibner et al., 2001), in which the α2 adrenergic receptors mediated inhibition of norepinephrine release is enhanced when the stimulation frequency is increased.

Prejunctional α2 adrenergic receptor function is impaired in some types of hypertension. A decrease in the functional activity of prejunctional α2 adrenoceptor may contribute to the enhanced release of norepinephrine from

caudal artery and portal vein of spontaneously hypertensive rats (Westfall et al., 1986). Impairment of $\alpha 2$ adrenergic autoreceptor function in sympathetic nerves associated with mesenteric arteries and veins from DOCA-salt rats results in increased NE release (Luo et al., 2004).

4.1.4 ET-1 modulation on sympathetic neurotransmission

ET-1 modulates sympathetic neuroeffector transmission to vasculature. ET-1 exerts both facilitatory effects, at low ET-1 concentration, and inhibitory effects, at high ET-1 concentration, on the neurogenically-induced release of sympathetic neurotransmitters ATP and NA in the rat tail artery (Mutafova-Yambolieva and Westfall, 1998), and there effects are blocked by selective ET_B receptor antagonist, which suggest that ET_B receptors may be important in prejunctional neuromodulation of sympathetic tone by ET-1 to blood vessels.

ET-1 modulation to sympathetic neurotransmission might be altered in hypertension. In isolated perfused mesenteric arteries, ET-1 enhances the responsiveness of alpha-adrenergic receptors to catecholamines, whereas it inhibits presynaptic adrenergic neurotransmission. And the modulation by ET-1 at the vascular neuroeffector junction in SHR is different from normotensive rats, which may explain the maintenance of hypertension in SHR (Tabuchi et al., 1990).

5 Antagonistic effects of sensory and sympathetic innervation to blood vessels

Sympathetic and primary sensory nerves appear to provide a vasoconstrictor-vasodilator balance to blood vessels, much like the "antagonistic"

balance between sympathetic and parasympathetic neurons in other effector organs. The evidence in support this includes: 1) Opposite effects are for the most part a reflection of different neurotransmitter phenotypes in two types of nerves: vasoconstrictive neurotransmitters, norepinephrine and ATP, released from sympathetic nerves, and vasodilatory neuropeptides, substance P (SP), calcitonin gene-related peptide (CGRP) and vasoactive intestinal peptide (VIP), released from sensory nerves. 2) The perivascular plexus of nerve terminals around mesenteric blood vessels contains the sympathetic postganglionic axon and primary sensory nerve terminals. The close association of sympathetic and sensory nerves provides an anatomical template for the interaction of these two types of nerves, which is important for the integration and specification of neural control of mesenteric arteries and veins (Luff et al., 2000). 3) Sensory nerves send collaterals to sympathetic ganglia to affect the activity of sympathetic nerves (Benarroch et al., 1992;Zheng et al., 1999). The sensory system originating in the kidney can activate increased sympathetic discharge through complex projection pathways involving forebrain systems (Brody, 1988). On the other side, the decrease in responsiveness of renal mechano-sensitive neurons contributes to an increase in renal sympathetic nerve activity and sodium retention (DiBona et al., 1999). Those studies support the idea that normal balance between sensory and sympathetic nervous system plays an important role in the maintenance of normal blood pressure. So far, how this interaction is altered in hypertension is not known.

6 Norepinephrine transporter (NET)

When tritiated norepinephrine is given intravenously to rats, it accumulated in sympathetically innervated organs. This effect can be blocked by administration of cocaine, leading to the conclusion that a specific transport system might be responsible for the inactivation of circulating norepinephrine (Axelrod et al., 1961). Neuronal uptake of norepinephrine was later designated as "uptake 1", now known as norepinephrine transporter (NET), to distinguish it from another cocaine-insensitive catecholamine uptake process in the heart and peripheral tissues, known as "uptake 2" (Iversen, 1963). The ability of desipramine to inhibit this neuronal norepinephrine transport system allows people to localize the NET in tissue slices by autoradiography and study its function by binding assay (Pacholczyk et al., 1991).

NET is located presynaptically on central and peripheral noradrenergic nerve terminals and it is responsible for the rapid clearance of 90 percent of neuronally released norepinephrine from the synaptic cleft. It also contributes to the inactivation of circulating catecholamines. After their transport into the nerve endings, these monoamines are taken up into storage vesicles in the nerve ending by the reserpine-sensitive vesicular monoamine transporters (VMAT) and/or degraded by the mitochondrial monoamine oxidase (MAO). This serves to shorten the time of effects of norepinephrine on adrenoceptors (Bruss et al., 1997;Eisenhofer, 1994).

6.1 Biochemical structure of NET

The molecular structure of NET was identified following its cloning from several species, include rat (Giros et al., 1991), human (Blakely et al., 1991), and

cow (Lingen et al., 1994). NET belongs to a large gene family of sodium (Na^+) and chloride (Cl^-) dependent transporters that translocate neurotransmitters and amino acids, such as dopamine, serotonin, GABA, glycine, and taurine (Masson et al., 1999). NET is a 617 amino acid transmembrane protein with 12 α-helical transmembrane domains (TMD) with configured intracellular and extracellular loops (with a large extracellular loop between TMD3 and TMD4), respective phosphorylation and glycosylation sites, and intracellularly located amino- and carboxyl-terminal residues (Bruss et al., 1997;Pacholczyk et al., 1991). The whole sequence of rat NET was cloned from rat pheochromocytoma cell line PC-12 cells by Bonisch and colleagues (Bruss et al., 1997). Rat NET amino acid sequence contains two potential N-glycosylation sites, while human NET has three. At the nucleotide level, the rat NET and the human NET share 87% identity in the coding region, while it exhibits only 65% identity to the rat dopamine transporter (DAT) (Bruss et al., 1997).

6.2 Pharmacological properties of the NET

Transport mediated by the NET is dependent on Na^+ and Cl^- ions and the inwardly directed Na^+ gradient (maintained by the action of the Na^+-K^+-ATPase) also contributes to the driving force for the active transport system. In addition, the inside negative membrane potential also contributes a driving force for inward transport (Bonisch et al., 1999). Transport by the NET is proposed to occur as a positively charged ternary complex, consisting of the transporter, one Na^+ ion, one Cl^- ion and the norepinephrine amine group (Harder and Bonisch, 1985).

NET has high specificity for norepinephrine and it is also able to

translocate the compounds with similar structure to norepinephrine, such as guanethidine (Galli et al., 1996). The substrates for NET include the endogenous catecholamines (norepinephrine and epinephrine), neurotoxic (1-methyl-4-phenylpyridinium, MPP^+), and the psychostimulant amphetamine. NET is blocked by the psychostimulant cocaine and tricyclic antidepressants such as desipramine (Blakely et al., 1991).

Mutations in the coding region, leading to amino acid substitutions in NET, can have crucial effects on the pharmacological properties of this transport system. The sequence between TMD1 and TMD2 of the NET is highly conserved in the Na^+/Cl^--dependent neurotransmitter transporter family and is very important for Na^+ and Cl^- co-transport. The sequence between TMD4 and TMD10 is very important for substrate and inhibitor binding. Some key nucleotide mutations, such as Ser399, Gly400 or Ala457, cause loss of uptake or binding ability to desipramine (Bonisch et al., 1999). Comparisons of pharmacological properties of rat, human and cow NET show small, but significant interspecies differences in the affinities for cocaine, Na^+ and some substrates, which support the notion that a few amino acid differences in the primary sequences of the transporters can influence the ligand recognition, translocation processes, and Na^+ dependence (Paczkowski et al., 1999). A single nucleotide mutation at TMD9 results in a total loss of NET function in an orthostatic intolerance patient (Shannon et al., 2000). The investigation of transporter amino acid mutations in disease states, especially in human essential hypertensive patients with genetic family history, offers much promise.

6.3 Physiological importance of the NET

NET limits norepinephrine-mediated neurotransmission by minimizing the duration of norepinephrine-receptor interaction. Thus, once norepinephrine is released, the duration and extent of presynaptic and postsynaptic G-protein-coupled-receptors (GPCRs) stimulation is largely limited by reuptake. Localization of NET presynaptically and along axons and dendrites, rather than within the synaptic cleft, supports this notion (Savchenko et al., 2003;Schroeter et al., 2000). This reuptake process is critical so that receptor desensitization is less likely to occur (Zahniser and Doolen, 2001).

The importance of NET in limiting neurotransmission, as well as in regulating presynaptic and postsynaptic transmitter homeostasis, is emphasized by experiments with transporter knockout mice (Xu et al., 2000). Compared to the wild type mice, the disruption of NET gene results in a 55-70% reduction in norepinephrine levels, approximately 60% reduction in the release of norepinephrine in response to electrical stimulation, and at least a 6-fold slower rate of norepinephrine clearance in rat brain. In spite of the decreased norepinephrine release, the effect of greatly reduced norepinephrine clearance rate predominates so that the extracellular norepinephrine concentration in the cerebellum is still 2-fold higher in NET knockout versus wild type mice (Xu et al., 2000).

6.4 Analysis of NET function

The function of NET can be assessed by a number of methods. These include measurement of cellular accumulation of exogenous radiolabeled

norepinephrine, transporter current, clearance of norepinephrine, norepinephrine metabolites in plasma, and clinical imaging (positron emission topography, PET, or single photon emission topography, SPET) (Eisenhofer, 2001;Galli et al., 1995). Due to the pharmacological properties of the NET, which is able to translocate compounds with similar structure to norepinephrine, a new fluorescent microscopy method can be used to measure NET uptake function by using ASP^+ (4-(4-(dimethylamino)-styrl)-N-methylpyridinium), a fluorescent analogue of the neurotoxin MPP^+ that can be accumulated in the cell by the NET (Schwartz et al., 2002).

6.5 Regulation of NET

Given the important physiological roles played by NET, its regulation is under investigation. The regulation of Na^+/Cl^- dependent neurotransmitter transporters occurs very rapidly on a time scale of seconds to minutes. One early study shows that [^{3}H]NE release is consistently potentiated during nerve stimulation. However, its major metabolite [^{3}H]3,4-dihydroxyphenylglycol (DHPG), which is produced only after neuronal reuptake of norepinephrine, does not appears in the perfusate until after the stimulation ends, suggesting that norepinephrine uptake is attenuated during depolarization (Dubocovich and Langer, 1976). Depolarization-induced reductions in uptake are consistent with the driving force for transport being the Na^+ electrochemical gradient. The transient inhibition of uptake during neuronal depolarization would allow the neurotransmitter a finite period of time to diffuse away from the presynaptic terminal and to interact with postsynaptic receptors, both within and outside of

the synapse (Zahniser and Doolen, 2001). Additionally, the regulation of Na^+/Cl^- dependent neurotransmitter transporters can also occur long-term on a time scale of days. Nine days of subcutaneous injection of reserpine, which selectively blocks the monoamine vesicular transporter and depletes biogenic amines, results in down-regulation of NET binding sites and reduced norepinephrine uptake in rat cerebral cortex. These findings suggest that a change in the amount or longevity of norepinephrine in and around the synaptic cleft may cause a change in the number or function of NET on noradrenergic neurons, a mechanism by which noradrenergic transmission is biologically regulated (Lee et al., 1983).

Many signaling systems are involved in the regulation of NET. The cloning of the NET in the early 1990s revealed the putative phosphorylation sequences for protein kinases, such as PKC and protein kinase A (PKA), suggesting that the transporters can be phosphorylated. PKC can be stimulated endogenously by the second messenger DAG, and pharmacologically by phorbol esters, such as phorbol 12-myristate 13-acetate (PMA). PMA-induced PKC activation leads to a decreased norepinephrine transport capacity (V_{max}) with no change in norepinephrine substrate affinity (Km) and a reduced density of [3H]nisoxetine binding sites (B_{max}) (Apparsundaram et al., 1998a). PKC activation also results in a reduction in radioligand binding to cell surface NETs and a decrease in the biotinylated labeled cell membrane transporter with no change in the total number of NETs (Apparsundaram et al., 1998b). These data led to the idea that PKC activation results in a distribution of transporters away from the cell surface

and that membrane trafficking is involved in the PKC-mediated transporter regulation. NET contains two conserved cysteine residues on the large extracellular loop similar to the other monoamine transporters and these cysteine residues are highly susceptible to oxidation (Zahniser and Doolen, 2001). Uptake mediated by the DAT, serotonin transporter (SERT), and GABA transporter (GAT) is inhibited by the generation of reactive oxidative species (ROS) (Zahniser and Doolen, 2001). However, the regulation of NET by ROS is controversial. Haughey et al. reports that the oxygen radical-generating enzyme, xanthine oxidase, dramatically reduces striatum DAT activity, but is unexpectedly without effect on rat hippocampus norepinephrine uptake (Haughey et al., 1999). However, Mao et al. showed that norepinephrine produced oxidative stress causes a dose-dependent reduction of norepinephrine uptake activity without affecting cell viability significantly. This decrease in norepinephrine uptake activity is associated with reductions in norepinephrine uptake binding sites and NET protein expression, but no changes in NET gene expression (Mao et al., 2004).

To date, most of the research investigating the regulation of NET has been done *in vitro* using substrates or/and blockers in stably transfected cell lines (Apparsundaram et al., 1998b;Bruss et al., 1995;Melikian et al., 1994;Zhu et al., 2000;Zhu et al., 1998) and in natively expressed cell lines, such as PC-12 cells (Zhu and Ordway, 1997) and human neuroblastoma (SK-N-SH) cells (Apparsundaram et al., 2001;Joyce et al., 2001). The reason for using the cell lines is that they are relatively easy to manipulate, ever since the molecular

structure of NET had been revealed. Those results demonstrate that the regulation of NET protein and mRNA and the function of NET are substrate-dependent. The changes in NET mRNA level, protein level, binding sites and binding affinities are inconsistent (Zhu et al., 1998;Zhu et al., 2000;Zhu and Ordway, 1997). Cells in culture lack synaptic contacts, therefore, the results only imply direct regulation as the result of occupation of NET. They do not inform us regarding secondary effects, such as changes in the activation of one or more of the synaptic receptors for norepinephrine or other trans-synaptic phenomena secondary to inhibition or activation of norepinephrine uptake (Zhu et al., 1998).

6.6 Clinical significance of NET in hypertension

Clinical studies suggest that the defective neuronal norepinephrine uptake by NET may be important in the pathogenesis of essential hypertension. Compared to normotensive patients, the spillover of norepinephrine from the heart is increased in some patients with essential hypertension (Esler et al., 1981;Kimura et al., 1983). There is evidence that norepinephrine reuptake increases with increased sympathetic nerve activity (Takimoto and Weiner, 1981). The half time of plasma norepinephrine clearance is longer in a fraction of essential hypertensive patients and normal subjects treated with desipramine, the specific blocker of NET, than in normal subjects treated with/without cortisol, the blocker of extraneuronal NET uptake 2 (Esler et al., 1980). This prolongation might result from unsuccessful elimination of norepinephrine resulting from defective uptake during the increased sympathetic activity in essential hypertension (Takeshita et al., 1984;VanNess et al., 1999).

Norepinephrine uptake is regulated by many potent key factors related to blood pressure regulation, such as norepinephrine, Ang II and angiotensin converting enzyme. The abnormal high plasma norepinephrine concentration in hypertensive patients might possibly regulate the expression or function of NET per se, because substrates for this transporter are capable of regulating its function (Lee et al., 1983). Ang II is a peptide hormone involved in the regulation of blood pressure and it can activate the peripheral sympathetic nervous system by inhibiting neuronal norepinephrine uptake (Malik and Nasjletti, 1976) and/or facilitating norepinephrine release from sympathetic nerves by activation of presynaptic Ang II receptors (Endo et al., 1977;Szabo et al., 1990). However, Ang II acutely and chronically stimulates the NET system and causes an increase in norepinephrine uptake and NET mRNA expression in a brainstem neuron culture from normal WKY rats. This stimulation is enhanced in spontaneously hypertensive rats (Lu et al., 1996). Distinctive central and peripheral effects of Ang II on the cardiovascular system may explain this controversy (Warren et al., 2001). Angiotensin converting enzyme inhibitors (ACEI) increase neuronal norepinephrine uptake acutely independent of the central sympathetic activity (Raasch et al., 2001).

7 Reactive oxygen species (ROS)

Accumulating evidence indicates that oxidative stress plays a major role in the initiation and progression of cardiovascular dysfunction associated with diseases, such as hypertension, diabetes mellitus, and chronic heart failure (Lassegue and Clempus, 2003). Oxidative stress is a state in which excess

reactive oxygen species (ROS) overwhelm endogenous antioxidant systems. ROS have distinct functional effects on tissues and cells and can play both physiological and pathological roles (Droge, 2002).

$O_2^{\cdot-}$ is formed by the univalent reduction of molecular oxygen (O_2) and this reaction is mediated by several enzyme systems including the NAD(P)H oxidases, xanthine oxidase (XO) and uncoupled nitric oxide synthase (NOS) (Droge, 2002). $O_2^{\cdot-}$ is one of the most important ROS and it is pivotal in generating other ROS. Reaction of $O_2^{\cdot-}$ with NO generates peroxynitrite anion, and dismutation of $O_2^{\cdot-}$ by superoxide dismutase (SOD) produces hydrogen peroxide (H_2O_2), which is then converted enzymatically into H_2O by catalase (Droge, 2002).

7.1 NAD(P)H oxidases as the major sources of ROS

NAD(P)H oxidases are the predominant source of ROS. Currently, attention is focused on NAD(P)H oxidases as critical determinants of the redox state in cardiovascular diseases. The activation of NAD(P)H oxidases leads to a variety of intracellular signaling events that cause dysfunction of systems (Lassegue and Clempus, 2003).

7.1.1 Structure

NAD(P)H oxidases were first found and cloned in phagocytic cells. The phagocytic NAD(P)H oxidases consist of four components that are essential for activity: two membrane bound components, $gp91^{phox}$ and $p22^{phox}$ (phox stands for phagocyte oxidase), and two cytosolic components $p47^{phox}$ and $p67^{phox}$. Additional components of the enzyme include the small GTPase(s) Rac, and

$p40^{phox}$, which is also associated with the oxidase and has an unclear functional role. Together $gp91^{phox}$ and $p22^{phox}$ form an integral membrane complex termed flavocytochrome b588 protein, located in cytoplasmic vesicles and plasma membrane. The catalytic subunit of this flavocytochrome, $gp91^{phox}$, binds three prosthetic groups: one flavin adenine dinucleotide (FAD) and two heme molecules. The cytosolic protein complex, composed of $p47^{phox}$ and $p67^{phox}$, does not interact with the cytochrome in resting cells (Babior et al., 2002). The phosphorylation of p47phox subunit by PKC serves as a switch to trigger the oxidase assembly and this results in a rearrangement of the conformation of the cytosolic complex. This activated cytoplasmic complex then associates with the cytochrome in the membrane to form a functional enzyme that is thought to include one copy of each phox subunit, as well as Rac. The reduced substrate NADPH binds to gp91phox on the cytoplasmic side of the membrane and releases two electrons, which are passed to FAD, then to the first and second heme group, and finally they are accepted by two successive molecules of oxygen on the opposite side of the membrane to produce two molecules of $O_2^{\bullet-}$. Once activated, phagocytes produce large quantities of superoxide, on the order of $10 nmol \cdot min^{-1} \cdot 10^6$ neutrophils^{-1} during the oxidative burst (Babior, 1999;Babior et al., 2002).

In the last decade, it became clear that the other non-phagocytic cells also produce $O_2^{\bullet-}$ via enzymes similar to the phagocytic NAD(P)H oxidases. Recently, it was discovered that the catalytic subunit is a member of a new family of homologous proteins termed NOX (NOX stands for NAD(P)H oxidases)

(Lambeth et al., 2000), such as NOX1, NOX2 ($gp91^{phox}$), NOX3, NOX4 et al. A lot of cell types express NOX, including vascular smooth muscle cells, endothelial cells and fibroblasts (Lassegue and Clempus, 2003), neurons and glial cells (Kim et al., 2002;Noh and Koh, 2000;Tammariello et al., 2000).

There are several differences between phagocytic and non-phagocytic NAD(P)H oxidases. First, non-phagocytic cells contain a number of homologues of $gp91^{phox}$, termed NOXs, such as NOX1. Second, the $O_2^{\cdot-}$ generation pathway is different. Phagocytic cells produce $O_2^{\cdot-}$ extracellularly via $gp91^{phox}$, while non-phagocytic cells can produce $O_2^{\cdot-}$ intracellularly via NOX1 or other NOX family members. Third, the phagocytic enzyme is normally silent, but upon stimulation, is activated rapidly. Non-phagocytic cells are constitutively active and also can be activated by agonist binding to G-protein coupled receptors (Griendling et al., 2000;Lassegue and Clempus, 2003).

The following part of the introduction will emphasize the properties of non-phagocytic NAD(P)H oxidases.

7.1.2 Mechanism of activation

The non-phagocytic NAD(P)H oxidases can be activated by hemodynamic forces, inflammatory mediators, and hormones, in addition to being constitutive. Bovine pulmonary artery endothelial cells exposed to shear stress exhibit an increased ROS production compared with continuously perfused cells. This can be inhibited by the NAD(P)H oxidase inhibitor diphenyleneiodonium (DPI) (Yermolaieva et al., 2000). Tumor necrosis factor α (TNF-α) stimulates NAD(P)H oxidase dependent $O_2^{\cdot-}$ production (De Keulenaer et al., 1998). ET-1 induced

vascular $O_2^{\cdot-}$ production is reduced by the NAD(P)H oxidase blockers apocynin and DPI (Li et al., 2003).

The activation mechanism of NAD(P)H oxidase in non-phagocytic cells shows similarities with that of the phagocytic enzyme. One is the activation of PKC pathway. Phosphorylation of the $p47^{phox}$ subunit by PKC is required for the activation of phagocytic oxidase and several studies demonstrate the indispensable role of PKC activation in vascular $O_2^{\cdot-}$ generation. Pulmonary endothelial cells showed an enhanced ROS generation upon stimulation with PMA, a PKC activator (Hohler et al., 2000). Treatment with a PKC inhibitor decreases Ang II induced $O_2^{\cdot-}$ production in mesangial cells (Jaimes et al., 1998). Another important activator is the small G protein Rac. In vascular smooth muscle cells, the expression of dominant-negative Rac in transgenic mice significantly inhibits Ang II-induced ROS production and overexpression of constitutively active Rac increased basal and Ang II induced ROS production (Seshiah et al., 2002).

Regulation of NAD(P)H oxidases activity occurs at two levels. First, activation of NADPH oxidase depends on the targeting of a cytoplasmic $p40^{phox}$-$p47^{phox}$-$p67^{phox}$ complex to the membrane bound heterodimeric $p22^{phox}$-$gp91^{phox}$ flavocytochrome and assembling a complex on the plasma membrane level (Paclet et al., 2000). Key to the assembly process is $p47^{phox}$, which contains two SH3 domains. This interaction is prevented in the resting state due to an auto-inhibited conformation of $p47^{phox}$. The X-ray structure of the auto-inhibited form of $p47^{phox}$ reveals that tandem SH3 domains function together to maintain the

cytoplasmic complex in an inactive form. Further structural and biochemical data show that phosphorylation of $p47^{phox}$ permits $p47^{phox}$ to interact with the cytoplasmic tail of $p22^{phox}$ and initiate formation of the active membrane bound enzyme complex (Groemping et al., 2003). Second, NAD(P)H oxidase activity can also be increased due to upregulation of NAD(P)H oxidase subunits mRNAs and proteins (Griendling et al., 2000). Ang II activates NAD(P)H oxidases to generate greater $O_2^{\cdot-}$ in cultures of rat vascular smooth muscle cells and in animals by upregulating mRNA levels of several components of this oxidase system, including $p22^{phox}$, $p67^{phox}$ and $p47^{phox}$ (Brandes et al., 2002;Fukui et al., 1997b;Pagano et al., 1998). NAD(P)H oxidase subunits are frequently upregulated by treatments leading to increased ROS production (Lassegue and Clempus, 2003).

7.2 Biological effects of NAD(P)H oxidases activation

ROS and NAD(P)H oxidases have been implicated in numerous cellular processes and disease conditions (Griendling et al., 2000;Lassegue and Clempus, 2003;Taniyama and Griendling, 2003;Zimmerman and Davisson, 2004)

In contrast to the cytotoxic amount of $O_2^{\cdot-}$ generation by phagocytes, nonphagocytic cells produce low amounts of ROS. Under physiological conditions, the intracellular ROS production does not alter the redox state of cells, which have large reserves of antioxidants, such as enzymes (SOD, glutathione peroxidases, and catalase), as well as non-enzymatic components (glutathione, ascorbate, α-tocopherol, and β-carotene) (Droge, 2002).

The reducing intracellular environment allows the agonist-induced ncreases in ROS to function as second messengers. Stimulation of cell surface eceptors with agonists or growth factors activate various cellular signaling athways, including protein kinases, phospholipases, and Ca^{2+}-dependent athways. Exogenous application of ROS stimulates many of the above cascade, nd the increased intracellular ROS induced by receptor activation also can ctivate those pathways (Griendling et al., 2000). The potential ROS-sensitive argets include MAPK, ERK, PKC, c-src, ras/rac, etc. (Griendling et al., 2000).

The regulation or expression of many genes is redox-sensitive. Elevated ROS concentrations can induce the expression of genes whose products exhibit ntioxidative activity in many cells, such as antioxidative enzymes and/or ntracellular glutathione (Droge, 2002). In addition, ROS can also induce ardiovascular related gene expression, such as adhesion molecules, and asoactive substances. The cytokine interleukin 1 β (IL-1 β) activates vascular ell adhesion molecule-1 (VCAM-1) gene expression through a mechanism that s repressed approximately 90% by the antioxidants pyrrolidine dithiocarbamate PDTC) and N-acetylcysteine (NAC) (Marui et al., 1993). The antioxidant NAC ould almost totally abolish the shear stress induced endothelial VCAM-1 gene xpression, whereas reduce approximately 70% of endothelial intercellular dhesion molecule-1 (ICAM-1) gene expression (Chappell et al., 1998). ntioxidants suppresses Ang II-induced ET-1 gene expression and DNA ynthesis in cardiac fibroblasts (Cheng et al., 2003).

7.2.1 Effects of ROS on the cardiovascular system

Many cardiovascular functions are affected by ROS. The most well studied functions are endothelium dependent vasorelaxation, cell growth and apoptosis.

7.2.1.1 Impaired endothelium dependent vasorelaxation

$O_2^{\cdot-}$ quenches the endogenous vasodilator, NO, to cause a loss of NO bioactivity in the vessel wall and impair the endothelium dependent vasorelaxation. In animal models, endothelial dysfunction occurs in association with increased ROS in numerous disease conditions, due to the inactivation of NO by $O_2^{\cdot-}$ (Cai and Harrison, 2000;Taniyama and Griendling, 2003). ROS-mediated endothelial dysfunction in Ang II infused rats (Laursen et al., 1997) and in DOCA-salt hypertensive rats (Somers et al., 2000a) can be reversed by antioxidant enzyme, endothelial NOS (Nakane et al., 2000) or SOD (Li et al., 2003).

7.2.1.2 Cell growth

ROS production leads to both hypertrophic and proliferative vascular cell growth. ROS are involved in the Ang II induced vascular smooth muscle cell hypertrophic response, which can be inhibited by catalase or $p22^{phox}$ antisense (Ushio-Fukai et al., 1996;Zafari et al., 1998). This also implicates the NAD(P)H oxidases-derived ROS in the hypertrophic response. ROS also mediates the thrombin triggered vascular smooth muscle cell proliferation and this response can be inhibited by the NAD(P)H oxidases inhibitor DPI (Patterson et al., 1999).

7.2.1.3 Apoptosis

ROS play a role in the apoptotic mechanisms induced by a variety of stimuli. ROS is causally involved in endothelial apoptosis induced by several pro-inflammatory and pro-atherosclerotic factors including Ang II, oxidized low density lipoprotein (LDL) or TNF-α, and antioxidants, such as SOD, catalase and antioxidant vitamins (Dimmeler and Zeiher, 2000). In contrast to the pro-apoptotic capacity of ROS in endothelial cells, in vascular smooth muscle cells emerging evidence suggests that endogenous ROS synthesis promotes cell proliferation and hypertrophy and does not affect cell survival. However, high concentrations of exogenous ROS can also stimulate smooth muscle cell apoptosis as shown for other cell types probably via activation of p53 (Dimmeler and Zeiher, 2000).

7.2.2 Effects of ROS on the nervous system

In the nervous system, ROS are best known for their contribution to oxidative damage and cell death in neurodegenerative diseases, such as amyotrophic lateral sclerosis and Parkinson's disease (Pong, 2003). More evidence is emerging to suggest that ROS may be involved in normal neuronal activity (Yermolaieva et al., 2000). In the CNS, ROS can serve as signaling molecules mediating the effects of neuroactive substances. For example, the Ang II/ROS signaling system mediates the action of Ang II to increase blood pressure (Zimmerman et al., 2002). In the peripheral nervous system, administration of H_2O_2, a type of ROS, in the vicinity of sympathetic preganglionic neurons projecting to the adrenal gland results in the activation of sympathetic preganglionic neurons innervating the adrenal gland (Lin et al., 2003). This opens the possibility that a change in the redox environment of peripheral nervous

system induced by $O_2^{\cdot-}$ may modulate neuronal activity directly. $O_2^{\cdot-}$ may also indirectly modulate the excitability of neurons by several other mechanisms. One possible mechanism is the ability of $O_2^{\cdot-}$ to modulate the neuronal excitability by quenching or inactivating nitric oxide (NO) (Li et al., 2003), which is known to exist in the sympathetic nervous system (Ceccatelli et al., 1994). We have shown previously that NO increases a Ca^{++}-activated K^+ current in isolated sympathetic neurons, an effect that would reduce the firing rate. By causing a reduction in ganglionic NO levels, $O_2^{\cdot-}$ would eliminate this inhibitory effect of NO and this would result in an increased excitability of sympathetic neurons (Browning et al., 1998). Another possible mechanism is that $O_2^{\cdot-}$ may act as an intracellular second messenger and regulate the gene expression of antioxidant enzymes, such as SOD (Park et al., 1998) and catalase (Sampath et al., 1994), in the sympathetic neurons as it does in blood vessels (Griendling et al., 2000).

7.3 Implication in hypertension

7.3.1 Experimental hypertension animal models

Compelling evidence has accumulated over the past years to support a role of ROS, especially $O_2^{\cdot-}$, in the pathogenesis of various hypertension animal models (Lassegue and Clempus, 2003;Zimmerman and Davisson, 2004).

The cardiovascular effects of ROS in animal models of hypertensive are mainly mediated by inactivation of NO by $O_2^{\cdot-}$ in the vasculature and by ROS induced vascular remodeling. An elevated vascular $O_2^{\cdot-}$ production is seen in several hypertensive animal models, including DOCA-salt (Li et al., 2003;Wu et al., 2001), Ang II infused animals (Nakane et al., 2000;Ushio-Fukai et al., 1996),

renal hypertension (Heitzer et al., 1999), and spontaneously hypertensive rats (Wu et al., 2001). The elevated $O_2^{\cdot-}$ production and hypertension can be reduced by antioxidants. The long-term treatment with cell-permeable SOD mimic tempol lowers the vascular $O_2^{\cdot-}$ levels and blood pressure in renal and DOCA-salt hypertension (Beswick et al., 2001b;Dobrian et al., 2001). Long-term treatment with the NADPH oxidase inhibitor apocynin significantly decreases aortic $O_2^{\cdot-}$ production and systolic blood pressure from DOCA-salt rats compared with sham-operated rats (Beswick et al., 2001a). Heparin-binding SOD significantly improves endothelium-dependent relaxation in DOCA-salt hypertension (Somers et al., 2000a).

Neural effects of ROS in hypertension are still under investigation. Several studies have implicated important roles for ROS in the neural control of blood pressure. ROS play critical roles in the central sympathetic neural control of blood pressure. The rostral ventral lateral medulla (RVLM) in brainstem is the vasomotor center that determines the basal sympathetic nerve activity (SNA) and maintains the basal vasomotor tone (Dampney, 1994). SNA is greater in spontaneously hypertensive rats (SHR), including stroke-prone SHR (SHRSP) (Judy et al., 1976;Kishi et al., 2002); and $O_2^{\cdot-}$ derived ROS signal is increased. This can be abolished by a hydroxyl radical scavenger, dimethylthiourea, in the RVLM in SHRSP. Bilateral microinjection of SOD mimic tempol into the RVLM decreases blood pressure in SHRSP, but not in normotensive control. Furthermore, SOD overexpression in the RVLM of SHRSP decreases blood pressure and inhibits sympathetic nerve activity (Kishi et al., 2004). Injection of

Ang II into the circumventricular organ (CVO), which receives inputs from systemic baroreceptors and chemoreceptors and projects to an extensive neural network responsible for maintaining homeostasis, leads to the increased blood pressure and heart rate. These changes are abolished by prior treatment with intracerebroventricular (ICV) injections of viruses encoding SOD (Zimmerman et al., 2002). In addition, isolated CVO neurons generate $O_2^{\bullet-}$ in response to Ang II *in vitro*. This response is blocked by infection with SOD encoding viruses (Zimmerman et al., 2002). These data demonstrate indirectly that $O_2^{\bullet-}$ plays a key role in the central neuronal and functional effects of Ang II. ROS also play critical roles in the peripheral sympathetic neural control of blood pressure. Sympathetic preganglionic neurons innervating the adrenal gland are activated by injection of H_2O_2 in their vicinity, followed by a subsequent release of catecholamine from adrenal medulla and the elevation in blood pressure and heart rate (Lin et al., 2003). Intravenous infusion of tempol decreases blood pressure. These effects are mediated by inhibition of renal sympathetic nerve activity (Shokoji et al., 2003;Xu et al., 2002).Taken together, oxidative stress in the sympathetic nervous system increases blood pressure, which might result from an increase in sympathetic nerve activity.

7.3.2 Clinical hypertension

A few clinical studies are investigating the role of ROS, especially $O_2^{\bullet-}$, in the pathogenesis of human hypertension. The presence of increased systemic oxidative stress is proven in hypertensive children and adolescents, irrespective of their body mass index (BMI). It can be determined by measuring the plasma

levels of nitrites and nitrates, an indirect measure of available nitric oxide, and the redox status of the red blood cell glutathione, as a new oxidative stress parameter (Turi et al., 2003). Ang II receptor blockers and angiotensin converting enzyme (ACE) inhibitors limit oxidative reactions in vascular tissues by blocking the activation of NAD(P)H oxidases. These findings have led to the study showing that the Ang II type 1 receptor antagonist losartan, and the ACE inhibitor enalapril, significantly increase plasma glutathione levels and plasma nitrate levels, indicating a reduced level of oxidative stress in essential hypertensive patients after the treatment period (Donmez et al., 2002). These findings suggest that Ang II receptor blockers and ACE inhibitors have clinically important antioxidant effects beyond lowering blood pressure (Oparil et al., 2003).

8 Issues to be solved

Compelling evidence demonstrates a key role of ET-1 related mechanisms in animal models of experimental hypertension and essential hypertension in human subjects, particularly salt-sensitive forms of hypertension. The DOCA-salt rat model of experimental hypertension was chosen in this study. This model has two characteristics useful in the study of salt-sensitive hypertension. First, sympathetic nervous system activity is increased in this experimental hypertensive model (de Champlain, 1990). Second, an elevated level of ET-1 in this model, a potent vasoconstrictor and neurotransmitter (Damon, 1998;Milner et al., 2000a;Sullivan and Morton, 1996), is thought to contribute to the development of salt-sensitive hypertension (Millette et al., 2003;Schiffrin, 2001;Yu et al., 2002).

Clinical studies suggest that impaired neuronal norepinephrine uptake and the consequent increase in norepinephrine levels contribute to the vasoconstriction and pathogenesis of essential hypertension (Esler et al., 1980;Ferrier et al., 1993). *In vitro* functional studies showed that the activity of NET located on the sympathetic innervation to mesenteric veins of DOCA-salt hypertensive rats is elevated compared to Sham normotensive rats. Furthermore, the content of norepinephrine in mesenteric veins from DOCA-salt hypertensive rats is decreased (Luo et al., 2003), indicating that the NET may play a role in the mechanism of DOCA-salt hypertension. However, no research has been done to investigate the regulation of NET expression and function in sympathetic neurons in hypertension.

Hypertension is associated with elevated reactive oxygen species (ROS), especially superoxide anions ($O_2^{\cdot-}$) (Sedeek et al., 2003;Somers et al., 2000b). A recent study shows that ET-1 is able to evoke arterial $O_2^{\cdot-}$ production in DOCA-salt hypertensive rats via ET_A receptor/NAD(P)H oxidase pathway (Li et al., 2003). This increase is thought to be very important for the development of hypertension through several mechanisms (Griendling et al., 2000;Somers et al., 2000b). In the CNS, ROS are hypothesized to mediate some effects of neuroactive substances. But very little is known about the roles of ROS in the peripheral sympathetic nervous system in hypertension.

This study will investigate the effects of the neurohumoral factor ET-1 on sympathetic ganglia innervating the mesenteric circulation in DOCA-salt hypertensive rats and normotensive rats. A major goal is to determine if the

abnormally high ET-1 level in DOCA-salt hypertensive rats contribute to the etiology of hypertension (Figure 2).

This study consists of five specific aims.

Specific aim 1: Compare the NET message RNA levels and protein expression in the sympathetic and sensory innervation to mesenteric vasculature in DOCA-salt hypertensive and Sham normotensive rats.

Specific aim 2: Determine the effects of ET-1 on NET mRNA levels, protein expression and norepinephrine uptake function in differentiated PC-12 cells with sympathetic neuronal phenotype.

Specific aim 3: Determine whether $O_2^{\cdot-}$ is generated and elevated in sympathetic neurons of DOCA-salt hypertensive rats, whether $O_2^{\cdot-}$ production is due to an action of ET-1, and which ET-1 receptor subtypes may mediate the increase in $O_2^{\cdot-}$ production.

Specific aim 4: Determine whether NAD(P)H oxidase is present in sympathetic neurons, and whether $O_2^{\cdot-}$ production in sympathetic neurons is mediated by NAD(P)H oxidase. Determine the change of NAD(P)H oxidase activity in sympathetic ganglia in DOCA-salt hypertensive rats.

Specific aim 5: Determine whether ET-1 induced $O_2^{\cdot-}$ production in sympathetic neurons is mediated via NAD(P)H oxidase and the possible links connecting ET-1 with NAD(P)H oxidase activation.

Figure 2: Schematic summarizing fundamental issues to be solved in present study. In hypertension, norepinephrine clearance is elongated, plasma norepinephrine spillover is increased, and neuronal norepinephrine metabolite dihydroxyphenylglycol (DHPG) is decreased, which imply impaired neuronal norepinephrine uptake through norepinephrine transporter (NET). However, it is not clear in hypertension whether NET mRNA and protein levels are changed, or how NET is regulated. In addition, compelling evidence has shown that reactive oxygen species (ROS) are involved in the pathogenesis of hypertension. Superoxide anion ($O_2^{\cdot-}$) is one of the most important ROS and is pivotal in generating other ROS. In the central sympathetic neural control, $O_2^{\cdot-}$ is increased along with increased sympathetic nerve activity in hypertension. Antioxidant treatment decreases $O_2^{\cdot-}$ generation as well as decreased sympathetic nerve activity and blood pressure. However, it is unknown if $O_2^{\cdot-}$ is playing a role in the peripheral sympathetic nervous system in hypertension. In present study, NET mRNA and protein levels were examined in sympathetic and sensory innervation to mesenteric circulation in DOCA-salt hypertensive rats, as well as the regulation of NET mRNA, protein and function by ET-1 in differentiated PC-12 cells. In addition, $O_2^{\cdot-}$ levels were examined in sympathetic neurons in DOCA-salt hypertension, as well as ET-1 effects on $O_2^{\cdot-}$ generation in sympathetic neurons. Furthermore, possible underlying pathways for $O_2^{\cdot-}$ generation via NAD(P)H oxidase in sympathetic neurons were also investigated.

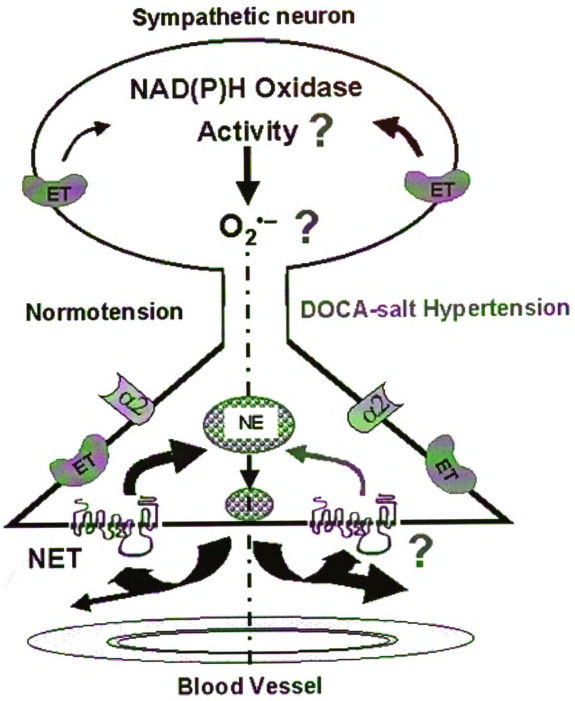
Sympathetic neuron
NAD(P)H Oxidase
Activity ?
ET
ET
$O_2^{\cdot-}$?
Normotension
DOCA-salt Hypertension
α2
α2
NE
ET
ET
NET
?
Blood Vessel

CHAPTER 2: REGULATION OF NOREPINEPHRINE TRANSPORTER

Introduction

In view of the demonstration of an elevated sympathetic drive coupled with an enhancement of vasomotor sympathetic modulation, sympathetic neurohumoral disturbances play a special role in essential hypertension. The defective neuronal norepinephrine uptake by norepinephrine transporter (NET) may be important in the pathogenesis of blood pressure elevation in some essential hypertensive patients (Esler et al., 1981). NET rapidly removes 90 percent of neuronally released norepinephrine from synaptic clefts; this reuptake back into nerve endings shortens the time of norepinephrine effects on adrenoceptors (Bonisch and Eiden, 1998;Eisenhofer, 1994). Compared to normotensive patients, there are increased norepinephrine spillover and longer plasma norepinephrine clearance in some essential hypertensive patients (Esler et al., 1980;Esler et al., 1981;Kimura et al., 1983;Takimoto and Weiner, 1981), which has been suggested to result from unsuccessful elimination of norepinephrine due to defective reuptake combined with increased sympathetic activity in essential hypertension (Takeshita et al., 1984;VanNess et al., 1999). Reduced norepinephrine reuptake increases the availability of norepinephrine for adrenergic receptors-mediated vasoconstriction, potentially leading to increased blood pressure. In contrast to this, some studies suggest a heightened activation of the adrenergic system in hypertension is accompanied by increased production of norepinephrine along with increased reuptake of norepinephrine from junctional clefts. For example, NET mRNA level is higher in brain regions

important for cardiovascular regulation including the rostral ventral lateral medulla (RVLM) and ventral medial hypothalamus (VMH) from spontaneously hypertensive rats (SHR) than from normotensive rats (Reja et al., 2002). Also, in mesenteric veins from DOCA-salt hypertensive rats, there is increased norepinephrine release and increased NET activity (Luo et al., 2003;Luo et al., 2004). However, the direct investigation of neuronal uptake of norepinephrine in blood vessels has been hampered by limitations of experimental technologies (Eisenhofer, 2001). Cloning of the human and rat NET (Bruss et al., 1997;Pacholczyk et al., 1991) opens the possibility of studying NET regulation from a molecular point of view in hypertension. So far, it is not clear if the expression or function of NET has been altered in hypertension.

We investigated NET expression in the sensory and sympathetic innervation to the splanchnic circulation, which is the largest single blood reservoir in the body. Its hemodynamic change is very important for cardiovascular homeostasis (Greenway, 1983b). Sympathetic and primary sensory nerves appear to provide a vasoconstrictor-vasodilator balance to blood vessels. The perivascular plexus of nerve terminals around mesenteric blood vessels contain the sympathetic postganglionic axon and primary sensory nerve terminals. The close association of sympathetic and sensory nerves provides an anatomical template for the interaction of these two types of nerves with one another, which is important for the integration and specification of neural control of mesenteric arteries and veins (Luff et al., 2000). The normal balance between sensory and sympathetic nervous system plays a very important role in the

maintenance of normal blood pressure (Wang et al., 2001).

DOCA-salt hypertensive rat, one of the established animal models to investigate the mechanisms of salt-sensitive hypertension in human due to salt retention and maintaining sympathetic hyperactivity (Iriuchijima et al., 1975;Reid et al., 1975;Takeda and Bunag, 1980), was used in present study. In DOCA-salt hypertension, there is an increased norepinephrine release from sympathetic nerves associated with mesenteric arteries and veins, resulting in the maintenance and/or increase in neurogenic constrictions (Luo et al., 2003). Preliminary studies from our laboratory showed the existence of NET mRNA in sensory neurons (Zheng et al., 2003). This study further examined NET mRNA and protein expression in sympathetic nerves, sensory nerves, and their regulatory effects on the sympathetic innervation to mesenteric arteries and veins.

Hypertension is a multifactorial disease. Alterations in many humoral factors that regulate hemodynamics under physiological conditions have been proposed to underlie the observed pathological changes accompanying the chronic increase in blood pressure (Oparil et al., 2003). Norepinephrine uptake can be regulated by many key factors related to blood pressure regulation, such as angiotensin II (Ang II) and endothelin-1 (ET-1). Both are increased in some essential hypertensive patients (Oparil et al., 2003). To date, the regulation of NET by Ang II has received the most attention (Lu et al., 1996;Sumners et al., 1985). The abnormal high plasma Ang II concentration in hypertensive animal models might possibly regulate NET expression or function *per se* (Endo et al.,

1977;Malik and Nasjletti, 1976). Acute and chronic exposure of brain neurons to Ang II upregulates NET mRNA and norepinephrine uptake and this upregulation is enhanced in SHR brain neurons (Lu et al., 1996).

ET-1, a potent vasoconstrictor originally discovered in endothelial cells (Yanagisawa et al., 1988b), is also present in sympathetic ganglia (Damon, 1999;Milner et al., 2000a), where it has multiple actions (Cao et al., 1993;Damon, 1999). The endothelin system is activated in salt-sensitive animal models of hypertension and hypertensives (Schiffrin, 2001), especially in DOCA-salt hypertension (Millette et al., 2003;Yu et al., 2002). ET-1 biological actions are mediated by two G-protein-coupled endothelin receptors, the ET_A and ET_B receptor (Mateo and de Artinano, 1997). The two receptors were believed to exist only on vascular tissues initially. Now they are known to be present on adrenal medulla chromaffin cells (Wilkes and Boarder, 1991a), the CNS, including neurons and glia (Hama et al., 1992;Sullivan and Morton, 1996), sympathetic ganglia (Damon, 1999), and the enteric nervous system (Nataf et al., 1996).

Rat pheochromocytoma PC-12 cells are derived from a rat catecholamine-secreting chromaffin tumor. They can differentiate to cells with a sympathetic neuronal phenotype after one week of nerve growth factor (NGF) treatment (Greene et al., 1998). Rat NET gene was first cloned from PC-12 cells (Bruss et al., 1997). PC-12 cells express NET in a high concentration and provide a useful system in which to study NET regulation and expression (Zhu and Ordway, 1997). ET receptors are present on PC-12 cells (Watanabe et al., 1997), and ET-1 significantly increases mRNA level and activity of tyrosine hydroxylase (TH),

the rate-limiting enzyme in catecholamine biosynthesis, in PC-12 cells, suggesting that ET-1 may modulate their function.

Furthermore, differentiated PC-12 cells were used to study the effects of ET-1 on the expression and function of NET in this study. We examined the effects of continuous exposure of differentiated PC-12 cells to different concentrations of ET-1 on NET mRNA levels, NET protein expression and the uptake.

Methods

Animals

All animal procedures were followed in accordance with the institutional guidelines of Michigan State University. DOCA-salt hypertensive rats were prepared as follows. Under sodium pentobarbital (50 mg/kg i.p.) anesthesia, male Sprague-Dawley rats (175-200g, Charles River Inc., Portage, MI) were uninephrectomized and deoxycorticosterone acetate (DOCA, 200 mg kg^{-1}) pellet was implanted subcutaneously. Postoperatively, the rats were given a solution of 1% NaCl and 0.2% KCl in the drinking water. Sham normotensive rats were uninephrectomized, received no DOCA and drank normal tap water. Rats were housed in temperature- and humidity-controlled rooms with a 12 h on/12 h off light cycle. Pellet rat chow and water were given *ad libitum*. Four weeks after surgery, the arterial blood pressure was measured using the tail cuff method. Rats with a mean arterial pressure of > 150 mmHg were considered hypertensive. The mean arterial pressures for the DOCA-salt and Sham rats are 122.9±2.1mmHg and 196.5±4.5mmHg respectively (n=36).

Tissue harvest

Rats were sacrificed with a lethal dose of sodium pentobarbital (65 mg/kg, i.p.). Celiac ganglia, dorsal root ganglia (DRG, spinal levels T13-L2, innervating colon, pelvic organs and mesenteric vasculature) (Baron and Janig, 1991), and mesenteric arteries and veins were dissected from rats. Crude preparation of mesenteric arteries and veins included smooth muscle cells, endothelial cells and the sympathetic and sensory nerve terminals around the blood vessels. Tissues of each type were placed into Hank's balanced salt solution (HBSS) plus HEPES (Invitrogen) and cleaned of fat and connective tissue. For RNA isolation, tissues were immediately placed in a tube containing RNAlater® (Ambion). For western blotting, the tissues were stored directly at –80°C.

Cell culture and drug exposure

Rat pheochromocytoma PC-12 cells were obtained from American Type Culture Collection (ATCC), and maintained in RPMI 1640 medium (Invitrogen) supplemented with 10% heat inactivated horse serum, 5% fetal bovine serum, 100U/ml penicillin, 100μg/ml streptomycin, and 0.25μg/ml Fungizone. Culture was performed at 37°C in a 95% humidified air with 5% CO_2 incubator. The cells were passaged once every four days when they had reached confluence. Feeding medium was changed every 2-3 days. PC-12 cells were cultured with 50ng/ml NGF 2.5 S (Chemicon) for one week and differentiated to cells with sympathetic neuronal phenotype (Greene et al., 1998). Drug exposure began after the cells were differentiated. Cells were cultured in the feeding media with 10, or 30 or 100nM ET-1 (Peninsula Laboratories Inc.) from 30 minutes to seven

days. Media were refreshed daily in all cases. Cells were washed with phosphorylate balanced salt solution (PBS) before harvesting for RNA isolation and western blotting. Cells were harvested and stored in TRIzol® at -80°C for RNA isolation or stored directly at -80°C for protein extraction later.

RNA isolation

Total RNA was isolated using the standard TRIzol® procedure (GIBCO Life Technologies). The RNA pellet was dried for 10 minutes, resuspended in 0.1% (v/v) diethyl pyrocarbonate (DEPC) treated water with 1μl RNase inhibitor (Roche) and RNA carrier polyinosinic acid (3μg) (Winslow and Henkart, 1991), and stored at -80°C. The concentration/purity/integrity of RNA was ascertained spectrophotometrically (A_{260}/A_{280}). To eliminate residual genomic DNA in the preparation, total RNA samples were treated with RNase-free DNase I (10U/μl) for 10 minutes at 37°C, and DNase I was inactivated by heating for 10 minutes at 75°C.

Reverse transcription polymerase chain reaction (RT-PCR)

A two-step RT–PCR was performed. The first strand complimentary DNA (cDNA) was synthesized by adding the following components into a nuclease-free microcentrifuge tube in a final 20 μl reaction volume: 1 μl $Oligo(dT)_{12-18}$ (500 μg/ml) (Invitrogen), 2μg total RNA, 1μl 10mM dATP, dGTP, dCTP and dTTP (dNTP) mix (Invitrogen), 4 μl 5 x first strand buffer, 2 μl 0.1 M DTT (dithiothreitol), 1μl RNase inhibitor (Roche), and 1μl Superscript II RNase H^- reverse transcriptase (Invitrogen). Samples were mixed, incubated at 42°C for 60 minutes, and inactivated by heating at 70°C for 15 minutes.

NET primers were derived from the *Rattus Norvegicus* NET gene (National Center for Biotechnology Information (NCBI) GenBank). Primers were developed using Primer3 software (Massachusetts Institute of Technology, 2003) to generate several possible primer pairs. A NCBI basic local alignment search tool (BLAST) search ensured the specificity of primer sequences for rat NET and the primers were synthesized at the Macromolecular Structure, Sequencing and Synthesis Facility at Michigan State University. Three primer pairs were designed in this study because of different requirements for sequencing, real-time RT-PCR and regular PCR. Predicted sequences of PCR amplification products were aligned with other rat sequences in GenBank to examine the stringency. Primer sequences are shown in Table 1.

Table 2.1: Primer sequences for NET, β-actin and GAPDH.

	Sequence	Amplicon Length (bp)	NCBI accession number
Regular PCR for NET	For:5' TCC TCA TTG CCC TCT ATG TTG 3'	203	Y13223
	Rev:5' CGG TGT GAA CTT GTA TTT GGA G 3'		
Real-time PCR for NET	For:5' GCC TGA TGG TCG TTA TCG TT 3'	123	Y13223
	Rev:5' CAT GAA CCA GGA GCA CAA AG 3'		
Sequencing for NET	For:5' GGT GCC TTC CTG ATT CCA T 3'	241	Y13223
	Rev:5' GCA CCT TCA AGG TGA AGG A 3'		
PCR for β-actin (Epperson et al., 2000)	For:5' GGC TAC AGC TTC ACC ACC AC 3'	500	V01217
	Rev:5' TAC TCC TGC TTG CTG ATC CAC 3'		
Real-time PCR for GAPDH	Purchased from Applied Biosystems	177	XM_237274

A 50 μl PCR reaction volume was prepared with 2 μl cDNA from the first-strand reaction, 5 μl 10x PCR buffer, 3 μl 25 mM $MgCl_2$, 1 μl 10 mM dNTP mix, 0.5μl forward primer (20 mM), 0.5 μl reverse primer (20 mM), 0.25 Taq DNA polymerase (Invitrogen) (5U/μl), and 37.25μl DEPC-treated distilled water. Amplification was performed as follows: pre-PCR denaturation at 94°C for 5 minutes, followed by 40 cycles of: denaturation at 94°C for 60 seconds, annealing at 60°C for 60 seconds, and elongation at 72°C for 90 seconds. This was followed by a final elongation step at 72°C for 7 minutes. PCR products were analyzed on 1.5% (w/v) agarose gel in 1x TAE buffer (2.42g Tris, 0.57ml glacial acetic acid, 0.37g EDTA-sodium) containing 0.5μg/ml of ethidium bromide. A 100bp DNA ladder was loaded on the gel to measure the length of RT-PCR products. Gels were visualized under UV light using a Bio-Rad Fluor-S Ethidium Bromide gel scanner. Samples from Sham and DOCA-salt tissues were run in parallel. In all cDNA preparations, RT-PCR for β-actin (Epperson et al., 2000) was also performed as an internal positive control to assure even loading and no genomic DNA contamination in each sample. The primers were designed to span a region of β-actin gene that encodes an intron. If the sample mRNA was contaminated with genomic DNA, a 700 bp PCR product would be detected. In addition, no cDNA template control (NTC) was also performed as the negative control.

Sequencing

For sequencing, PCR amplicons were run on the low melting temperature agarose gel. The positive bands with predicted size were extracted from the gel using QIAquick Gel Extraction Kit (Qiagen) and further purified free of primers,

nucleotides, enzymes, salts, agarose, ethidium bromide, and other impurities from DNA samples using QIAquick PCR Purification Kit (Qiagen). The concentrations of purified DNA amplicons were determined spectrophotometrically. The identities of amplicons were confirmed by sequencing the mixture of 20ng DNA amplicon and 30 picomoles forward PCR primer (or reverse PCR primer) on an ABIPRISM® 3100 Genetic Analyzer (Applied Biosystems) at the Genomic Technology Support Facility (GTSF) at Michigan State University.

Relative quantification of gene expression using real-time PCR

Real-time PCR was performed to compare the relative quantities of NET mRNA in tissues and cells. Quantitative real-time PCR was performed using an iCycler® Real Time PCR thermal cycler (Bio-Rad). One-tenth of the first strand cDNA was taken through the reaction system with 12.5μl SYBR® Green Master Mix (Applied Biosystems), 1μl forward and reverse primers (10μM) and DEPC treated distilled water. Amplification was performed as follows: pre-PCR denaturation at 94°C for 10 minutes, followed by 40 cycles of: denaturation at 94°C for 15 seconds, annealing and elongation at 60°C for 60 seconds. A dissociation protocol (60-95°C melt) was performed at the end of the experiment to verify that only one amplicon was formed during the process of amplification.

Primers were optimized and validated by calculating the efficiency of primer sets for NET and glyceraldehyde-3-phosphate dehydrogenase (GAPDH), an internal control calibrator reference. Triplicates for a 10x dilution series (1:1, 1:10, 1:100 and 1:1000) of cDNA from 4μg total RNA were performed. In terms of

generating amplification plots in serially diluted cDNA samples (Bio-Rad Laboratories, 2001), the efficiency (E) of primers was calculated using the formula $E=(10^{-1/slope})-1$ and a reaction with 100% efficiency generates a slope of –3.32. Only the primers for NET, which had the identical efficiency as primers for GAPDH, were used. Samples for the target gene were run in parallel with samples for GAPDH. Samples without cDNA were also taken along as no template controls (NTC).

SYBR green was used as the fluorescence detector in the quantitative real-time PCR. SYBR green intercalates into the minor groove of double stranded DNA, therefore the dissociation protocol (60-95°C melting temperature) was performed at the end of experiments to verify the specific amplification in which one product was present and melted at the appropriate temperature. In addition, PCR products were run on the 2% Tris-acetate-EDTA (TAE) agarose gel to confirm that the correct sizes of amplicons were present.

Western blotting

Tissues or cells were homogenized in a 15 ml tissue grinder (PYREX®) containing 11 ml of homogenization buffer [10mM Hepes (Sigma), 0.15M NaCl (VWR), 1mM EDTA (Sigma), 1mM phenol methane sulfanyl fluoride (PMSF, Roche), 1μg/ml leupeptin (Roche), and 1μg/ml aprotinin (Roche)] and centrifuged (Sorvall RC 5B Plus) at 2500*xg* for 15 minutes at 4°C. The pellet which contained the nuclear and cell debris were discarded and the supernatant was centrifuged at 100,000*xg* for one hour at 4°C to obtain the membrane protein pellet, which was resuspended in homogenization buffer and stored at -80°C. Protein

concentrations were determined using the Lowry method (Lowry et al., 1951). Proteins were resolved by polyacrylamide gel electrophoresis (PAGE). Samples containing 45μg protein were prepared, loaded into 4% stacking gel/ 10% resolving gels with 5X Laimlee buffer and run at 90 V for 90 minutes until the leading edge of samples traveled to the bottom of gel. The gel was transferred to the polyvinylidene fluoride (PVDF) membrane (Bio-Rad) at a constant voltage of 100 V, 250mA at 4°C for 60 minutes. The membrane was blocked with 4% non-fat dry milk in PBS containing 0.1% Tween 20 (Sigma) for one hour, and incubated overnight at 4°C with the primary antibody rabbit anti-rat NET (Chemicon, Temecula, CA) diluted as 1:2000 in 4% milk solution. The membrane was rinsed with PBS containing 0.1% Tween 20 and incubated for one hour at 4°C into the secondary antibody conjugated with anti-rabbit IgG horseradish peroxidase (HRP) (Santa Cruz Biotech) diluted 1:2000 in 4% milk solution. Immunoreactivity was detected using a chemiluminescence kit (Pierce) to visualize bands. The membrane was exposed to Kodak Biomax Light scientific imaging film (Kodak). The film was scanned and quantified using ImagePro (Media Cybernetics, Inc.). Membranes were stained with Coomassie Blue (Invitrogen) to verify equal protein loading. To verify the specificity of antibody binding, the primary antibody was incubated with the control peptide prior to application to the membrane. The absence of bands at 54 KD confirmed the specificity of the antibody for NET protein.

NET function measurement: ASP^+ uptake assay

Differentiated PC-12 cells were plated on poly-L-lysine coated Costar® 24-

well tissue culture dishes at $2x10^5$ cells per well prior to performing transport function assay. The medium was removed by aspiration. Cells were then preincubated for 10 minutes in Kreb's-Hepes (KH) buffer. The fluorescence probe 4-(4-(dimethylamino)styryl)-*N*- methylpyridinium iodide (ASP+, 10μM(4-Di-1-ASP)) (Schwartz et al., 2002) was used as a substrate for NET in KH solution (pH 7.4, 320 mOsm) throughout the experiments. ASP^+ is an analogue of 1-methyl-4-phenylpyridinium (MPP^+) which can be accumulated by monoamine transporters without producing neurotoxicity (Paczkowski et al., 2002;Peter et al., 1996;Smith and Levi, 1999). Trypan blue (30μM) was added to the dishes with ASP^+ (10 μM) to quench unbound extracellular ASP^+ (Scott and Woods, 2000;Van Amersfoort and Van Strijp, 1994). Cells pre-incubated with the selective NET blocker desipramine (DMI, 30nM) were taken as the control group to measure the DMI sensitive ASP+ uptake. The fluorescence intensities were normalized to DMI treated cells. The cells were incubated with ASP+ (10nM) for 30 minutes and the ASP+ fluorescent signal was measured with a Biotek FL600 fluorescence plate reader (Bio-Tek Instruments, Inc., Winooski, Vermont). The fluorescent signal was detected using excitation filter of 485±40nm and emission filter of 590±35nm.

Data analysis

Data were presented as mean ± standard error of the mean for the number of animals or cell groups. For real-time PCR, relative amounts of mRNA were compared by determining the number of cycles when reaching a critical threshold (C_T). C_T values were derived as the threshold cycle at which the

product was first detected and were reported as cycle numbers. The threshold was normalized to the endogenous reference GAPDH and the relative quantification value was expressed as the following formula: $= 2^{-(S\Delta C_T - C\Delta C_T)}$. When there is no difference in the amount of mRNA between the two samples, the relative quantitative value is 1(Applied Biosystems, 1998). All data from Sham and DOCA blood vessels were normalized to those from Sham arteries and all data from DOCA ganglia were normalized to those from Sham ganglia. All data from cell groups were normalized to the no treatment control groups. For western blotting of tissues, the changes in the NET protein levels in blood vessels were determined by the ratio of optical densities of bands from blood vessels to those from Sham mesenteric arteries, and the changes in the NET protein levels in DOCA ganglia were determined by the ratio of optical densities of bands from DOCA-salt ganglia to those from Sham ganglia. For western blotting of cells, the changes in NET protein levels were determined by the ratio of total pixel intensities of bands from treated groups to those from no treatment control group. For uptake study, the percentage of change in uptake was obtained by comparing the uptake from the treatment groups to that of the no treatment group. Statistical significance was assessed using the non-parametric Mann-Whitney test in Prism version 3.0 (GraphPad Software, San Diego CA), with $P<0.05$ taken as a level of statistical significance.

Results

RT-PCR analysis of NET mRNA levels in mesenteric arteries and mesenteric veins, celiac ganglia and DRG from Sham and DOCA-

hypertensive rats

RT-PCR was performed using specific primers for rat NET in tissues of mesenteric arteries, mesenteric veins, celiac sympathetic ganglia and DRG from Sham and DOCA-salt hypertensive rats. The amplicons for NET were detected in all four tissues from Sham and DOCA-salt hypertensive rats at the expected size of 203 bp, as well as β-actin of 500 bp (Figure 3). The band intensities of PCR amplicons for β-actin from all tissues were equal, which means that the same amount of mRNA was loaded in each sample. The band intensities of PCR amplicons for NET of mesenteric arteries and veins and celiac ganglia from DOCA rats were higher than those from Sham rats. However, the band intensity of PCR amplicon of DRG from DOCA rats was lower than that from Sham rats (Figure 3). These results indicate that NET was expressed in harvested tissues of mesenteric arteries, mesenteric veins, and their innervating sympathetic celiac ganglia and sensory DRG. There was higher NET mRNA expression in mesenteric arteries, mesenteric veins and celiac ganglia, but not in DRG, from DOCA-salt hypertensive rats when compared to those from Sham rats.

Sequencing of PCR amplicon

The amplicon from PCR for NET was sent to the GTSF to be sequenced directly. The detected sequence of PCR amplicon was aligned in GenBank and the nucleotide sequence of PCR amplicon for NET was identical to the predicted amplification part of rat NET GenBank sequence (Accession number: Y13223). Out of 209 identified nucleotides, 207 of them (99%) matched the published sequences (Figure 4). This verifies the stringency of PCR amplification in the

Figure 3: Reverse transcription polymerase chain reaction (RT-PCR) for NET and β-actin in RNA extracts of mesenteric arteries (MA), mesenteric veins (MV), celiac ganglia (CG) and dorsal root ganglia (DRG) from Sham normotensive rats and DOCA-salt hypertensive rats. RT-PCR for β-actin was used as the internal control, which showed the same amount of mRNA in each sample. Representative 1.5% agarose gel images from three preparations: Upper panel: NET with an expected size of 203bp; lower panel: β-actin with an expected size of 500bp.

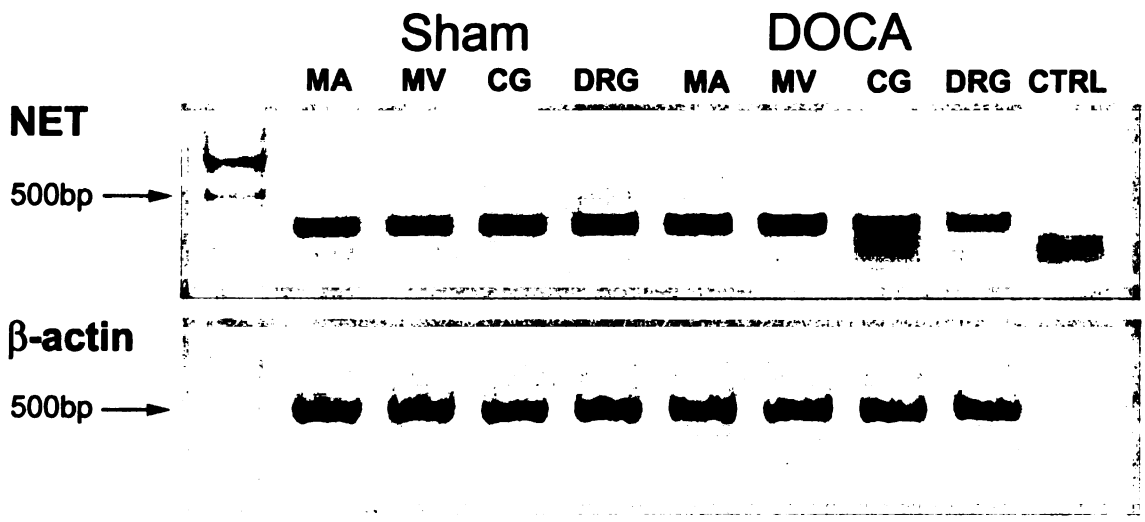
Sham
DOCA
MA
MV
CG
DRG
MA
MV
CG
DRG
CTRL
NET
500bp
β-actin
500bp

Figure 4: The comparison of the sequenced result of RT-PCR amplicon to the expected RT-PCR amplicon sequence. The RT-PCR amplicon sequence was blasted in GenBank with the published rat NET sequence (Y13223). Out of 209 identified nucleotides, 207 of them (99%) matched the published sequence. The asterisks indicate the misamplified nucleotides.

```
                     *           *
Query: 4   catcattgctggtatgcctctgttctacatggagctggctctggggcagttcaaccggga 63
           |||||||||||| |||||||||| ||||||||||||||||||||||||||||||||||||
Sbjct: 306 catcattgctgggatgcctctgttttacatggagctggctctggggcagttcaaccggga 365

Query: 64  gggggcagccacagtgtggaagatctgccctttcttcaaaggagtgggctatgctgtgat 123
           ||||||||||||||||||||||||||||||||||||||||||||||||||||||||||||
Sbjct: 366 gggggcagccacagtgtggaagatctgccctttcttcaaaggagtgggctatgctgtgat 425

Query: 124 cctcattgccctctatgttggcttttactacaatgtcatcattgcctggtcactgtacta 183
           ||||||||||||||||||||||||||||||||||||||||||||||||||||||||||||
Sbjct: 426 cctcattgccctctatgttggcttttactacaatgtcatcattgcctggtcactgtacta 485

Query: 184 cctcttcgcgtccttcaccttgaacctgc 212
           |||||||||||||||||||||||||||||
Sbjct: 486 cctcttcgcgtccttcaccttgaacctgc 514
```

present study and further demonstrates the existence of rat NET mRNA in mesenteric arteries, mesenteric veins, CG and DRG.

Validation and optimization of primers

Primers used in real-time PCR for NET and the internal control gene GAPDH were validated and the efficiencies of primers were calculated. The real-time PCR amplification plots demonstrate that the amplification curves of NET or GAPDH, which were amplified in serial dilutions of cDNA (1:1, 1:10, 1:100 and 1:1000), were parallel during the phase of exponential amplification (Figure 5A and 2.3B) and the iCycler® software automatically calculated the threshold of relative fluorescence unit (RFU) value. The cycle number at the threshold (C_T) was determined when the fluorescence intensity reached the threshold number. The difference in C_T between adjacent curves was the slope of the plot of log input amount of cDNA to the C_T (Figure 5C) and the plots for NET and GAPDH were parallel. PCR amplification plots using primers for NET generated a slope of –3.53 or 91.9% efficiency, with a correlation coefficient of 0.9938 (Figure 5C). The PCR amplification plots using primers for GAPDH generated a slope of –3.74 or 85.1% efficiency, with a correlation coefficient of 0.996 (Figure 5C). The efficiency difference between these two primers was 6.8%. Values less than a 10% difference are generally acceptable (Bio-Rad Laboratories, 2002). The dissociation curves for NET and GAPDH are shown in Figure 5D (with cDNA) and 3E (no cDNA template control). Only one peak occurred in each curve in Figure 5D when the cDNA was present and there was no peak present in the absence of cDNA of curves in Figure 5E. These results demonstrate that only

Figure 5: Validation and optimization of real-time PCR primers for NET and GAPDH. A and B: Representative real-time PCR amplification plots demonstrating that the amplification curves for NET (A) and GAPDH (B) in serial dilutions of cDNA (1:1, 1:10, 1:100, 1:1000) from 4ug total RNA of differentiated PC-12 cells were parallel and the difference between the cycle number at the threshold (C_T) from the adjacent two curves was equal. C: Plots of the log of dilution factor of input amount of cDNA to C_T demonstrating that the primers for NET and GAPDH have similar efficiencies. The plot of input amount of cDNA to threshold cycle number was generated from panel A and B. The linear regression curves for norepinephrine transporter and GAPDH are y=-3.465x+38.075 (R^2=0.9938), with the efficiency of 91%, and y=-3.74x+36.75 (R^2=0.996), with the efficiency of 85%, respectively. D and E: Dissociation curves of samples with cDNA (D) and with no cDNA (no template control, NTC) (E) representing by the derivative d(fluorescence intensity) / d(Temperature) (df/dT) plotted against the temperature. Each pair of primers showed its characteristic peak. Only one peak was shown in each curve in samples with cDNA (D) representing the presence of only one amplification product. No peak was shown in curves in samples with NTC (E) representing no amplification product formation. F: A 2% TAE agarose gel stained with ethidium bromide showing the PCR amplicons from NET (123bp) and GAPDH (177bp). Only one band was shown in each lane, representing only one amplification product formation and no primer-dimer existence

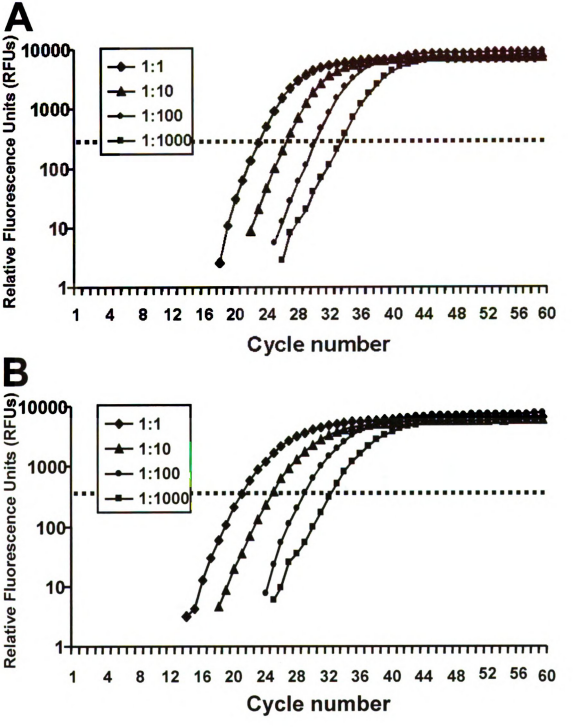
A
Relative Fluorescence Units (RFUs)
10000
1000
100
10
1
1:1
1:10
1:100
1:1000
1 4 8 12 16 20 24 28 32 36 40 44 48 52 56 60
Cycle number
B
Relative Fluorescence Units (RFUs)
10000
1000
100
10
1
1:1
1:10
1:100
1:1000
1 4 8 12 16 20 24 28 32 36 40 44 48 52 56 60
Cycle number

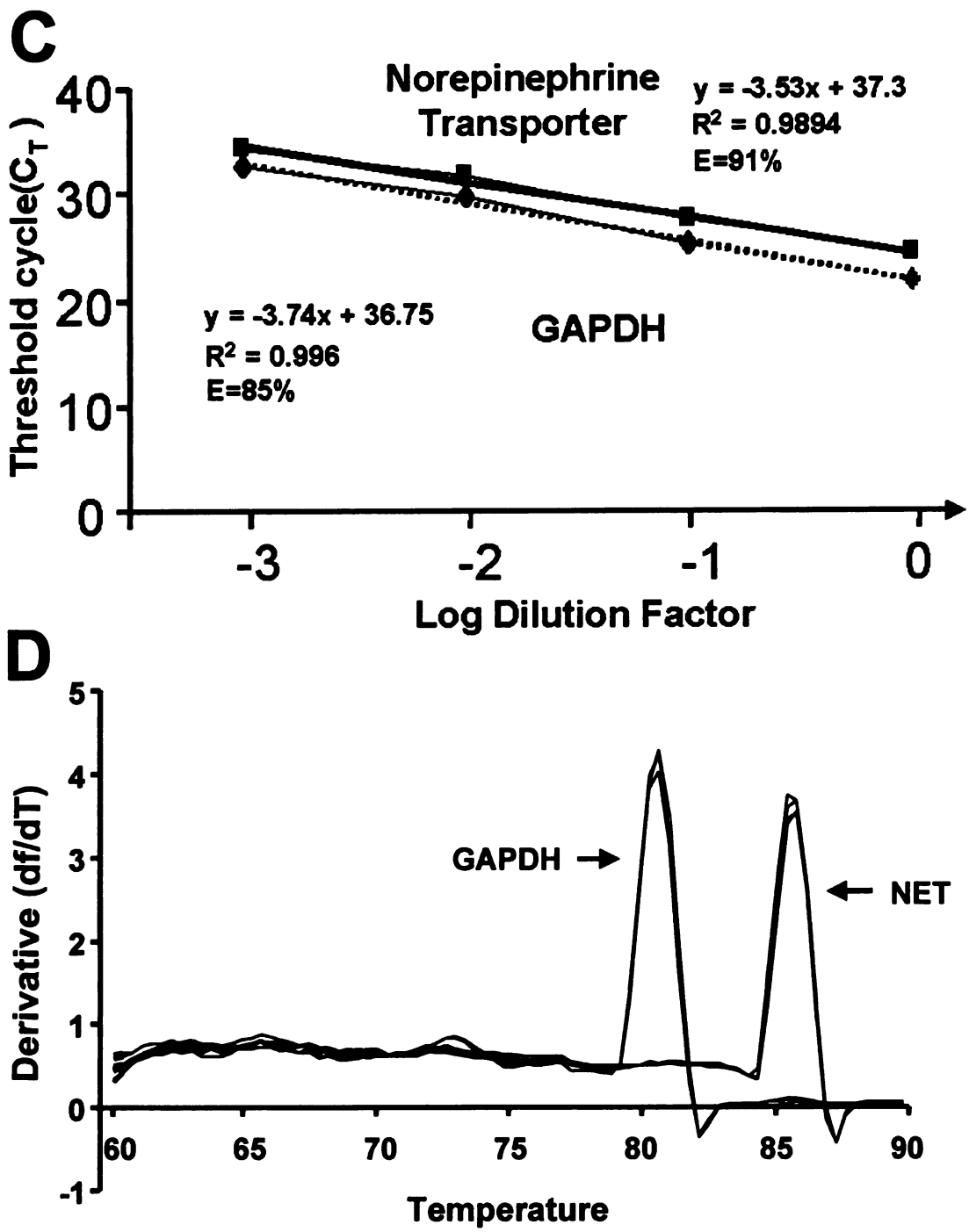
C
Norepinephrine Transporter
y = -3.53x + 37.3
R2 = 0.9894
E=91%
y = -3.74x + 36.75
R2 = 0.996
E=85%
GAPDH
Threshold cycle(CT)
40
30
20
10
0
-3
-2
-1
0
Log Dilution Factor
D
Derivative (df/dT)
5
4
3
2
1
0
-1
GAPDH
NET
60
65
70
75
80
85
90
Temperature

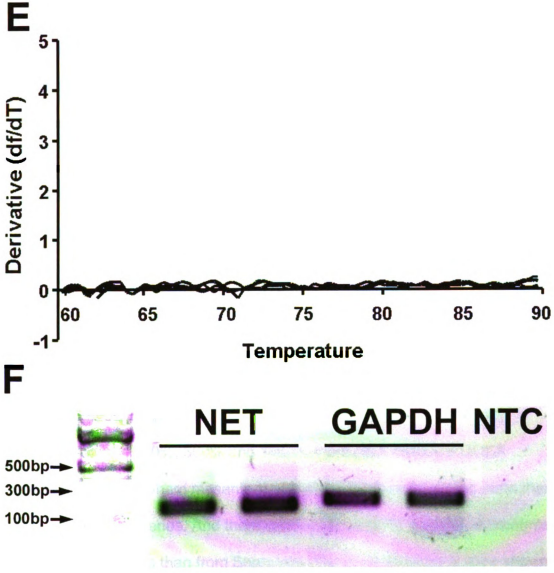
E
Derivative (df/dT)
5
4
3
2
1
0
-1
60
65
70
75
80
85
90
Temperature
F
NET
GAPDH
NTC
500bp
300bp
100bp

one amplicon was formed. Furthermore, no genomic DNA and/or the existence of a primer-dimer contamination was seen in any samples. Therefore, the increased SYBR green fluorescence intensity associated with the amplification process only represented formation of PCR amplicons. The agarose gel images shown in Figure 5F demonstrate that the correct band sizes of amplicons were present, which were 123 bp for NET and 177 bp for GAPDH, respectively. There was no existence of a primer-dimer band, further implying the good qualities of primers. Optimized and validated primers for real-time PCR of NET and GAPDH were used in this study.

Quantification of NET mRNA levels in mesenteric arteries and mesenteric veins, celiac ganglia and DRG from Sham and DOCA-hypertensive rats using real-time PCR

NET mRNA levels in tissues of mesenteric arteries, mesenteric veins, celiac ganglia and DRG from Sham normotensive rats and DOCA-salt hypertensive rats were quantified by quantitative real-time PCR analysis using optimized primers (Figure 6).

There were 150%, 300% and 1400% more NET mRNA in DOCA mesenteric arteries, Sham mesenteric veins and DOCA mesenteric veins than in Sham mesenteric arteries. And there was 248% more NET mRNA in mesenteric veins from DOCA rats than from Sham rats. These upregulations were shown in the relative quantification values of 1, 2.5±0.45, 4.0±0.72, and 15.5±3.30 in Sham mesenteric arteries, DOCA mesenteric arteries, Sham mesenteric veins and DOCA mesenteric veins, respectively (Figure 6A).

Figure 6: Real-time RT-PCR for NET and GAPDH in RNA extracts of mesenteric arteries and veins (A), sympathetic celiac ganglia (CG) (B) and dorsal root ganglia (DRG) (C) from Sham normotensive rats and DOCA-salt hypertensive rats. GAPDH was used as an internal control. n=5; $P<0.05$ indicating the significance. #: versus Sham arteries; @ versus DOCA arteries; X versus Sham veins; * versus Sham CG; & versus Sham DRG.

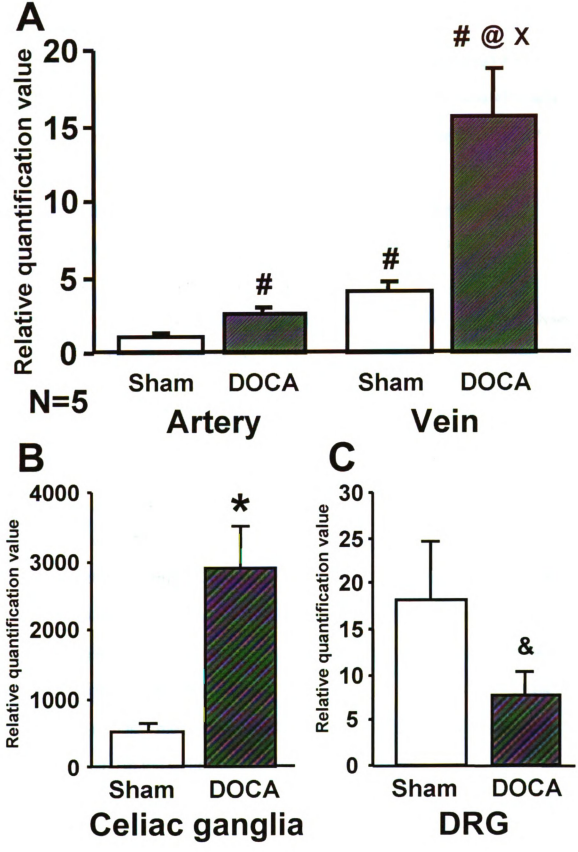
A
Relative quantification value
20
15
10
5
0
#
#
@ x
Sham
DOCA
Sham
DOCA
N=5
Artery
Vein
B
Relative quantification value
4000
3000
2000
1000
0
*
Sham
DOCA
Celiac ganglia
C
Relative quantification value
30
25
20
15
10
5
0
&
Sham
DOCA
DRG

There was 453% more NET mRNA in celiac ganglia from DOCA-salt hypertensive rats than from Sham rats. This upregulation is reflected in the relative quantification value of 523±115.1 for Sham rats and 2895±593.8 for DOCA rats (Figure 6B). In contrast, the NET mRNA level in DRG was 42% less in DOCA rats than it from Sham rats, with the relative quantification values of 18±6.3 in Sham rats and 7.7±2.57 in rats (Figure 6C).

Detecting NET protein expression in mesenteric arteries and mesenteric veins, celiac ganglia and DRG from Sham and DOCA-hypertensive rats using western blotting

The protein expression of NET was examined by western blotting analysis using a polyclonal antibody detected against amino acids 185 to 206 on the second extracellular loop of the NET. A single band reacting with anti-NET antibody was observed at 54KD in the membrane fractions of mesenteric arteries, mesenteric veins, celiac ganglia and DRG from DOCA-salt hypertensive and Sham rats (Figure 7A).

There were 51% and 33% more NET protein in mesenteric arteries and veins, respectively, from DOCA rats than them from Sham rats (Figure 7B). And there were 64.8% and 65.2% less NET protein expression in mesenteric veins than in mesenteric arteries from DOCA rats and Sham rats, respectively (Figure 7C). These changes were represented by 151±18.1%, 35±2.6% and 53±2.0% NET protein in DOCA mesenteric arteries, Sham mesenteric veins and DOCA mesenteric veins of the values in Sham arteries (Figure 7B).

Figure 7: Western immunoblotting for NET in mesenteric arteries, mesenteric veins and sympathetic celiac ganglia (CG) and sensory DRG of Sham and DOCA-hypertensive rats. (A) Representative immunoblot showing a 54 KDa band for NET in membrane enriched extracts from mesenteric arteries, mesenteric veins, CG, and DRG of Sham normotensive and DOCA-hypertensive rats. Proteins from Sham and DOCA rats of each tissue were always run on the same gel and Coomassie Blue staining was used to verify equal protein loading of all lanes (not shown). B) Comparison of changes in band densities for NET in arteries, veins, CG and DRG. For blood vessels, the density is represented as a percentage change compared to Sham arteries. For CG or DRG, the density is represented as a percentage change compared to Sham CG or DRG. (n=4; $P<0.05$ indicating significance; #: versus Sham arteries; @ versus DOCA arteries; X versus Sham veins; * versus Sham CG; & versus Sham DRG.) C) Comparison of changes in band densities for NET in arteries and veins and the density is represented as a percentage changes compared to arteries from DOCA and Sham rats. Asterisks indicate significant change compared to arteries.

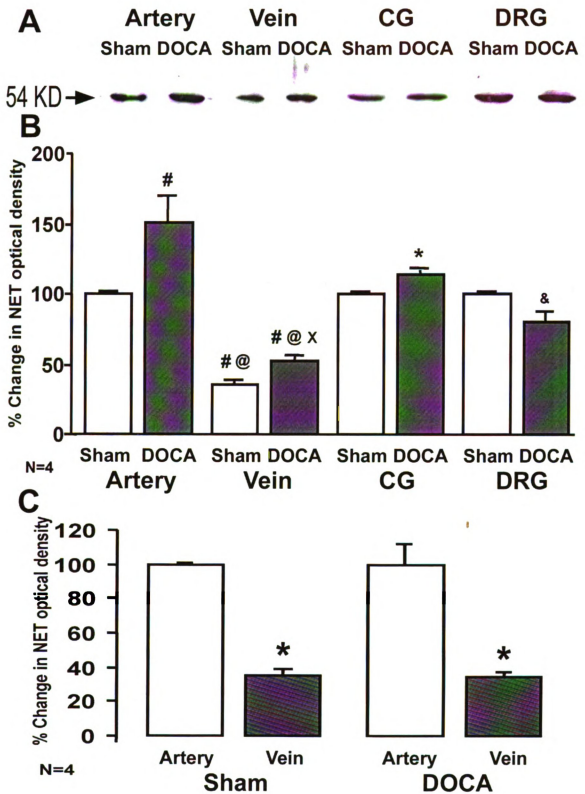
A
Artery
Vein
CG
DRG
Sham DOCA Sham DOCA Sham DOCA Sham DOCA
54 KD
B
% Change in NET optical density
200
150
100
50
0
#
#@
#@ x
*
&
Sham DOCA Sham DOCA Sham DOCA Sham DOCA
N=4
Artery
Vein
CG
DRG
C
% Change in NET optical density
120
100
80
60
40
20
0
*
*
Artery Vein Artery Vein
N=4
Sham
DOCA

There was more NET protein in sympathetic celiac ganglia from DOCA-salt hypertensive rats than from Sham rats. However, there was less NET protein in DRG from DOCA rats than from Sham rats. The NET protein expression level in DOCA sympathetic celiac ganglia was 14±3.5% higher than in the comparable tissues of Sham-operated control and NET protein expression level in DRG of DOCA-salt hypertensive rats was 20% less than that of Sham rats (Figure 7B).

Finally, there was much less NET protein in mesenteric blood vessels than in sympathetic and sensory ganglia. A much longer exposure time of PVDF membranes to X-ray films was needed for samples of blood vessels compared to samples of ganglia in western blotting in order to detect the positive bands of NET protein and achieve the bands with relatively similar optical intensities (Data not shown).

Cells morphology

Morphology of cells treated with ET-1 was checked and no gross morphological changes in drug-treated cells were observed. In addition, the amount of total protein in wells of ET-1 treated groups and control groups was measured and there was no difference between drug-treated and drug-free cells in terms of total protein of cells per well at any time points (data were not shown.). It was concluded from these findings that the drug exposure was not toxic to cells and all data were normalized to the no treatment control group. In another study, undifferentiated PC-12 cells are exposed to ET-1 at up to a concentration of 1μM from 10 minutes to one day and no toxic effect is reported (Takekoshi et al., 2002).

Effects of ET-1 on NET mRNA levels in differentiated PC-12 cells

The effects of a seven day exposure of differentiated PC-12 cells to ET-1 (10, 30 and 100nM) on the relative levels of NET mRNA were evaluated and a two-phase change in NET mRNA levels was observed (Figure 8). All three concentrations produced a similar decrease in NET mRNA in the first 12 hours, followed by a return to the control level as early as 24 hours in 30nM and 100nM ET-1 treatment groups, and an increase at 7 days treatment in all three concentrations groups.

NET mRNA levels in cells treated with 10nM ET-1 were 52±11.9, 38±11.4, 56±18.3, 41±14.3 and 48±13.0% of the control (ET-1 treatment for 0 hour) at 0.5, 2, 12, 24 and 48 hours, respectively (Figure 8). This was followed by an increase in NET mRNA level at 7 days (750±180% of the control) (Figure 8). NET mRNA levels in cells treated with 30nM ET-1 were 30±12.8, 50±11.9, 50±13.8% of the control at 0.5, 2, and 12 hours respectively (Figure 8). This was followed by a return to control levels at 24 and 48 hours (59±20.0 and 235±179.4% of the control, respectively), and an increase at 7 days (660±193.3% of the control) (Figure 8). NET mRNA levels in cells treated with 100nM ET-1 were 43±11.6, 39±7.6, 49±15.0% of the control at 0.5, 2, and 12 hours, respectively (Figure 8). This was followed by a return to the control level at 24 and 48 hours (92±42.6 and 216±130.3% of the control, respectively), and an increase at 7 days (750±122.5% of the control) (Figure 8).

Effects of ET-1 on the plasma membrane NET protein expression in differentiated PC-12 cells

Figure 8: Quantitative real-time RT-PCR for NET in cells treated with ET-1 (10, 30 and 100nM) for 30 minutes to 7 days. Data are represented by the percentage change to the no treatment control group. $p<0.05$ indicating significance. * Significant difference in all three groups; # Significant difference in 10 nM group; @ Significant difference in 30 and 100nM groups (n=4).

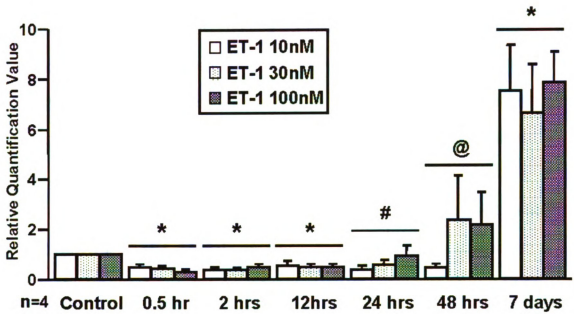
Relative Quantification Value
10
8
6
4
2
0
ET-1 10nM
ET-1 30nM
ET-1 100nM
*
*
*
#
@
*
n=4
Control
0.5 hr
2 hrs
12hrs
24 hrs
48 hrs
7 days

Treatment of differentiated PC-12 cells with ET-1 (10, 30 and 100nM) also produced two phases of changes in the plasma membrane NET protein expression. Western blotting revealed a 54 KD band recognized by the NET antibody (Figure 9A, 9C, 9E and 9G) and the total pixel intensities of bands were quantified (Figure 9B, 9D, 9F and 9H). When the cells were treated with 10nM ET-1, there was an initial decrease in the NET protein expression at 0.5, 2, 12, 24 and 48 hours (50±6.5, 40±4.3, 41±3.2, 46±3.2 and 34±4.7% of the control) (Figure 9A and 9B), respectively. This was followed by a return to control levels at 7 days (109±4.8% of control) (Figure 9G and 9H). Treatment with 30nM ET-1 resulted in an initial decrease in NET protein level at 0.5, 2, 12, 24 and 48 hours (47±9.2, 35±8.4, 51±5.4, 43±5.9, and 35±7.0% of the control, respectively) (Figure 9C and 9D). NET protein levels returned to control levels at 7 days (103±1.8% of the control) (Figure 9G and 9H). Treatment with 100nM ET-1 resulted in an initial decrease in NET protein level at 0.5, 2, 12, 24 and 48 hours (47±6.5, 30±6.1, 32±4.1, 38±6.4, and 42±4.1% of the control, respectively) (Figure 9E and 9F). This initial decrease in protein levels was followed by a return to the control level at 7 days (98±1.0% of the control) (Figure 9G and 9H).

Figure 9: Western immunoblotting for NET in differentiated PC-12 cells treated with ET-1 (10, 30 and 100nM) for 30 minutes to 7 days. (A, C, E, G): Representative immunoblotting images showing a 54KDa band for NET in membrane-enriched protein extracts from ET-1 treated cells at different treatment time points. (A, C, E): ET-1 treatment for 30 minutes to 48 hours. (A) 10 nM ET-1 treatment group; (C) 30nM ET-1 treatment group; (E) 100nM ET-1 treatment group. (G) ET-1 treatment for seven days. The Coomassie Blue staining was used to verify equal protein loading of all lanes (not shown). (B, D, F, H): Comparison of changes in total pixel intensities of treatment groups to the control group. (B, D, F): ET-1 treatment for 30 minutes to 48 hours. (B) 10nM ET-1 treatment group; (D) 30nM ET-1 treatment group; (F) 100nM ET-1 treatment group. (H) ET-1 treatment for seven days. Asterisks indicate significant change compared to the control group ($p<0.05$ indicating significance; n=5~8).

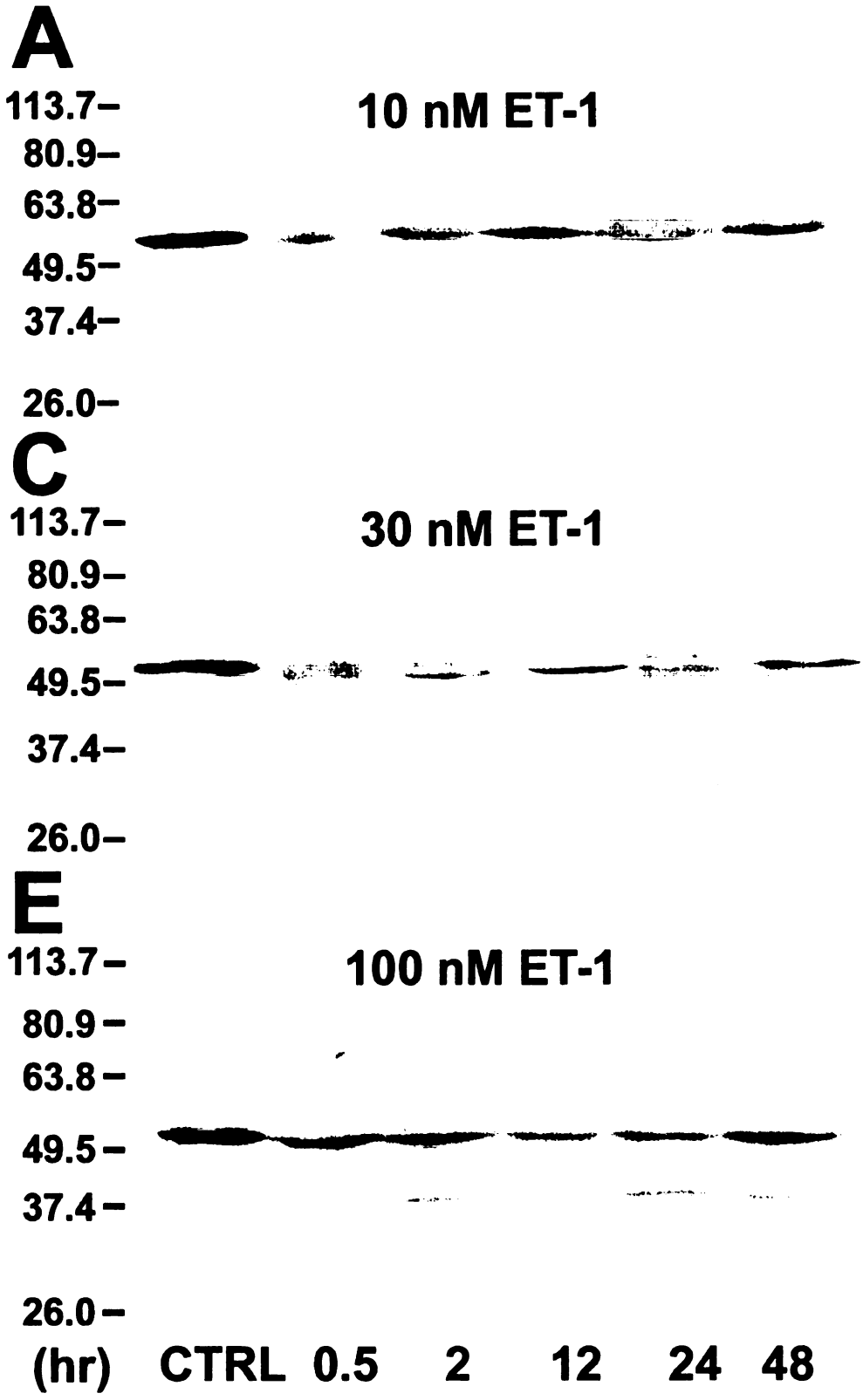
A
113.7–
80.9–
63.8–
49.5–
37.4–
26.0–
10 nM ET-1
C
113.7–
80.9–
63.8–
49.5–
37.4–
26.0–
30 nM ET-1
E
113.7–
80.9–
63.8–
49.5–
37.4–
26.0–
100 nM ET-1
(hr) CTRL 0.5 2 12 24 48

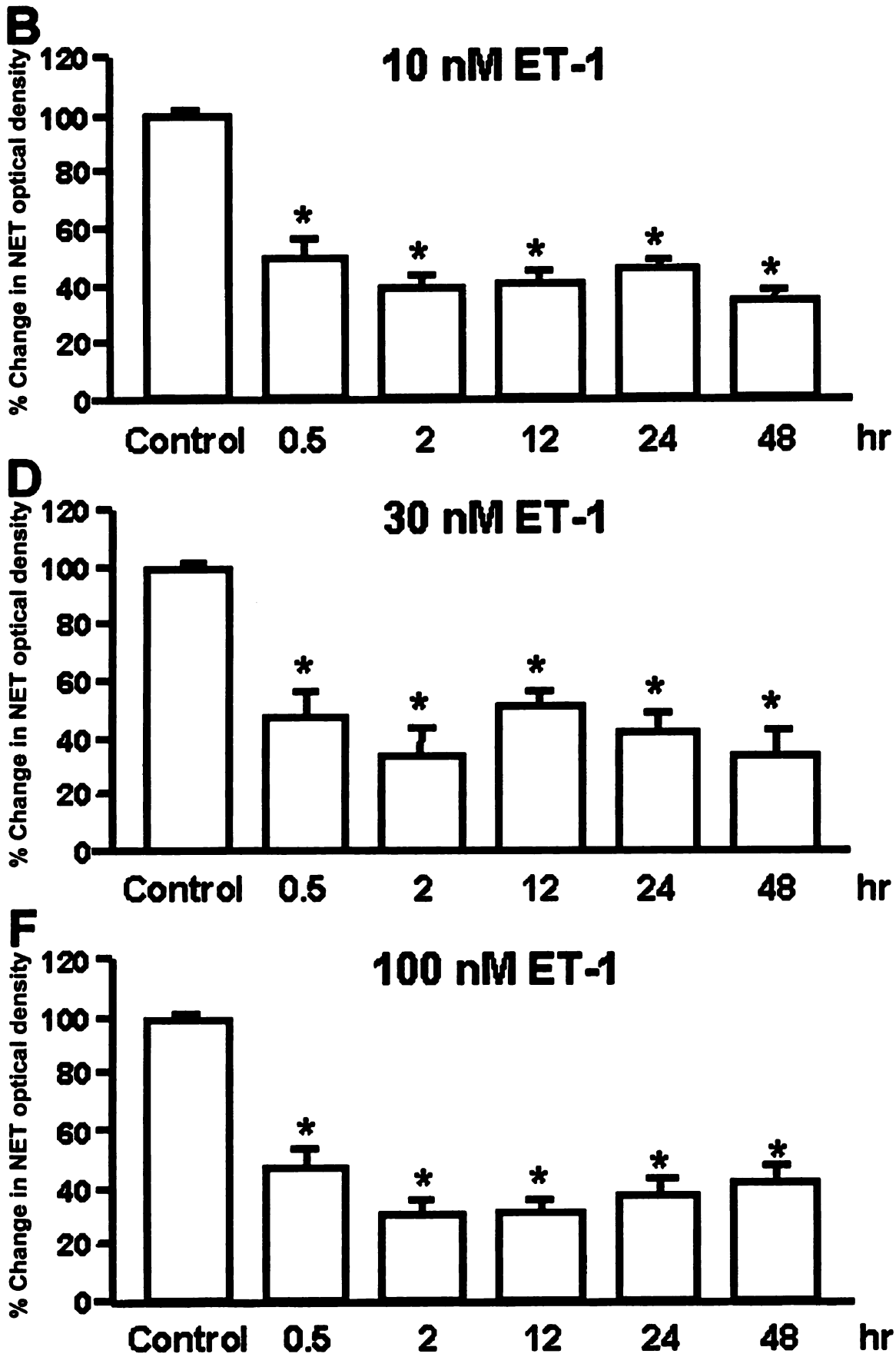
B
10 nM ET-1
% Change in NET optical density
120
100
80
60
40
20
0
Control
0.5
2
12
24
48
hr
D
30 nM ET-1
% Change in NET optical density
120
100
80
60
40
20
0
Control
0.5
2
12
24
48
hr
F
100 nM ET-1
% Change in NET optical density
120
100
80
60
40
20
0
Control
0.5
2
12
24
48
hr

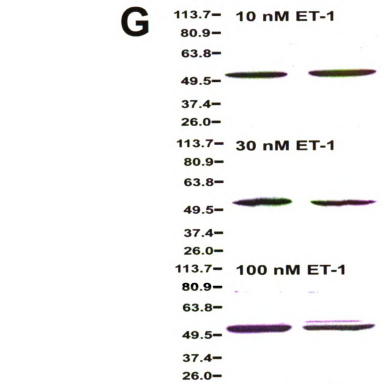
G
113.7–
80.9–
63.8–
49.5–
37.4–
26.0–
10 nM ET-1
30 nM ET-1
100 nM ET-1
Control 7 days

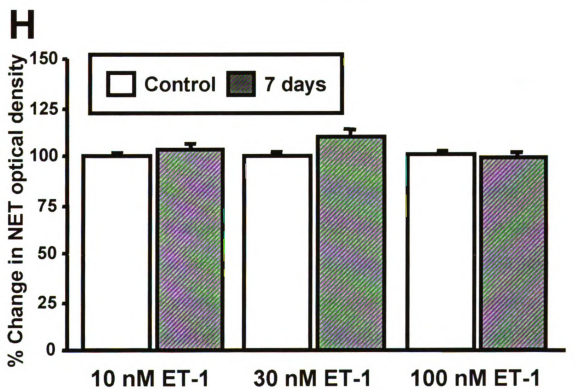
H
% Change in NET optical density
150
125
100
75
50
25
0
Control
7 days
10 nM ET-1
30 nM ET-1
100 nM ET-1

Effects of ET-1 on uptake of Asp+ via NET in differentiated PC-12 cells

Desipramine sensitive Asp+ uptake was measured in differentiated PC-12 cells treated with ET-1 for 30 minutes to 7 days (Figure 10). ET-1 treatment (10, 30 and 100nM) produced a decrease in the NET uptake, which could be seen as early as 30 minutes with 100nM ET-1 with a gradual further decrease occurring a function of time. Although the amount of NET mRNA and protein was beginning to increase at 7 days of treatment, the uptake in all treatment groups was still lower than the control.

When cells were treated with 10nM ET-1, uptake was 90±2.9, 57±1.8, 14±1.8, and 42±9.0% of the control at 0.5, 12, 24 hours and 7 days, respectively (Figure 10). Uptake activity was 80±2.9, 53±1.9, 19±2.9, and 56±9.0% of the control at 0.5, 12, 24 hours and 7 days, respectively (Figure 10) in the 30nM ET-1-treated group. In cells pretreated with 100nM ET-1, uptake was 67±1.4, 68±2.3, 28±7.5, and 68±4.4% of the control at 0.5, 12, 24 hours and 7 days, respectively (Figure 10).

Discussion

In the present study, NET mRNA level and protein expression were investigated. This is the first demonstration of NET mRNA and protein in tissues extracts of mesenteric arteries, mesenteric veins, celiac ganglia and DRG from DOCA-salt hypertensive and Sham rats. Both NET mRNA level and protein expression were upregulated in mesenteric arteries, mesenteric veins and sympathetic celiac ganglia, but not in DRG, from DOCA-salt hypertensive rats

Figure 10: Effects of exposure of differentiated PC-12 cells to ET-1 (10, 30 and 100nM) for 30 minutes, 12 hours, 24 hours, and 7 days on desipramine-sensitive NET uptake using Asp+ as the substrate. Data are represented by the percentage change to the no treatment control group. Asterisks indicate significant change compared to the control group ($p<0.05$ indicating significance; n=8).

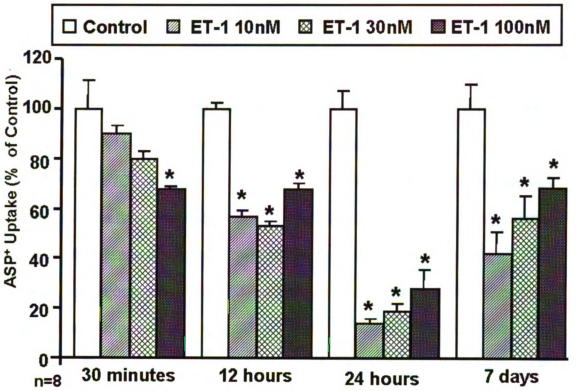
Control
ET-1 10nM
ET-1 30nM
ET-1 100nM
ASP+ Uptake (% of Control)
120
100
80
60
40
20
0
n=8
30 minutes
12 hours
24 hours
7 days

compared to Sham rats. The present study also shows that exposure of differentiated PC-12 cells, which naturally express NET mRNA and protein, to ET-1 produced a two-phase change in mRNA expression and protein level of NET. Exposure to ET-1 resulted in an initial decrease in NET mRNA level up to 48 hours, followed by an increase at 7 days, and an initial decrease in NET protein level up to 48 hours, followed by a return to the control level at 7 days. However, uptake was downregulated by ET-1 treatment from 30 minutes to 7 days.

Regulation of NET

NET activity can be regulated at several levels, including the functional level, the mRNA level and the protein level (Zahniser and Doolen, 2001). The regulation of Na^+/Cl^- dependent neurotransmitter transporters can be regulated very rapidly on a time scale of seconds to minutes or long-term on a time scale of days. [^{3}H]NE release is consistently potentiated during nerve stimulation. However, its major metabolite [^{3}H]3,4-dihydroxyphenylglycol (DHPG), which is produced only after neuronal reuptake of norepinephrine, does not appear in the perfusate until after the stimulation ends, suggesting that norepinephrine uptake is attenuated during depolarization (Dubocovich and Langer, 1976). Nine days of treatment with reserpine, which selectively blocks the monoamine vesicular transporter and depletes biogenic amines, results in down-regulation of NET binding sites and reduced norepinephrine uptake in rat cerebral cortex (Lee et al., 1983). To date, most of the research investigating the regulation of NET has been done *in vitro* with cloned transporter expressed heterologously transfected

cell lines (Apparsundaram et al., 1998b;Bruss et al., 1995;Melikian et al., 1994;Zhu et al., 1998;Zhu et al., 2000), or with native NET expressed in cell lines, such as PC-12 cells (Zhu and Ordway, 1997) and human neuroblastoma (SK-N-SH) cells (Apparsundaram et al., 2001;Joyce et al., 2001). The advantage of using cell lines lies on the fact of relatively easy manipulation of the transporter, ever since its molecular structure is known. Those results demonstrate that the direction of regulation of NET mRNA level, protein level, binding sites and binding affinities are inconsistent (Zhu et al., 1998;Zhu et al., 2000;Zhu and Ordway, 1997). Nevertheless, the cultured cells lack of synaptic contacts and other necessary nerve growth factors and environmental factors, which are preserved in native tissues and are important for the growth and differentiation of neurons and expression of phenotypic NET. However, only a few studies have investigated regulation of NET in native tissues, such as in brain locus coeruleus (Cubells et al., 1995;Hebert et al., 2001;Zhu et al., 2002), and ventromedial hypothalamus (VMH) and rostral ventrolateral medulla (RVLM) (Reja et al., 2002). No research that I am aware of has examined NET regulation in blood vessels and their innervating peripheral nervous systems. Regulation of NET in native tissues may occur as a direct result within cells per se, or as indirect effects, such as the activation of one or more synaptic receptors or other transsynaptic phenomena.

Regulation of NET in hypertension

Impaired neuronal reuptake of norepinephrine by NET might contribute to essential hypertension. This idea was initially suggested by findings of reduced

[^{3}H]norepinephrine in tissues of hypertensive rats (de Champlain et al., 1966). Subsequent clinical studies indicate that a subgroup of patients with essential hypertension have increased plasma norepinephrine and reactivity to norepinephrine and decreased norepinephrine uptake and secretion of norepinephrine (Mendlowitz, 1975). Measurements of norepinephrine spillover, norepinephrine concentration, and sympathetic nerve activity demonstrate in essential hypertensive patients demonstrated that there was reduced neuronal norepinephrine reuptake and increased rates of sympathetic nerve firing. Both of these could contribute to sympathetic activation in hypertension (Schlaich et al., 2004). Impaired function of NET may become involved in the pathogenesis of essential hypertension in some patients by reducing norepinephrine reuptake and thus increasing the amount of locally available norepinephrine. This in turn would lead to more persistent and pronounced α-adrenergic receptors mediated-vasoconstriction, which could be followed by an increase in blood pressure. Interestingly, a family of patients with orthostatic intolerance and human NET gene Ala457Pro variant has an almost complete loss of NET function with a very high plasma norepinephrine concentration and reduced systemic norepinephrine clearance. They exhibits a dramatic increase in heart rate, but only moderate increase in blood pressure, upon changing from supine to upright position (Shannon et al., 2000). Several mutations of NET gene have been reported in some essential hypertensive patients, however, none of them result in abnormal norepinephrine uptake. This may be due to the small number of patients observed in the study, or to the fact that NET gene variants in hypertension do

not affect norepinephrine uptake (Paczkowski et al., 2002). Possibly, changes in NET mRNA and protein levels, followed by changes in NET function, may shed light on the impaired neuronal uptake in hypertension. This study is the first reported examination of changes in NET mRNA and protein level in vascular tissues and its innervation in an accepted model of hypertension.

Upregulated NET in sympathetic ganglia in hypertension

Most of previous work investigating NET function was done *in vivo* using radiolabeled tracer. Cloning of the NET gene provides a new way to examine the expression and function of NET from a molecular biological point of view. NET mRNA level is significantly higher in central brain regions associated with control of arterial blood pressure from spontaneously hypertensive rats than from normotensive rats (Reja et al., 2002). Present study extended the study of expression of NET to the peripheral sympathetic nervous system regulating blood pressure and showed that there was a significant increase in the level of NET mRNA and protein in celiac ganglia from DOCA-salt hypertensive rats.

In hypertension, several factors may possibly regulate the level of NET mRNA and protein. The first candidate may be norepinephrine. Depletion of norepinephrine with reserpine reduces the number of uptake sites, whereas increasing the amount of norepinephrine induced by treatment with monoamine oxidase inhibitors raises the number of binding sites in brain neurons (Lee et al., 1983). In DOCA-salt hypertensive rats, increased sympathetic nerve activity (Reid et al., 1975) along with impaired neuronal uptake of norepinephrine in splanchnic vasculature (Wang et al., 2002) may contribute to an increased

release of norepinephrine from nerve terminals around mesenteric arteries and veins (Luo et al., 2004). Possibly, locally increased norepinephrine may upregulate sympathetic NET mRNA and protein expression. Other circulating hormones may also influence NET function. Angiotensin II (Ang II) upregulates mRNA of NET in brain neurons and this upregulation is potentiated in spontaneously hypertensive rats (Lu et al., 1996). However, Ang II activity is markedly depressed peripherally in DOCA-salt hypertension (Ueno et al., 1988b). The upregulated levels of NET mRNA and protein in DOCA hypertension may possibly come from the effects of other humoral hormones, such as endothelin-1 (ET-1). In human essential hypertension, circulating levels of ET-1 are elevated in many hypertensive patients, especially those with severe hypertension (Kohno et al., 1990;Saito et al., 1990). Expression of ET-1 mRNA and production of ET-1 peptide are increased in endothelial cells in DOCA-salt hypertension (Millette et al., 2003;Yu et al., 2002). ET-1, secreted from the endothelium layer toward outer layers of blood vessels and produced within sympathetic ganglia (Damon, 1998), may act on ET receptors located on sympathetic nerve terminals (Damon, 1998;Mutafova-Yambolieva and Westfall, 1998) and furthermore to regulate NET.

Downregulated NET in sensory ganglia in hypertension

NET mRNA and protein were detectable in sensory DRG. Previous data from our laboratory (Zheng et al., 2000) has suggested that guanethidine, acting as a substrate for NET (Berfield et al., 1999;Sachs, 1970), has actions on primary sensory nerves. We recently detected the presence of NET mRNA in a

single sympathetic celiac neuron and a sensory DRG neuron and we were also able to image NET uptake using a fluorescent marker and NET substrate Asp+ in dissociated DRG neurons. Uptake of Asp+ via NET is the selective NET blocker desipramine-sensitive (Zheng et al., 2003). In this study, we further supported previous findings by showing that NET mRNA and protein were present in the whole DRG. There was 10 fold less NET mRNA in DRG than in celiac ganglia from Sham rats when using quantitative real-time PCR method.

In contrast to the upregulated levels of NET mRNA and protein in sympathetic ganglia in DOCA-salt hypertensive rats, NET mRNA and protein levels were downregulated in sensory DRG in DOCA hypertensive rats. This may come from an antagonistic balance between sympathetic and sensory nerves, in which sympathetic and primary sensory nerves provide a vasoconstrictor-vasodilator balance to blood vessels. The evidence includes: 1) Opposite effects are reflected for the most part in different neurotransmitter phenotypes in two types of nerves, such as vasoconstrictive neurotransmitters, norepinephrine and ATP, released from sympathetic nerves, and vasodilatory neuropeptides, SP, CGRP and VIP, released from sensory nerves. 2)Sensory nerves send collaterals to sympathetic ganglia to affect sympathetic nerve activity (Kreulen and Peters, 1986;Zheng et al., 1999). The normal balance between the sensory and sympathetic nervous system plays an important role in the maintenance of normal blood pressure (Wang et al., 2001). NET in DRG neurons may transport norepinephrine, facilitate the removal of norepinephrine released from adjacent sympathetic nerve terminals and terminate vasoconstrictive effects provided by

norepinephrine. In DOCA-salt hypertensive rats, decreased NET in sensory nerve terminals would reduce the speed of norepinephrine removal. Considering an increased release of norepinephrine in DOCA-salt hypertension (Luo et al., 2004), this effect would result in more norepinephrine acting on postjunctional adrenergic receptors and cause greater constriction, followed by an increased blood pressure.

Upregulated NET in blood vessels in hypertension

NET mRNA and protein were also detectable in mesenteric arteries and veins. Tissues of mesenteric arteries and veins harvested for this study contain adventitia, smooth muscle cells, endothelial cells and sensory and sympathetic nerve terminals. NET mRNA and protein may come from two possible sources. The first source is sympathetic and sensory nerve terminals located on arteries and veins. Classically, it was believed that mRNA exists only in neuron cell bodies and protein is present from cell bodies to nerve terminals. Nevertheless, many mRNAs, including members of the glutamate receptor family, and second messenger systems, such as calcium/calmodulin-dependent protein kinase II (CaMK II) are reported to be present on individual processes of cultured brain neurons (Job and Eberwine, 2001;Miyashiro et al., 1994). NET mRNA and protein are present in sympathetic celiac ganglia and sensory DRG, where neuron cell bodies are, and highly possibly on sympathetic and sensory nerve terminals extended from cell bodies. If NET mRNA and protein in blood vessels come only from their surrounding nerve terminals, lower levels of NET mRNA and protein in mesenteric blood vessels than in ganglia may result from lower

amount of NET mRNA and protein in nerve terminals than in cell bodies. These results may demonstrate that there is less locally synthesized NET mRNA in nerve terminals compared to neuron cell bodies. The second possible source of NET mRNA and protein is non-neuronal cells. There are several extraneuronal cell types that express the same NET as in noradrenergic neurons, including mouse capillary endothelial cells (Wakayama et al., 2002) and human placenta (Bzoskie et al., 1995;Bzoskie et al., 1997). Unlike neuronal reuptake of norepinephrine, the non-neuronal NET appears to function primarily as a mechanism for inactivating norepinephrine (Eisenhofer, 1994).

The mechanism underlying the upregulated NET in mesenteric blood vessels is unknown. Considering the possibility that NET mRNA and protein may come from their innervating sensory and sympathetic nerves, the upregulated levels of NET mRNA and protein in mesenteric arteries and veins in DOCA hypertension may be the sum of increased NET mRNA and protein in sympathetic neurons and decreased NET mRNA and protein in sensory neurons. The preparation of plasma membrane-enriched protein was used in this study and this is different from the preparation of whole-cell homogenate protein in other studies (Kantor et al., 2001;Zhu et al., 1998). Those studies demonstrate that the changes in the level of NET protein represent the loss of total NET protein, which is the combination of an intracellular pool NET protein and the cell membrane bound NET protein. Recent studies strongly argue that only NET protein trafficking to the cell membrane has the potential to carry out the reuptake function of norepinephrine (Apparsundaram et al., 1998b;Hahn et al.,

2003;Savchenko et al., 2003). Consequently, the upregulated vascular NET protein may be due to an increased level of surface protein trafficking in hypertension. However, we couldn't rule out the possibility of an increased level of total protein, which needs to be examined in later study.

Different levels of NET mRNA and protein in arteries and veins

The differences in NET mRNA and protein levels of arteries and veins may rise from different sympathetic innervation to them. Sympathetic innervation to arteries and veins is different and there exist arterial and venous sympathetic neurons, which have different electrophysiological properties and use different neurotransmitters (Browning et al., 1999;Hottenstein and Kreulen, 1987). More NET mRNA, but less NET protein, was present in veins than in arteries in both DOCA and Sham rats, and the ratio of NET protein in arteries to it in veins is the same in DOCA rats as in Sham rats. These results indicate that the levels of NET mRNA and protein may be regulated in a complex manner in hypertension, and the regulation may happen at several levels, such as post-transcription, translation or protein degradation (Zhu et al., 2002).

Differentiated PC-12 cells vs. undifferentiated PC-12 cells and transfected cells

Much of our knowledge about NET has been derived from some cell lines that do not normally express NET and are transfected with human NET, or cell lines that express native NET, such as rat pheochromocytoma (PC-12) cell line. PC-12 cells express NET because they are derived from the adrenal medulla tumor that secretes norepinephrine. We chose to use differentiated PC-12 cells

for several reasons. First, regulation of NET in transfected cells may use completely different biomedical mechanisms compared to cells expressing native NET. Some studies have investigated NET regulation in cell lines transfected with the NET gene (Bauman and Blakely, 2002). The promoters driving NET transcription in those cells are heterologous and very active (Zhu et al., 1998). For example, HEK-hNET cell is the HEK-293 cell stably transfected with human NET (hNET) cDNA; expression of this cDNA is under the control of CMV promoter (Galli et al., 1995). This promoter is extremely powerful, and transcription of the hNET gene in HEK-293 cells is constitutively active (Foecking and Hofstetter, 1986). Therefore transfected cells are not good models for studying native NET gene regulation. Second, in native adrenergic neurons, NET protein or mRNA might be directly regulated by available catecholamines in synaptic clefts (Lee et al., 1983) and indirectly regulated by other factors, which may also regulate the enzymes responsible for catecholamine synthesis and/or metabolism (Cubells et al., 1995;Weinshenker et al., 2002). However, transfected cells do not contain metabolic enzymes for catecholamines, and in turn they are unable to release catecholamines. Hence, regulation of NET in transfected cells may not reliably illustrate NET regulation in "real" synaptic terminals. Finally, differentiated PC-12 cells have extensive neurites growth and form abundant synaptic contacts with each other. In contrast, both undifferentiated PC-12 cells and transfected cells lack synaptic contacts. Regulation of NET in those cells may occur as a direct result within each cell, as opposed to indirect effects, such as the activation of one or more presynaptic receptors or other transsynaptic

phenomena, which may be critical for *in vivo* NET regulation.

Acute regulation

The acute regulation of NET membrane protein expression and uptake in differentiated PC-12 cells is due to an ET receptor-dependent pathway. Regulation of NET can occur rapidly. We observed an initial rapid regulation of NET mRNA, plasma membrane protein and uptake after treating PC-12 cells with ET-1. One hour treatment of cultured hypothalamic-brainstem neurons with Ang II or PMA, a PKC activator, rapidly upregulates NET mRNA, accompanied by upregulated uptake of [^{3}H]NE. These effects can be inhibited by bisindolymaleimide, a selective PKC inhibitor (Lu et al., 1996). Incubation of PC-12 cells with ET-1 (100nM) for 10 minutes is capable of activating the PKC pathway (Takekoshi et al., 2002). Incubation of SK-N-SH cells with the PKC activator PMA for 10 minutes downregulates the cell membrane NET protein expression and uptake (Apparsundaram et al., 1998b). ET-1 activated PKC pathway may be responsible for the acute regulation of NET mRNA, cell membrane protein and function in differentiated PC-12 cells in this study. Compared to the regular RT-PCR used in a previous study (Lu et al., 1996), in which the mRNA level was examined based on the densities of bands on agarose gels at the end of PCR amplification, quantitative real-time PCR was performed in our study. Real-time PCR allowsus to measure mRNA level based on the PCR cycle number at the threshold in the process of PCR amplification. This quantitative real-time PCR can discover smaller differences in mRNA levels that regular PCR could not detect (Bio-Rad Laboratories, 2002). As a result, we

were able to detect a decrease in NET mRNA level as early as 30 minutes.

Downregulation

The levels of NET mRNA, protein and uptake can be downregulated. Activated PKC pathway via the binding of ET-1 to ET receptors (Kodama et al., 1989) may result in downregulation of NET mRNA and protein. Exposure of differentiated PC-12 cells to ET-1 resulted in a decrease in NET mRNA, cell membrane protein and uptake as early as 30 minutes. PMA, a PKC activator, downregulates NET membrane protein expression and uptake function in HEK-hNET cells and SK-N-SH cells (Apparsundaram et al., 1998a;Apparsundaram et al., 1998b;Savchenko et al., 2003). However, in brainstem neurons, Ang II increases NET surface protein expression (Savchenko et al., 2003). Ang II and PMA upregulate NET mRNA level and uptake, which is proposed to be mediated through a PKC pathway (Lu et al., 1996). The inconsistence of regulation might reflect differences between characteristics of brain neurons and other cell types. For example, Zhu *et al.* reported that NET protein was unchanged in rat brain locus coeruleus (LC) after three days of treatment with desipramine, whereas NET protein was decreased in SK-N-BE(2)M17 cells given the same treatment (Zhu et al., 2002).

Time course of changes in NET mRNA and protein

The dissociation between mRNA and protein levels of NET was observed in this study. The effects of ET-1 treatment on both NET mRNA and protein levels were biphasic, with an early transient fall and a late rise. Changes in NET mRNA were most rapid and earliest while changes in NET membrane protein

lagged behind changes in mRNA. NET mRNA level returned to control levels as early as 24-hour of ET-1 treatment whereas NET protein level was still reduced despite a marked increase in NET mRNA level. The levels of NET mRNA and protein were all elevated after 7-day of ET-1 treatment. Similar disparities between mRNA and protein level are observed in other studies of regulation of NET. For example, treatment of HEK-hNET cells with desipramine for three days produces a concentration-dependent decrease in NET protein with no change in NET mRNA (Zhu et al., 1998). Furthermore, this phenomenon is also observed in other catecholamine transporters after drug treatments. Treatment with selective SERT inhibitors paroxetine or sertraline decreases brain SERT protein density, without a change in SERT mRNA (Benmansour et al., 1999).

Several mechanisms could underlie this inconsistent change of NET mRNA and protein in the presence of ET-1. First, downregulation of cell membrane protein after 30-minute of ET-1 treatment might come from decreased insertion of NET protein into cell surface. For example, confocal microscopy and flow cytometry methods reveal that 30-minute of PMA treatment results in a substantial decrease in cell membrane NET protein accompanied with a concomitant increase in cytoplasmic NET protein (Apparsundaram et al., 1998b;Savchenko et al., 2003). Second, the delayed increase in the level of NET mRNA and protein might be a compensatory response to its initial decrease in response to drug exposure. In this study, NET protein level remained decreased until 7-day of ET-1 treatment, even with a return of NET mRNA to control levels by 24 hours and an increased NET mRNA level at 48-hour of ET-1 treatment. It

could be argued that the increased expression of NET mRNA might not be adequate to restore the reduction in NET protein until after 7-day of ET-1 treatment. Third, the downregulated NET protein expression induced by ET-1 treatment may result from decreased translation, or increased protein turnover/degradation. The loss of transporter protein resulting from protein degradation is demonstrated in the glucose transporter system, in which the src oncogene is associated with an increase in type 1 glucose transporter protein due to a decrease in the degradation rate of this protein (Shawver et al., 1987). At last, downregulation of NET mRNA and plasma membrane protein levels in differentiated PC-12 cells could result from a combination of several processes, such as changes in transcription, translation, or protein trafficking.

Relationship between NET uptake and plasma membrane protein

The initial decrease in desipramine-sensitive Asp+ uptake by NET after exposure to ET-1 was associated with a loss of cell membrane protein expression. This may result from a decrease in the amount of transporter protein trafficked to cell membrane. Although not much is known about molecular mechanisms underlying the intracellular trafficking of NET, a large body of evidence suggests that PKC activation leads to the internalization of NET from cell membrane to cytoplasm and the subsequent downregulation of plasma membrane NET (Apparsundaram et al., 1998b;Apparsundaram et al., 1998a). Therefore, exposure of cells to ET-1 might trigger a signal transduction cascade, in which PKC activation results in an increase in the amount of transporter trafficking to intracellular compartments and a decrease in cell membrane

transporter expression.

There was a persistent reduction in desipramine-sensitive Asp+ uptake even though the level of plasma membrane NET protein had returned to control levels after 7-day of ET-1 exposure. A time lag between protein expression and uptake is also observed in rat brain γ-aminobutyric acid (GABA) transporter (GAT1) expressed in *Xenopus* oocytes, in which the ability of PMA to upregulate transporter activity is decreased as the transporter expression level is increased (Corey et al., 1994). The transport capacity of NET is determined by the combination of several factors. Besides protein expression, the kinetics of uptake and substrate binding ability also contribute to the transporter function (Yoshimura et al., 2001). In turn, regulation of any of above parameters by drugs will potentially regulate the capacity of transporter to uptake substrates.

One noteworthy difference between present study and previous investigations is that different protein samples were used. Protein from whole-cell homogenates are examined in other studies (Kantor et al., 2001;Zhu et al., 1998); in contrast, the plasma membrane-enriched protein preparation was used in this study. Results form present study stood for changes in the amount of NET protein on cell membrane, and represented more closely to changes in the functional NET protein than other studies.

ET-1 concentration

The concentration of ET-1 applied to cells ranged from 10nM to 100nM in this study, which were based on the EC50 of ET-1 in an *in vitro* vasoconstriction study (Johnson et al., 2002) and functional studies of ET-1 on neurons or PC-12

cells (Mutafova-Yambolieva and Westfall, 1998;Takekoshi et al., 2002). NET mRNA level was returned to the control level earlier in 30nM and 100nM ET-1 treatment group than in 10nM ET-1 treatment group after the initial decrease. It appears that regulation of NET protein level and uptake was not ET-1concentration-dependent, at least within the concentration range in present study. The lowest ET-1 concentration that we chose in this study may be already high enough to occupy all ET receptors, and consequently, NET regulation is not concentration dependent at all.

Stringency of PCR amplification products and antibody in this study

The possibility of identifying the protein and mRNA of a closely related, but functionally distinct gene was ruled out in this study. Stringent sequences of PCR primers and antibody antigen for NET were used in this study. First, the rat NET gene exhibits a 65% identity to the rat DAT gene and has very low identity to genes from other members in Na^+/Cl^- dependent neurotransmitter transporter family. It is necessary to avoid conserved regions with other transporter genes when we design PCR primers and choose the antibody for western blotting to examine the existence of NET mRNA or protein (Bruss et al., 1997). Three pairs of primers were designed in this study because sequencing, real-time RT-PCR and regular PCR have different requirements for primer selection. Predicted sequences of PCR amplification products were aligned with all other rat gene sequences in GenBank and they only matched 100% with the rat NET gene. This assured the stringency of primers. Besides, only six amino acids out of 22 amino acids in the recognition site of NET antibody was identical to the rat DAT gene.

This demonstrates low homology of NET antibody with DAT and further assures the stringent binding of antibody to antigen. Furthermore, there is no DAT present in sympathetic neurons. This notion is supported by a study showing that, in rat superior cervical ganglia (SCG), NET and SERT are expressed in ganglionic neurons, but not DAT mRNA (Nishimura et al., 1999). In addition, there is no other evidence showing the presence of other monoamine transporters besides NET and SERT in the peripheral sympathetic or sensory nervous systems, although a lot of research has investigated the existence of monoamine transporters in the CNS (Nelson, 1998).

Detection of NET protein

The western blotting was performed in this study using an antibody from Chemicon and a 54KD immunoreactive band was detectable. NET is detected in three forms according to the molecular weight recognized in western blotting, 46 (or 50) KD, 54 (or 58) KD and 80 KD (Bruss et al., 1995;Melikian et al., 1994). There exists inconsistency among studies as to which form of NET is detectable using immunoblotting method. A single 54 KD immunoreactive band is detected in the transfected Hela-hNET cell line, but three forms of NET are detected in stably transfected LLC-NET cells using the same NET antibody (Melikian et al., 1994). A 58 KD (or 54KD) protein is predominant in SK-N-SH cell line with native NET expression and in transfected COS-7 cells (Bruss et al., 1995). In addition, a protein from the adrenal medulla is characterized by a molecular weight of 50-53 KD representing the NET by means of low and high pressure liquid chromatography using anion exchange, gel filtration or lectin affinity columns

(Bonisch et al., 1991). The only immunoreactivity of NET detected in all tissues in this study was a 54 KD size using a commercial available antibody, although a form of 80 KD size is detected in undifferentiated PC-12 cells using the same antibody (Kantor et al., 2001). These discrepancies may come from the possibilities that different tissues or cells, or antibodies are employing in different studies.

Perspectives

This study is the first to demonstrate that NET mRNA and protein were present in mesenteric blood vessels and their sympathetic and sensory innervation celiac ganglia and DRG from DOCA-salt hypertensive and Sham rats. NET mRNA and protein levels were upregulated in mesenteric arteries, mesenteric veins and sympathetic celiac ganglia, but not in DRG, from DOCA-salt hypertensive rats compared to Sham rats. This study also demonstrates for the first time that NET can be regulated by ET-1 in differentiated PC-12 cells. ET-1 produced both acute and long-term changes in NET mRNA and protein level. However, the reduced uptake of Asp+ via NET was persistent through the 7 days of study. Considering the impairment of neuronal norepinephrine reuptake and/or increased ET-1 production in some essential hypertensive patients, we speculate that the impairment of neuronal norepinephrine reuptake could be mediated through ET-1 dependent regulation of NET. The expression and function NET in the sympathetic and sensory nervous systems may be important targets for therapeutic treatment of hypertension.

CHAPTER 3: SUPEROXIDE ANION IN SYMPATHETIC NEURONS

CHAPTER 3A: INCREASED $O_2^{\cdot-}$ PRODUCTION AND UPREGULATION OF ET_B RECEPTORS BY SYMPATHETIC NEURONS IN DOCA-SALT HYPERTENSIVE RATS

Introduction

Many factors are potentially responsible for changes that occur in the sympathetic nervous system in hypertension. In vascular tissues, there is a profound increase in ROS, including $O_2^{\cdot-}$, in several models of hypertension (Sedeek et al., 2003;Somers et al., 2000b). However, it is not known whether sympathetic neurons generate ROS, such as $O_2^{\cdot-}$, and whether this is elevated in hypertension as it is in the vascular system. ROS contribute to oxidative damages and cell death in neurodegenerative diseases, such as amyotropic lateral sclerosis and Parkinson's disease (Pong, 2003). But there is no evidence of degenerative changes in sympathetic ganglia in hypertension. In the CNS ROS can serve as signaling molecules mediating the effects of neuroactive substances. For example, Angiotensin II(Ang II)/ROS signaling system mediates the action of Ang II to increase the blood pressure (Zimmerman et al., 2002).

Endothelin-1 (ET-1), a peptide originally described as a potent vasoconstrictor synthesized in endothelial cells, is also present in the nervous system and it has multiple actions on sympathetic and sensory neurons (Damon, 1999;Milner et al., 2000a;Sullivan and Morton, 1996). ET-1 contributes to salt-sensitive hypertension in animals and humans (Schiffrin, 2001), and the pathogenesis is associated with ROS, especially $O_2^{\cdot-}$, which are increased in

blood vessels in DOCA-salt hypertension as well as in several other experimental models of hypertension (Sedeek et al., 2003;Somers et al., 2000b). ET-1 evokes arterial $O_2^{\bullet-}$ production in DOCA-salt hypertensive rats via ET_A receptors (Li et al., 2003). The effects of ET-1 on ROS in the sympathetic nervous system, especially in hypertension, are not known.

We investigated $O_2^{\bullet-}$ levels in sympathetic ganglia of DOCA-salt hypertensive rats. The focus of this study is on the inferior mesenteric ganglia (IMG) and celiac ganglia (CG) innervating the splanchnic circulation, which stores 38% of total blood and up to 64% of that can be mobilized by direct stimulation of sympathetic nerves due to their rich innervation (Greenway, 1983b). Due to the characteristically high ET-1 released from endothelial cells in DOCA-salt hypertension (Millette et al., 2003;Yu et al., 2002), we examined the effects of ET receptor agonists on $O_2^{\bullet-}$ generation in dissociated sympathetic postganglionic neurons and differentiated PC-12 cells. We also sought to establish the possible mechanism involved in the $O_2^{\bullet-}$ production in sympathetic ganglia in DOCA-salt hypertension by investigating ET-1 levels and ET receptors expression in celiac ganglia.

Methods

Animals

See Chapter 2 Methods.

The mean arterial pressure for the DOCA-salt rats and Sham rats are 181.3±3.1 mmHg and 111.8±4.3 mmHg separately.

Sympathetic ganglia tissue harvest and cell culture

See Chapter 2 Methods.

Measurement of superoxide anion generation

Levels of superoxide anion were examined by measuring fluorescence signal intensity resulting from intracellular probe oxidization. IMGs or cells were loaded with the oxidant-sensitive fluorogenic probe Dihydroethidine (DHE) ($2x10^{-6}$mol/L, Molecular Probes) for 30 or 45 minutes before measuring fluorescence (excitation: 514 nm; emission: 560 nm) with a confocal microscope. DHE is oxidized to fluorescent ethidium by $O_2^{\bullet-}$. Ethidium will intercalate with DNA to further amplify the fluorescent signal and the intensity of the fluorescent signal is proportional to $O_2^{\bullet-}$ levels (Becker et al., 1999;Benov et al., 1998). IMG were from 4 groups: Sham rats, DOCA-salt hypertensive rats, Sham rats incubated with ET-1 ($3x10^{-8}$mol/L) for 30 minutes *in vitro*, and Sham rats incubated with ET_B receptor antagonist BQ788(10^{-7}mol/L) for 45 minutes followed by ET-1 incubation for 30 minutes *in vitro*. IMG were loaded with DHE for 45 minutes at 37°C. Cells were divided into 2 treatment groups: one group using ET-1 as the agonist and another group using sarafotoxin 6c (S6c, 10^{-8}mol/L) as the agonist. The ET_A receptor antagonist BQ610(10^{-7}mol/L), or the ET_B receptor antagonist BQ788 was tested against both agonists. Control cultures received no drug treatments. Cells were incubated with/without antagonists for 45 minutes, followed by incubation with agonists for 30 minutes, and then loaded with DHE for 30 minutes at 37°C. Confocal images consisting of an 0.36 m optical slice through the approximate center of ganglia or cells were captured at a resolution of 1024x1024 pixels and stored for analysis using image analysis software

ImagePro® Plus (Media Cybernetics, Inc.). A scale bar was added to each image to indicate the size of neuron.

RNA isolation

See Chapter 2 Methods.

Reverse transcription polymerase chain reaction (RT-PCR)

See Chapter 2 Methods.

Regarding ET_B receptor (GenBank accession number NM_017333), primers for PCR are ATGACGCCACCCACTAAGAC and CACGAGGCATGATACAATCG and the length is195bp.

Western blotting

See Chapter 2 Methods.

Sympathetic ET-1 content measurement

CG were removed from rats, frozen in liquid nitrogen and stored at -80°C until ET-1 extraction. CG were homogenized in 1ml 1M acetic acid containing protease inhibitor and immediately heated to 100°C for 10 min followed by chilling on ice. The homogenate was centrifuged at 14,000g for 30 min at 4°C. The supernatant was dried in a Speed-Vac and reconstituted in 250µl calibrator diluents. ET-1 content was measured by the quantitative sandwich enzyme immunoassay technique using an ET-1 QuantiGlo Chemiluminescent Assay Kit (R&D systems) (Wang et al., 2002).

Data analysis

Data are presented as means ± standard error of the mean for the number of animals. Statistical significance was assessed by student t-test or one-way

ANOVA test with Dunnett's Multiple Comparison post-test using Prism 3.0 (GraphPad Software) (*P<0.05* indicating statistical significance).

Drugs

ET-1, S6c, BQ610 and BQ788 were obtained from Peninsula Laboratories and they were solubilized in deionized water or dimethylsulphoxide. DOCA salt was purchased from Sigma Chemical Co. and soluble in water.

Results

Fluorogenic detection of $O_2^{\cdot-}$ levels in inferior mesenteric ganglia

Cells were grouped by diameter so that the fluorescent intensity of both neurons and glia were quantified. Cells with diameter ranging from 15 to 35 μm were identified as neurons and from 5 to 10 μm as glia. Representative optical slices through Sham and DOCA-salt IMGs are shown in Figure 11 (n=Sham rats; n=4 DOCA-salt rats). $O_2^{\cdot-}$ levels were higher in IMG from a DOCA-salt rat (Figure 11B) than from a Sham rat (Figure 11A). Neurons displaying elevated $O_2^{\cdot-}$ levels were distributed throughout ganglia. Compared to Sham ganglia, fluorescent intensities of neurons and glia were 250% and 200% greater, respectively, in DOCA-salt ganglia (Figure 11C).

Effects of ET-1 administration on $O_2^{\cdot-}$ levels in sympathetic ganglia

$O_2^{\cdot-}$ levels were evaluated in IMG of Sham rats incubated with ET-1 or ET-1 plus the ET_B receptor antagonist BQ788 (n=4 rats in each group). Example optical slices of control and treated ganglia are shown in Figure 12. The control Sham IMG received no ET-1. $O_2^{\cdot-}$ levels in both neurons and glia were higher in

Figure 11: Superoxide levels in inferior mesenteric ganglia (IMG) neurons and glial cells from Sham and DOCA-salt rats. $O_2^{\cdot-}$ levels, indicated by DHE fluorescence intensity in confocal images of IMG, are higher in DOCA-salt rats than in Sham rats. Cells with a soma diameter of 15 to 35 μm were identified as neurons and cells with a diameter of 5 to 10 μm were identified as glial cells. Arrows indicate examples of neurons and arrowheads indicate examples of glial cells. (A) IMG from a Sham rat; (B) IMG from a DOCA-salt rat. (C) Comparison of mean fluorescence intensity of 146 Sham neurons to 70 DOCA-salt neurons and 510 Sham glial cells to 534 DOCA glial cells (n=4 Sham rats; n=4 DOCA-salt rats). Fluorescence of both types of cells was significantly ($P<0.05$) greater in DOCA ganglia compared to Sham. The calibration bar in B applies to both panels.

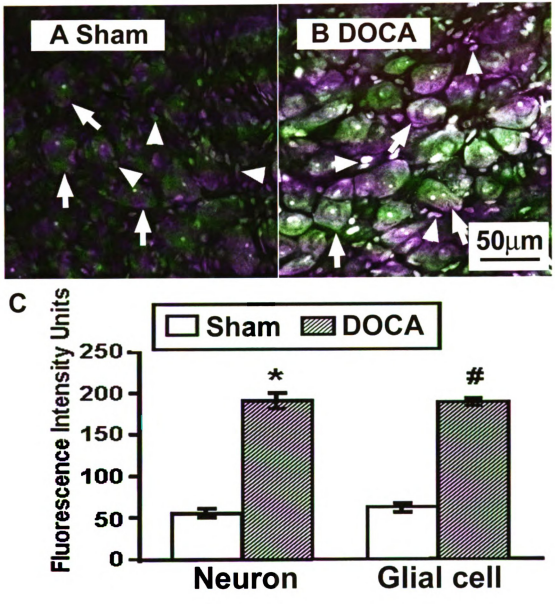
A Sham
B DOCA
50μm
C
Sham
DOCA
Fluorescence Intensity Units
250
200
150
100
50
0
*
#
Neuron
Glial cell

Figure 12: Superoxide levels in inferior mesenteric ganglia (IMG) neurons and glial cells from Sham rats treated with ET-1 or the ET_B receptor antagonist BQ788 plus ET-1. $O_2^{\cdot-}$ levels, indicated by DHE fluorescence intensity in confocal images, are higher in IMG *in vitro* treated with ET-1 than in control IMG, and this ET-1 induced increase is attenuated by BQ788 pretreatment. Cells with a soma diameter of 15 to 35 μm were identified as neurons and cells with a diameter of 5 to 10 μm were identified as glial cells. Arrows indicate examples of neurons and arrowheads indicate examples of glial cells. (A) Control Sham IMG; (B) IMG *in vitro* treated with ET-1; (C) IMG *in vitro* treated with the BQ788 plus ET-1; (D) Comparison of mean fluorescence intensity of 72 to 146 neurons or from 468 to 587 glial cells (n=4 Sham rats in each group). The significance ($P<0.05$) is indicated by * vs. control in neurons and by # vs. control in glial cells (n=4). The calibration bar in C applies to all panels.

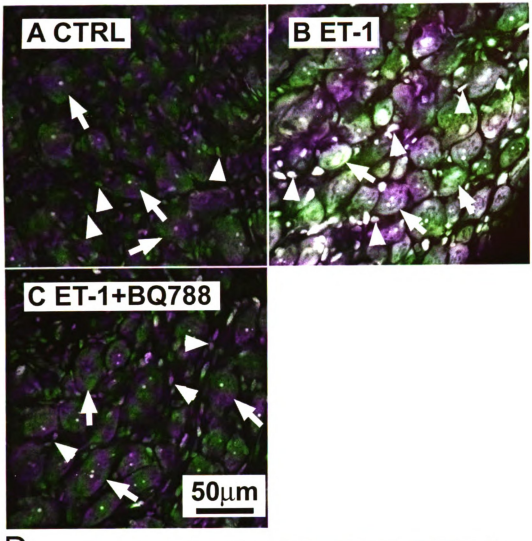
A CTRL
B ET-1
C ET-1+BQ788
50μm
D
CTRL
ET-1
ET-1+BQ788
Fluorescence Intensity Units
250
200
150
100
50
0
*
#
n=146
n=94
n=72
n=510
n=587
n=468
Neuron
Glial cell

the ET-1 treated IMG (Figure 12B) compared to the control (Figure 12A). ET-1 treatment resulted in 250% and 215% increase in fluorescent intensity in neurons and glia respectively (Figure 12D). Ganglia pretreated with ET_B receptor antagonist BQ788 followed by ET-1 treatment showed no increase in $O_2^{\cdot-}$ fluorescence (Figure 12C) compared to the control (Figure 12A). This indicates that ET-1 is acting on ET_B receptors to elevate $O_2^{\cdot-}$ levels in prevertebral sympathetic ganglia.

Fluorogenic detection of $O_2^{\cdot-}$ level in dissociated celiac ganglionic neurons and PC-12 cells

To determine whether ET-1 acts on neurons directly to elevate $O_2^{\cdot-}$ levels, we incubated freshly dissociated celiac ganglionic neurons from normal rats and differentiated PC-12 cells with ET-1 and measured $O_2^{\cdot-}$ levels. Representative confocal images of DHE fluorescence in treated cells are shown in Figure 13 and Figure 14 (n=4 dishes of cultured cells in each group). Changes in fluorescent intensity were quantified (Figure 15). Phase-contrast images of control cells were shown in Figure 13A and Figure 14A in parallel with the corresponding confocal images of control cells.

Compared with the control (Figure 13B, 38 ±4.5 Arbitrary Fluorescence Units (AFUs)), sympathetic ganglionic cells incubated with ET-1 showed a 400% increase in fluorescence indicating elevated $O_2^{\cdot-}$ levels (Figure 13C, 201 ±6.3 AFUs). The response was limited to cells with typical neuronal morphology with soma diameters ranging from 15 to 35μm. Of 175 neurons counted over four sets of independent experiments, 174 (99.5%) were DHE positive when they were

incubated with ET-1, whereas no control neurons (58 neurons counted) exhibited the fluorescence intensity above background levels. The ET-1-induced increase in the fluorescence intensity was attenuated to 45% by pretreatment with ET_B receptor antagonist BQ788 (Figure 13E, 90±6.5 AFUs). Pretreatment of cells with the ET_A receptor antagonist BQ610 did not reduce the ET-1-induced increase in the fluorescence intensity (Figure 13D, 213±9.5 AFUs). Likewise, cells treated with S6c showed a 400% increase in $O_2^{\cdot-}$ levels (Figure 13F, 203±5.7 AFUs). The S6c-induced increase was attenuated to 31% by pretreatment with ET_B receptor antagonist BQ788 (Figure 13H, 65 ±3.8 AFUs) but not by pretreatment with BQ610 (Figure 13G, 210±8 AFUs). These experiments indicate that ET_B receptors mediate superoxide anions production in sympathetic neurons.

The actions of ET receptors activation on $O_2^{\cdot-}$ generation were also evaluated in PC-12 cells, a catecholamine-secreting tumor cell line derived from chromaffin cells, that have functional ET receptors (Wilkes and Boarder, 1991b). ET-1 incubation induced a 225% increase in the fluorescence intensity (Figure 14C, 192±8 AFUs) compared to control cells (Figure 14B, 59 ±3 AFUs). The ET-1-induced increase in the fluorescence intensity was attenuated to 40% by pretreatment with ET_B receptor antagonist BQ788 (Figure 14E, 78±6 AFUs). Pretreatment with ET_A receptor antagonist BQ610 did not change the effects of ET-1 (Figure 14D, 209±8 AFUs). Cells treated with S6c showed a 270% increase in the fluorescence intensity (Figure 14F, 219±6 AFUs). This increase was not blocked by BQ610 (Figure 14G, 199±4.5 AFUs) but was attenuated to

Figure 13: ET_B receptor activation elevates $O_2^{\bullet-}$ levels in celiac ganglia (CG) neurons from normal rats *in vitro*. (A) Phase-contrast microscopy image of the control group. (B-H): Confocal fluorescent images of (B) Control group; (C) ET-1; (D) BQ610 plus ET-1; (E) BQ788 plus ET-1; (F) S6c; (G) BQ610 plus S6c; (H) BQ788 plus S6c. The calibration bar in H applies to all panels.

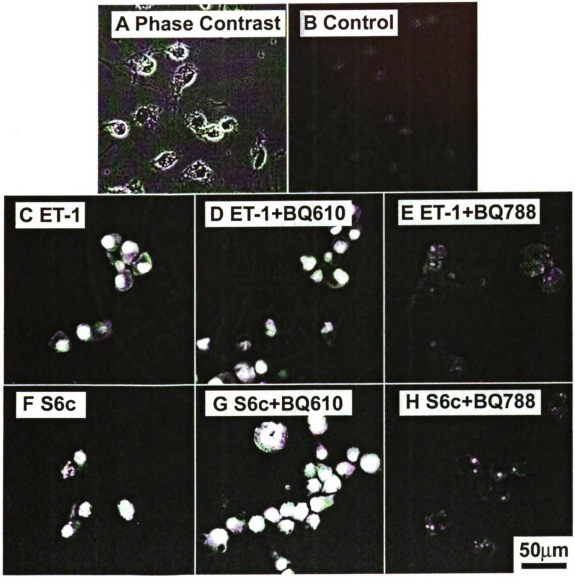
A Phase Contrast
B Control
C ET-1
D ET-1+BQ610
E ET-1+BQ788
F S6c
G S6c+BQ610
H S6c+BQ788
50μm

Figure 14: ET_B receptor activation elevates $O_2^{\bullet-}$ levels in differentiated PC-12 cells *in vitro*. (A) Phase-contrast microscopy image of the control group. (B-H): Confocal fluorescent images of (B) Control group; (C) ET-1; (D) BQ610 plus ET-1; (E) BQ788 plus ET-1; (F) S6c; (G) BQ610 plus S6c; (H) BQ788 plus S6c. The calibration bar in H applies to all panels.

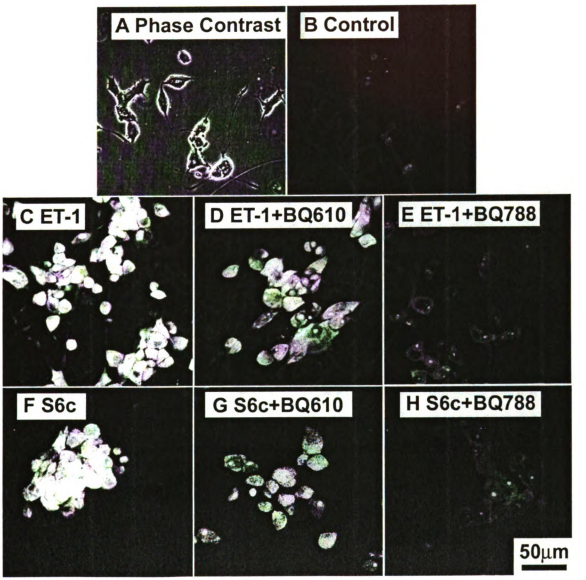
A Phase Contrast
B Control
C ET-1
D ET-1+BQ610
E ET-1+BQ788
F S6c
G S6c+BQ610
H S6c+BQ788
50μm

Figure 15: Effects of ET-1 receptor agonists and/or antagonists on $O_2^{\bullet-}$ levels in celiac ganglia (CG) neurons from normal rats and differentiated PC-12 cells *in vitro*. Results are expressed as mean±SE. Control cells received no agonist treatment. The significance (P<0.05) is indicated by * vs. control in CG cells and # vs. control in PC-12 cells.

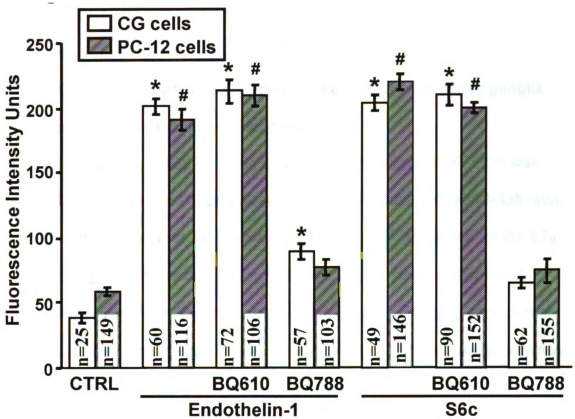
CG cells
PC-12 cells
Fluorescence Intensity Units
250
200
150
100
50
0
n=25
n=149
n=60
n=116
n=72
n=106
n=57
n=103
n=49
n=146
n=90
n=152
n=62
n=155
CTRL
BQ610
BQ788
BQ610
BQ788
Endothelin-1
S6c

34% by ET_B receptor antagonist BQ788 (Figure 14H, 74±10 AFUs). These results indicated that ET-1 acts on the ET_B receptors to induce $O_2^{\cdot-}$ production in PC-12 cells.

Measurement of ET-1 levels

In the crude protein fractions extracted from celiac ganglia of Sham and DOCA-salt rats (n= 4 Sham rats; n=4 DOCA-salt rats), there were 695.6±40.9 and 723.3±71.7 picograms of ET-1 per gram of wet weight of ganglia, respectively. They were not significantly different ($p>0.05$).

ET_B receptor mRNA level and protein expression in celiac ganglia from Sham and DOCA-salt hypertensive rats

Using primers designed stringently for the ET_B receptor, RT-PCR was done in CG of Sham and DOCA-salt rats (n= 4 Sham rats; n=4 DOCA-salt rats). The representative images are shown in Figure 16. PCR amplicons for the ET_B receptor and β-actin were detected in CG at the expected size, 195bp and 500bp, respectively, in 1.5% ethidium-stained agarose gel (Figure 16A). Equal densities of β-actin bands indicate the equal loading of samples. Band densities of PCR amplicons for the ET_B receptor from DOCA-salt rats were 32% higher than from Sham rats (Figure 16B). This result indicates that ET_B receptor mRNA levels were upregulated in celiac ganglia from DOCA-salt hypertensive rats compared to Sham rats.

Levels of ET_B receptor protein were measured in CG of Sham and DOCA-salt rats (n= 4 Sham rats; n=4 DOCA-salt rats) using the western blotting analysis. As shown in Figure 17A, a single 40KD band was present in both

Figure 16: Elevated ET_B receptor mRNA levels in celiac ganglia (CG) from DOCA-salt rats. Two samples from four Sham and DOCA salt animals were run on the same ethidium bromide–stained agarose gel to show PCR amplicons for the ET_B receptor (195bp) and β-actin (500bp), seen in (A). No cDNA template control (NTC) was performed as a negative control. Optical densities of positive bands were quantified and mean values are shown in panel B, which is 32% higher in DOCA rats than in Sham rats. The significance ($P<0.05$) is indicated by * vs. Sham rats (n=4).

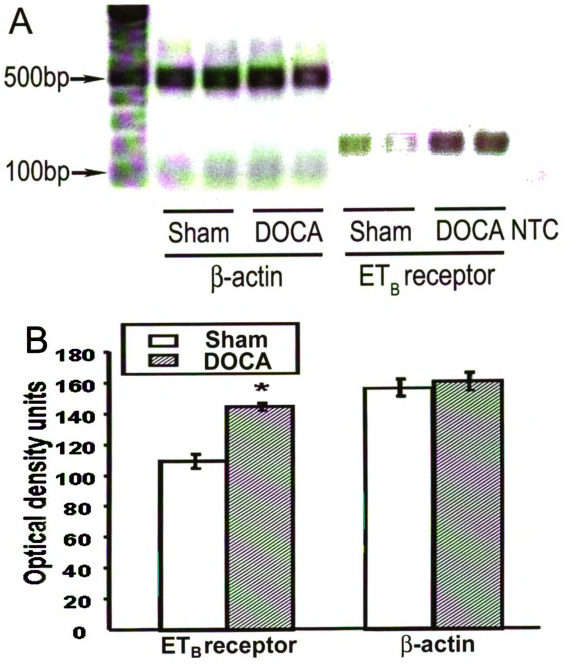
A
500bp
100bp
Sham
DOCA
Sham
DOCA
NTC
β-actin
ET$_B$ receptor
B
Sham
DOCA
Optical density units
180
160
140
120
100
80
60
40
20
0
*
ET$_B$ receptor
β-actin

Figure 17: Elevated ET_B receptor protein levels in celiac ganglia (CG) from DOCA-salt rats. Immunoblotting for the ET_B receptor in CG from Sham and DOCA-salt rats shows a single 40KDa band (A). Optical densities of bands were quantified and densities were normalized to Sham. The change in ET_B receptor protein levels was determined by the ratio of optical densities of bands from DOCA-salt rats to those from Sham rats. The percentage change is shown in panel B, which is 20% higher in DOCA rats than in Sham rats. The significance ($P<0.05$) is indicated by * vs. Sham rats (n=4).

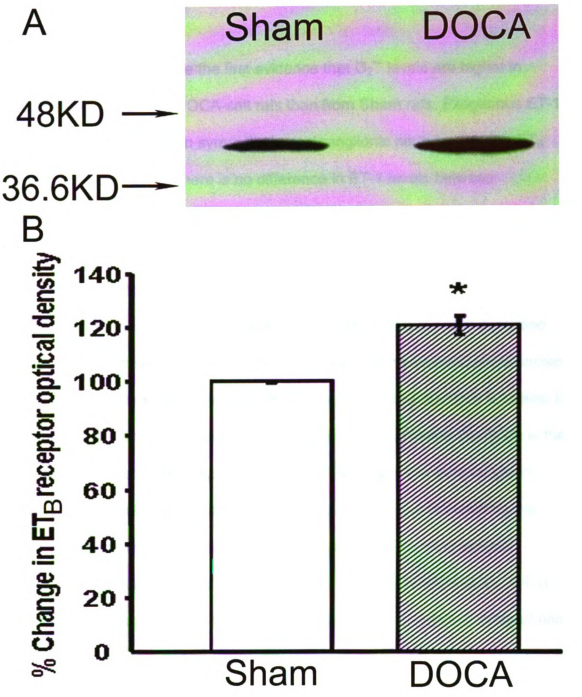
A
Sham
DOCA
48KD
36.6KD
B
% Change in ET_B receptor optical density
140
120
100
80
60
40
20
0
*
Sham
DOCA

DOCA-salt and Sham rats. The density of ET_B band was 20% higher in DOCA-salt ganglia than in Sham ganglia (Figure 17B). This indicates that the level of ET_B receptor protein is upregulated in sympathetic ganglia of DOCA-salt rats.

Discussion

These results provide the first evidence that $O_2^{\bullet-}$ levels are higher in sympathetic ganglia from DOCA-salt rats than from Sham rats. Exogenous ET-1 stimulates $O_2^{\bullet-}$ production in sympathetic postganglionic neurons through ET_B receptor activation. While there is no difference in ET-1 levels between sympathetic ganglia from DOCA-salt rats compared to Sham rats, the levels of ET_B receptor mRNA and protein are upregulated in sympathetic celiac ganglia from DOCA-salt rats.

Although the actions of $O_2^{\bullet-}$ on blood vessels have been well-described, the effects of $O_2^{\bullet-}$ production in sympathetic ganglia are not known, nor is known how elevated $O_2^{\bullet-}$ production in sympathetic neurons of hypertension is related to the pathogenesis of hypertension. Administration of H_2O_2, one of the ROS, in the vicinity of sympathetic preganglionic neurons projecting to the adrenal gland results in the activation of sympathetic preganglionic neurons innervating the adrenal gland and the subsequent release of catecholamine from adrenal medulla, which in turn elevates blood pressure and heart rate (Lin et al., 2003). This opens the possibility that a change in the redox environment of sympathetic ganglionic neurons induced by $O_2^{\bullet-}$ may activate sympathetic neurons and result in vasoconstriction and hypertension. $O_2^{\bullet-}$ may also indirectly modulate the excitability of sympathetic neurons by several mechanisms. One possible

mechanism is the ability of $O_2^{\bullet-}$ to modulate sympathetic excitability by quenching or inactivating nitric oxide (NO) (Li et al., 2003), which is known to exist in the sympathetic nervous system (Ceccatelli et al., 1994). We have shown previously that NO increases a Ca^{++}-activated K^+ current in isolated sympathetic neurons, an effect that would reduce the firing rate. By causing a reduction in ganglionic NO levels, $O_2^{\bullet-}$ would eliminate this inhibitory effect of NO and this would result in an increased excitability of sympathetic neurons (Browning et al., 1998). Another possible mechanism is that $O_2^{\bullet-}$ may act as an intracellular second messenger and regulate gene expression of antioxidant enzymes, such as SOD (Park et al., 1998) and catalase (Sampath et al., 1994), in sympathetic neurons as it does in blood vessels (Griendling et al., 2000).

In sympathetic ganglia from Sham rats, incubation with ET-1 elevated $O_2^{\bullet-}$ production to the levels found in ganglia of DOCA-salt rats. Similarly, ET-1 increases intracellular $O_2^{\bullet-}$ production in dissociated ganglionic neurons. This demonstrates that the mechanisms responsible for ET-1 induced $O_2^{\bullet-}$ generation are endogenous to neuron cell bodies and do not require the presence of vasculature or glia. Sympathetic neurons projecting to mesenteric arteries are distinct from neurons projecting to mesenteric veins by their localization, neurochemical phenotypes, and electrophysiological properties (Browning et al., 1999). There was no evidence that subpopulations of neurons were affected differently because the increased $O_2^{\bullet-}$ signal was evenly distributed throughout the IMG, including both ganglionic neurons and glia. Likewise, when dissociated neurons were incubated with ET-1, $O_2^{\bullet-}$ levels increased in all neurons. By

contrast, in the central nervous system, Ang II administration increases $O_2^{\cdot-}$ in 40% of neurons in the lamina terminalis (Zimmerman et al., 2002). Furthermore, it appears that the glia in sympathetic ganglia also have the capacity to generate $O_2^{\cdot-}$, which is similar to the increased superoxide production mediated through NAD(P)H oxidase in microglia of the ventral mesencephalon in Parkinson's disease (Gao et al., 2003).

ET-1 levels in protein extracts of celiac ganglia were the same in Sham and DOCA-salt rats. In contrast, in superior cervical ganglia of SHRs, there is an increased intracellular ET-1 immunoreactivity and mRNA (Milner et al., 2000b). This may reflect different ganglia and/or different hypertensive models. ET-1 can be released from cultured sympathetic neurons (Damon, 1999) analogous to endothelial cells. The crude ganglionic protein extracts included both intracellular and extracellular ET-1, and therefore didn't differentiate between stored and released ET-1. Particularly the higher sympathetic outflow present in DOCA-salt hypertensive rats (Reid et al., 1975) would result in elevated ET-1 release.

Two G-protein coupled ET-1 receptors, ET_A and ET_B, have been identified and cloned (Arai et al., 1990;Sakamoto et al., 1991); both are widely distributed in vascular tissues (Watts et al., 2002), the central nervous system including neurons and glia (Hama et al., 1992;Sullivan and Morton, 1996), the sympathetic nervous system (Damon, 1999), and PC-12 cells (Watanabe et al., 1997). The activation of ET receptor subtypes may be tissue specific. Elevated $O_2^{\cdot-}$ production in the vasculature of DOCA-salt hypertension is mediated by ET_A receptors (Li et al., 2003) and $O_2^{\cdot-}$ production in sympathetic ganglia, which

include neurons and glia, dissociated sympathetic neurons and PC-12 cells, is elevated by the activation of ET_B receptors, but not by ET_A receptors. ET_A receptor knockout mice have developmental defects in great vessels (Kurihara et al., 1999). By contrast, homozygous ET_B receptor gene knockout mice have lethal developmental defects in the enteric nervous system (Gershon, 1995;Kurihara et al., 1999). In addition, the ET_B receptor is essential in neural crest development (Gershon, 1995), from where neurons and glia of the sympathetic nervous system and the enteric nervous system are differentiated.

The levels of ET_B receptor mRNA and protein were upregulated in celiac ganglia from DOCA-salt rats when compared to Sham rats. Upregulation of ET_B receptors also occurs in the vasculature in DOCA-salt hypertension (Watts et al., 2002) where it is thought to be important in mediating the enhanced contractile response to ET-1 that occurs in veins but not in arteries. A similar mechanism may occur in ET-1-mediated increase in $O_2^{\bullet-}$ production in sympathetic ganglia. In the face of similar ET-1 levels in normotensive and hypertensive ganglia, upregulated ET_B receptors may be mediating the enhanced $O_2^{\bullet-}$ production. However, the possibility of upregulated activity or mRNA expression of NAD(P)H oxidase cannot be ruled out (Fukui et al., 1997a). For example, Ang II upregulates vascular NAD(P)H oxidase subunits nox1, nox4, $gp91^{phox}$, and $p22^{phox}$ mRNA expression; an effect that is thought to mediate Ang II stimulated $O_2^{\bullet-}$ production (Higashi et al., 2003).

Perspectives

This study demonstrates that $O_2^{\bullet-}$ is elevated in prevertebral sympathetic

ganglia in DOCA-salt hypertensive rats. Furthermore, we have identified ET-1 as a stimulus to increase $O_2^{\cdot-}$ levels in sympathetic postganglionic neurons and PC-12 cells, and this increase can be attenuated by pretreatment wih specific ET_B receptor antagonist BQ788. Finally, ET-1 may be a potent stimulus for the elevation of $O_2^{\cdot-}$ levels in sympathetic ganglia in DOCA-salt hypertension, an effect that is mediated by the upregulated ET_B receptor pathway. We propose that $O_2^{\cdot-}$ production evoked by ET-1 may play roles in the increased sympathetic excitability and pathogenesis in the DOCA-salt hypertension. We further speculate that ROS in the sympathetic nervous system may be an important target for therapeutic treatment of hypertension.

CHAPTER 3B: GENERATION OF $O_2^{\cdot-}$ IN SYMPATHETIC GANGLIA THROUGH NAD(P)H OXIDASE

Introduction

Vascular endothelial cells, smooth muscle cells and fibroblasts generate ROS, such as $O_2^{\cdot-}$ and hydrogen peroxide (H_2O_2), to play critical roles in the normal function of vascular cells, including the modulation of redox-sensitive signaling pathways and gene expression, or in the pathophysiology of hypertension and atherosclerosis (Griendling et al., 2000;Lassegue and Clempus, 2003). In several models of hypertension, there is a profound increase in vascular $O_2^{\cdot-}$ (Sedeek et al., 2003;Somers et al., 2000b) and this increased $O_2^{\cdot-}$ may impair endothelium-dependent relaxation by inactivating the potent endogenous vasodilator nitric oxide (NO) and result in hypertension (Griendling et al., 2000;Lassegue and Clempus, 2003). ROS can also induce cardiovascular related gene expression, such as adhesion molecules and vasoactive substances. The cytokine interleukin 1 β (IL-1 β) activates vascular cell adhesion molecule-1 (VCAM-1) gene expression through a mechanism that is repressed approximately 90% by antioxidants pyrrolidine dithiocarbamate (PDTC) and N-acetylcysteine (NAC) (Marui et al., 1993).

In hypertension, many factors are potentially responsible for changes occurring in the sympathetic nervous system, such as the increased sympathetic nerve activity along with more released vasoconstrictive neurotransmitters, norepinephrine and ATP, from nerve terminals. One of the factors might be ROS. ROS not only contribute to the oxidative damage and cell death in the nervous

system (Pong, 2003), but also serve as signaling molecules to activate kinase pathways or mediate the effects of neuroactive substances (Griendling et al., 2000;Lassegue and Clempus, 2003). Angiotensin II(Ang II)/ROS signaling system mediates the action of Ang II to increase blood pressure(Zimmerman et al., 2002). H_2O_2 can activate PKC pathway (Droge, 2002), which is capable of facilitating neurotransmitter release from nerve terminals (Majewski and Iannazzo, 1998). Recently we showed that sympathetic neurons generate $O_2^{\cdot-}$ (Dai et al., 2004b), and that $O_2^{\cdot-}$ production is elevated in hypertension.

NAD(P)H oxidase was first found and cloned in phagocytes. It comprises a membrane-bound cytochrome b_{558} composed of a $p22^{phox}$-$gp91^{phox}$ heterodimer and several cytosolic subunits ($p47^{phox}$, $p40^{phox}$, $p67^{phox}$, and Rac). In phagocytes, this enzyme is normally silent, but upon stimulation, cytosolic subunits are phosphorylated and translocate to the membrane and associate with cytochrome b_{558}, resulting in the rapid activation of oxidase. NADPH oxidase in non-phagocytic cells such as endothelial cells and vascular smooth muscle cells exhibits significant differences from the phagocytic enzyme. In particular, recent studies have indicated the presence of a number of homologues of $gp91^{phox}$, termed NOXs (Lambeth et al., 2000), and it has been suggested that the substitution of $gp91^{phox}$ (also known as NOX2) by NOX1 or NOX4 may account for different behaviors of non-phagocytic enzymes (Lassegue and Clempus, 2003).

NAD(P)H oxidase is present in mouse sympathetic neurons and cortical neurons and astrocytes contributing to neuronal apoptosis (Noh and Koh,

2000;Tammariello et al., 2000). However, it was not specified which sympathetic ganglia was studied and if the NAD(P)H oxidase was also present in rat sympathetic ganglia, especially in sympathetic ganglia innervating the splanchnic circulation, which stores 38% of total blood and up to 64% of that can be mobilized by the direct stimulation of sympathetic nerves due to their rich innervation (Greenway, 1983b).

We investigated the presence of rat NAD(P)H oxidase subunits in one-day cultured sympathetic neurons and differentiated PC-12 cells with sympathetic neuronal phenotype. We also investigated if sympathetic NAD(P)H oxidase was functional by measuring $O_2^{\cdot-}$ production after the activation of NAD(P)H oxidase by an PKC activator, PMA. Due to the increased $O_2^{\cdot-}$ production in sympathetic ganglia of DOCA-salt hypertensive rats (Dai et al., 2004b), we further examined the effects of NAD(P)H oxidase inhibitor on the increased $O_2^{\cdot-}$ production and the NAD(P)H oxidase activity in sympathetic ganglia of DOCA-salt hypertensive rats.

Methods

Animals

See Chapter 2 Methods.

The mean arterial pressure for the DOCA-salt rats and Sham rats was 204.5.3±8.1 mmHg and 121.8±2.4 mmHg respectively.

Tissue harvest and cell culture

See Chapter 2 Methods.

NAD(P)H oxidase is the key enzyme in phagocytes (Babior et al., 2002) and blood cells containing phagocytes were used as the positive control to

examine the presence of $gp91^{phox}$ in PCR amplification. After normal rats were sacrificed, the blood was withdrawn from the heart and stored in EDTA coated tubes. The blood was centrifuged at 2000*xg* for 20 minutes in order to collect the lower layer blood cells and blood cells were stored at –80°C.

RNA isolation

See Chapter 2 Methods.

Reverse transcription polymerase chain reaction (RT-PCR)

See Chapter 2 Methods.

Primer sequences are shown in Table 2.

Sequencing

See Chapter 2 Methods.

Measurement of superoxide anion generation

See Chapter 3A Methods.

Cells were divided into 3 groups: control (no treatment), treated with the PKC activator, PMA (1ug/ml), as the agonist, and treated with PMA plus pretreatment with NADPH oxidase inhibitor apocynin. IMGs were divided from 3 groups: Sham rats, DOCA-salt hypertensive rats, and DOCA-salt hypertensive rats incubated with apocynin (10^{-7}mol/L) for 45 minutes.

Table 3.1: Primer sequences for NAD(P)H oxidase subunits gp91^{phox}, NOX1, p47^{phox} and p22^{phox}, and β-actin.

	Sequence	Amplicon Length (bp)	NCBI accession Number
gp91^{phox}	For:5' GAT CTT CTT CAT CGG CCT TG 3'	340	AJ295950
	Rev:5' AGG ATG AGT GAC CAC CTT GG 3'		
NOX1	For:5' GTG GAG TGG TGT GTG AAT GC 3'	324	AF298656
	Rev:5' TCC ACG TAC AAT TCG CTC AG 3'		
p47^{phox}	For:5' GGC CAA AGA TGG CAA GAA TA 3'	221	AF260779
	Rev:5' TGT CAA GGG GCT CCA AAT AG 3'		
p22^{phoxphox}	For:5' TTG TTG CAG GAG TGC TCA TC 3'	282	RNO295951
	Rev:5' TAG GCT CAA TGG GAG TCC AC 3'		
β-actin (Epperson et al., 2000)	For:5' GGC TAC AGC TTC ACC ACC AC 3'	500	V01217
	Rev:5' TAC TCC TGC TTG CTG ATC CAC 3'		

Measurement of NAD(P)H oxidase activity

Fluorescence spectrometry of tissue $O_2^{\cdot-}$ production was performed by using a modification of methods described by Benov et al (Benov et al., 1998) and Zou et al (Zou et al., 2001). Oxidase activity in cells may be limited by the available cytosolic concentrations of NADH and NADPH (Lassegue and Clempus, 2003), and when measuring vascular cells NAD(P)H oxidase activity, the increase in $O_2^{\cdot-}$ production can be observed only when NAD(P)H oxidase substrates were added to whole cells or tissues (Lassegue and Clempus, 2003). In a microtiter plate, freshly prepared CG homogenates were incubated with DHE (10µmol/L), salmon testes DNA (0.5mg/mL, Qiagen) and the corresponding substrate for NAD(P)H oxidase, β-NADH (0.1mmol/L) or β-NADPH (0.1mmol/L), for 30 minutes at 37°C. The ethidium-DNA fluorescence was measured at an excitation of 485±40nm and an emission of 590±35nm using a Biotek FL600 fluorescence plate reader (Bio-Tek Instruments, Inc.). Salmon testes DNA was added to bind to ethidium and consequently stabilize ethidium fluorescence, thereby increasing the sensitivity of $O_2^{\cdot-}$ measurement (>40-fold) (Yang and Zou, 2003;Zou et al., 2001). The enzyme activity was expressed as fluorescence units per minute per milligram tissue homogenate.

Data analysis

See Chapter 3A Methods.

Drugs

Deoxycorticosterone acetate, PMA, apocynin, β-NADH and β-NADPH were purchased from Sigma Chemical Co.. DHE was purchased from Molecular

Probes and salmon testes DNA was purchased from Stratagene.

Results

mRNA expression of NAD(P)H oxidase in dissociated celiac ganglionic neurons and differentiated PC-12 cells

PCR amplicons of NAD(P)H oxidase subunits $p47^{phox}$, $p22^{phox}$, and NOX1 were detected in dissociated CG neurons (Figure 18A) and differentiated PC-12 cells (Figure 18B) at the expected sizes of 221bp, 282bp, and 324bp, respectively. However, the presence of $gp91^{phox}$ mRNA was not detected in dissociated CG neurons and differentiated PC-12 cells. Even though the quality of $gp91^{phox}$ primers was confirmed by the presence of $gp91^{phox}$ RT-PCR amplicon of expected size, 340bp, from blood cells mRNA (Figure 18C). The sequenced PCR amplicons were aligned in GenBank. Greater than 99% of sequenced amplicons of $p47^{phox}$, $p22^{phox}$ and NOX1 in CG neurons and PC-12 cells and $gp91^{phox}$ in blood cells matched published sequences. These results indicate the presence of mRNAs of NAD(P)H oxidase subunits $p47^{phox}$, $p22^{phox}$, and NOX1, but not $gp91^{phox}$, in dissociated sympathetic postganglionic neurons and differentiated PC-12 cells.

Fluorogenic detection of $O_2^{\bullet-}$ levels in dissociated celiac ganglionic neurons and PC-12 cells

To determine whether the activation of PKC generates $O_2^{\bullet-}$ production in sympathetic neurons, and if so, if this PKC activated $O_2^{\bullet-}$ generation is mediated through NAD(P)H oxidase, we examined the effects of PMA or PMA plus apocynin on $O_2^{\bullet-}$ production in sympathetic neurons and differentiated PC-12

Figure 18: NAD(P)H oxidase subunits $p47^{phox}$, $p22^{phox}$, and NOX1, but not $gp91^{phox}$, are present in dissociated celiac ganglia (CG) neurons and PC-12 cells. PCR amplicons from dissociated CG neurons (A) and differentiated PC-12 cells (B) were run on ethidium bromide–stained agarose gels to show PCR amplicons for $p47^{phox}$ (221bp), $p22^{phox}$ (282bp), NOX1 (324bp) and β-actin (500bp). PCR amplicons from dissociated CG neurons, differentiated PC-12 cells and blood cells were run on ethidium bromide–stained agarose gels and showed the presence of $gp91^{phox}$ (340bp) in blood cells, but not in dissociated CG neurons and differentiated PC-12 cells, even though all three samples showed positive bands for β-actin (500bp) (C). No cDNA template control (NTC) was performed as a negative control (A-C).

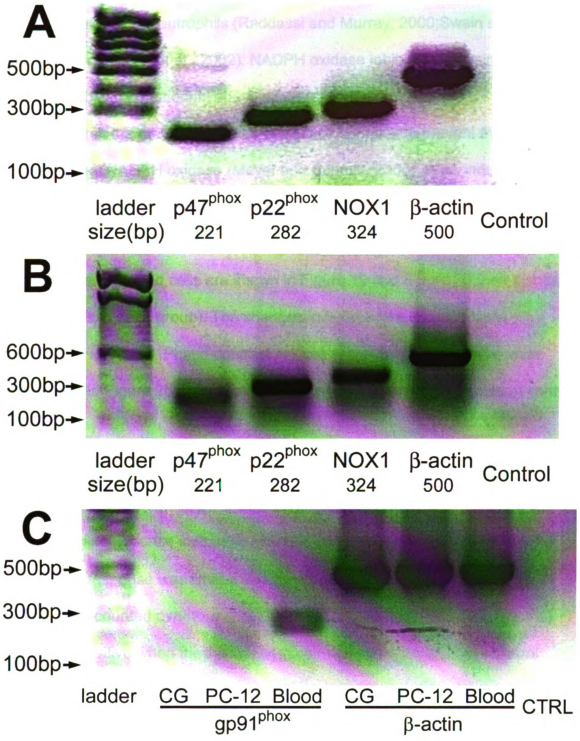
A
500bp
300bp
100bp
ladder size(bp)
p47phox 221
p22phox 282
NOX1 324
β-actin 500
Control
B
600bp
300bp
100bp
ladder size(bp)
p47phox 221
p22phox 282
NOX1 324
β-actin 500
Control
C
500bp
300bp
100bp
ladder
CG PC-12 Blood
gp91phox
CG PC-12 Blood
β-actin
CTRL

cells. PMA activates the PKC pathway to phosphorylate $p47^{phox}$ and the phosphorylated $p47^{phox}$ translocates to the cell membrane and form a functional NAD(P)H oxidase in neutrophils (Raddassi and Murray, 2000;Swain et al., 1997) and vascular cells (Li et al., 2002). NADPH oxidase inhibitor apocynin is a methoxy-substituted catechol and it impedes the assembly of $p47^{phox}$ and $p67^{phox}$ subunits within the membrane NADPH oxidase complex to prevent the formation of a functional NADPH oxidase (Meyer and Schmitt, 2000). PMA induced $O_2^{\cdot-}$ production is almost completely inhibited by treatment with apocynin in rat neutrophils (Salmon et al., 1998). Representative confocal images of DHE fluorescence in treated cells are shown in Figure 19 and Figure 20 (n=4 dishes of cultured cells in each group). The changes in fluorescent intensity were quantified (Figure 21). Phase-contrast images of control cells were shown in Figure 19 and Figure 20 in parallel with corresponding confocal images of control cells.

Compared with the control (Figure 18A, 46.6±2.5 Arbitrary Fluorescence Units (AFUs)), sympathetic ganglionic cells incubated with PMA showed a 317% increase in fluorescence indicating elevated $O_2^{\cdot-}$ levels (Figure 18B, 194.4±2.7 AFUs). The response was limited to cells with typical neuronal morphology. Of 121 neurons counted over four sets of independent experiments, 119 (98.5%) were DHE positive when they were incubated with PMA, whereas no control neurons (45 neurons counted) exhibited fluorescence intensity above control levels. Pretreatment with apocynin attenuated PMA-induced increase in fluorescence intensity to the control level (Figure 20C, 47.4±3.0 AFUs). PC-12

Figure 19: NAD(P)H oxidase activation by PMA elevates $O_2^{\cdot-}$ levels in dissociated celiac ganglia (CG) neurons *in vitro* and this increase is attenuated by pretreatment with NADPH oxidase inhibitor apocynin. Left column: Confocal fluorescent images of (A) Control group; (B) PMA; (C) PMA plus apocynin; right column: Phase-contrast microscopy images of (A) Control group; (B) PMA; (C) PMA plus apocynin. The calibration bar in C applies to all panels.

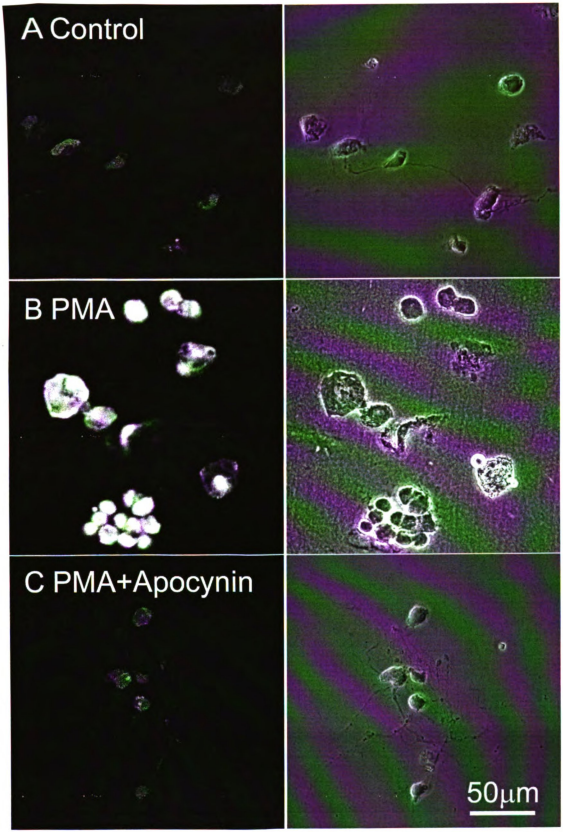
A Control
B PMA
C PMA+Apocynin
50μm

Figure 20: NAD(P)H oxidase activation by PMA elevates $O_2^{\cdot-}$ levels in differentiated PC-12 cells *in vitro* and this increase is attenuated by pretreatment with NADPH oxidase inhibitor apocynin. Left column: Confocal fluorescent images of (A) Control group; (B) PMA; (C) PMA plus apocynin; right column: Phase-contrast microscopy images of (A) Control group; (B) PMA; (C) PMA plus apocynin. The calibration bar in C applies to all panels.

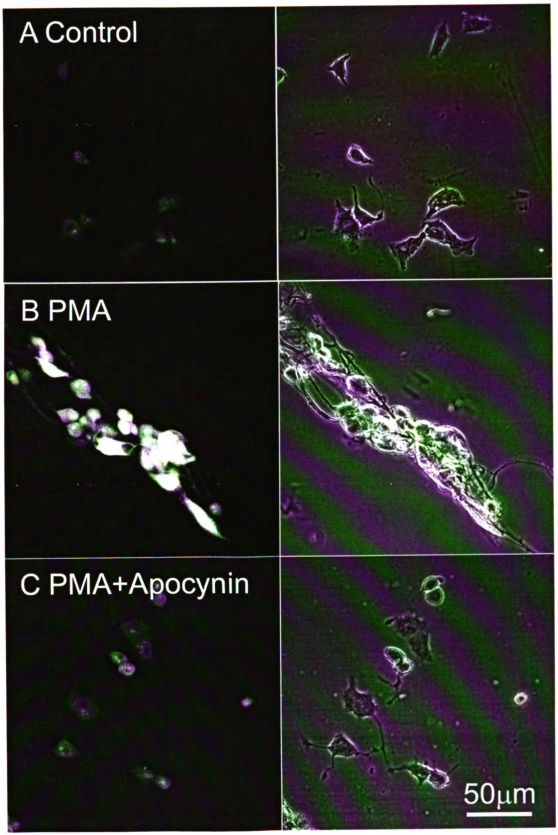
A Control
B PMA
C PMA+Apocynin
50μm

Figure 21: Effects of NAD(P)H oxidase activation on $O_2^{\bullet-}$ levels in celiac ganglia (CG) neurons and PC-12 cells *in vitro*. Results are expressed as mean±SE. Control cells received no agonist treatment. The significance ($P<0.05$) is indicated by # vs. control in CG cells and PC-12 cells (n=4 dishes in each treatment group).

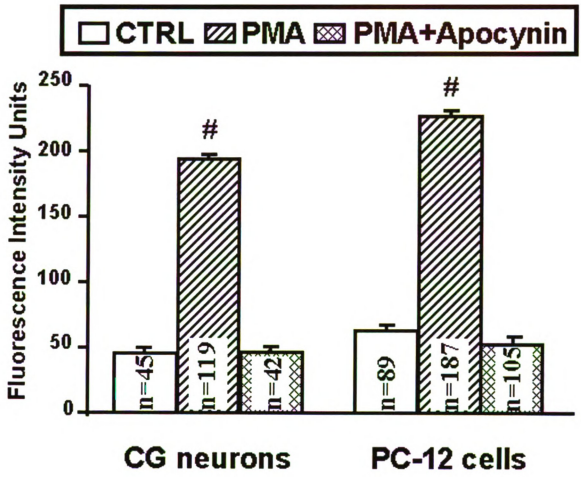
CTRL
PMA
PMA+Apocynin
Fluorescence Intensity Units
250
200
150
100
50
0
#
#
n=45
n=119
n=42
n=89
n=187
n=105
CG neurons
PC-12 cells

cells incubated with PMA showed a 254% increase in fluorescence intensity (Figure 20B, 226.6±1.5 AFUs) compared to control cells (Figure 20A, 64.1±2.6 AFUs). The PMA-induced increase in the fluorescence intensity was attenuated to 23.2% by pretreatment with apocynin (Figure 20C, 52.7±1.6 AFUs). These experiments indicate that PKC activation induces $O_2^{\cdot-}$ production in sympathetic postganglionic neurons and differentiated PC-12 cells, and this is mediated by NAD(P)H oxidase activation.

Fluorogenic detection of $O_2^{\cdot-}$ levels in inferior mesenteric ganglia

$O_2^{\cdot-}$ levels were evaluated in intact IMG (n=4 rats in each group) incubated with DHE in vitro. $O_2^{\cdot-}$ levels in both neurons and glial cells were greater in IMG from a DOCA-salt rat (Figure 22B) than from a Sham rat (Figure 22A), 267% and 186% fluorescent intensity higher in neurons and glial cells respectively (Figure 22D). Neurons displaying elevated $O_2^{\cdot-}$ levels were distributed throughout the ganglia. DOCA IMG *in vitro* treated with apocynin showed no difference in $O_2^{\cdot-}$ fluorescence (Figure 22C) compared to Sham IMG (Figure 22A). This indicates that there is higher $O_2^{\cdot-}$ production in neurons and glia in prevertebral sympathetic ganglia from DOCA than from Sham rats and the increased $O_2^{\cdot-}$ production in rat prevertebral sympathetic ganglia from DOCA rats can be blocked by treatment with NAD(P)H oxidase inhibitor apocynin.

NAD(P)H oxidase activity in CG from Sham and DOCA-salt hypertensive rats

Tissue homogenates of CG from Sham rats and DOCA-salt hypertensive rats (n=6 Sham rats; n=6 DOCA-salt hypertensive rats) were incubated with

Figure 22: $O_2^{\cdot-}$ levels, indicated by DHE fluorescence intensity in confocal images of inferior mesenteric ganglia (IMG), are higher in IMG from DOCA-salt rats than from Sham rats, and this increase is attenuated by pretreatment with NADPH oxidase inhibitor apocynin. Cells with a soma diameter of 15 to 35 μm were identified as neurons and cells with a diameter of 5 to 10 μm were identified as glial cells. Arrows indicate examples of neurons and arrowheads indicate examples of glial cells. (A) IMG from a Sham rat; (B) IMG from a DOCA-salt rat; (C) Apocynin pretreated IMG from a DOCA-salt hypertensive rat; (D) Comparison of mean fluorescence intensity of 157 Sham neurons to 70 DOCA-salt neurons and 496 Sham glial cells to 543 DOCA glial cells (n=4 rats in each group). Fluorescence of both types of cells was significantly ($P<0.05$) greater in DOCA ganglia compared to Sham. The calibration bar in C applies to all panels.

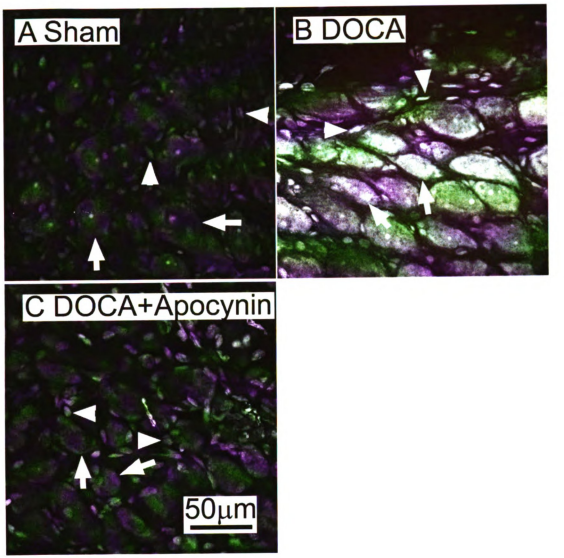
A Sham
B DOCA
C DOCA+Apocynin
50μm
D
Sham
DOCA
DOCA+Apocynin
Fluorescence Intensity Units
250
200
150
100
50
0
#
#
n=157
n=70
n=62
n=496
n=505
n=543
Neuron
Glial cell

Figure 23: NAD(P)H oxidase activity is higher in celiac ganglia (CG) from DOCA-salt hypertensive rats than from Sham rats. NAD(P)H oxidase activities of CG from Sham rats and DOCA-salt hypertensive rats are 482.7±42 and 723.3±42 fluorescence intensity units per minute per milligram wet tissue respectively when using β-NADH as the NAD(P)H oxidase substrate, and 586.3±19.0 and 1047.3±37.7 fluorescence intensity units per minute per milligram wet tissue respectively when using β-NADPH as the NAD(P)H oxidase substrate. The significance ($P<0.05$) is indicated by * vs. Sham (n=6 Sham rats; n=6 DOCA-salt hypertensive rats).

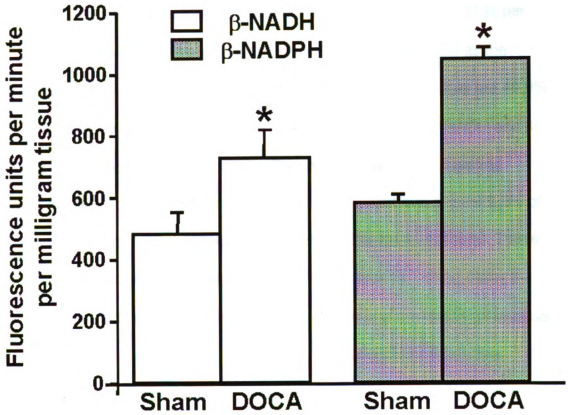
Fluorescence units per minute per milligram tissue
1200
1000
800
600
400
200
0
β-NADH
β-NADPH
*
*
Sham
DOCA
Sham
DOCA

β-NADH or β-NADPH, which are substrates for NAD(P)H oxidase and the formation of $O_2^{\cdot-}$ was detected in reaction mixtures. $O_2^{\cdot-}$ production of homogenates from DOCA ganglia was greater than it from Sham ganglia regardless of substrates (Figure 23). NAD(P)H oxidase activities of Sham and DOCA homogenates are 482.7±42 and 723.3±42 fluorescence intensity units (FIUs) per minute per milligram wet tissue respectively when using β-NADH as the NAD(P)H oxidase substrate, and 586.3±19.0 and 1047.3±37.7 FIUs per minute per milligram wet tissue respectively when using β-NADPH as the NAD(P)H oxidase substrate (Figure 23). NAD(P)H oxidase activities are 49.9% and 78.6% higher in DOCA CG than in Sham CG when using β-NADH and β-NADPH as the substrate, respectively. The control group without adding substrates showed very low fluorescence intensity, which was around 6.0% of the average of experimental groups and considered to be background. These results indicate that tissue homogenates of CG produce $O_2^{\cdot-}$ using either β-NADH or β-NADPH as NAD(P)H oxidase substrates and the NAD(P)H oxidase enzymatic activity is greater in CG from DOCA rats than from Sham rats regardless of substrates.

Discussion

These results provide the first evidence that mRNAs of NAD(P)H oxidase subunits NOX1, $p22^{phox}$ and $p47^{phox}$, but not $gp91^{phox}$, are present in rat sympathetic postganglionic neurons and differentiated PC-12 cells. The activation of NAD(P)H oxidase by exogenous PMA administration in sympathetic postganglionic neurons and PC-12 cells resulted in an increased $O_2^{\cdot-}$ production,

which can be blocked by pretreatment with NAD(P)H oxidase inhibitor apocynin. $O_2^{\cdot-}$ production was higher in sympathetic ganglia from DOCA-salt rats than from Sham rats, and this increase can be reduced by treatment with NAD(P)H oxidase inhibitor apocynin. The increased $O_2^{\cdot-}$ production in sympathetic ganglia from DOCA-salt hypertensive rats may rise from an upregulated NAD(P)H oxidase activity.

Presence of mRNA of NADPH oxidase in sympathetic CG neurons

NAD(P)H oxidase mRNA is present in rat sympathetic ganglionic neurons and differentiated PC-12 cells. Our previous study observed $O_2^{\cdot-}$ signal in rat sympathetic ganglia using DHE staining method (Dai et al., 2004b), however, it is not known which enzyme is responsible for $O_2^{\cdot-}$ production in sympathetic ganglia. NAD(P)H oxidase is firstly detected in phagocytes for $O_2^{\cdot-}$ generation and it includes subunits of $p22^{phox}$, $p47^{phox}$, $p67^{phox}$, $p40^{phox}$ and $gp91^{phox}$ (Babior et al., 2002). Vascular cells also contain phagocyte-type NAD(P)H oxidase (Griendling et al., 2000;Lassegue and Clempus, 2003) to generate $O_2^{\cdot-}$, as well as mouse sympathetic neurons (Tammariello et al., 2000) and cortical neurons and astrocytes (Noh and Koh, 2000), and rat cortical neurons (Kim et al., 2002). Recently, a new NAD(P)H oxidase subunit, NOX1, which is the homologue of $gp91^{phox}$, is cloned from vascular smooth muscle cells (Lassegue et al., 2001). We are the first to observe that mRNAs of $p22^{phox}$, $p47^{phox}$ and NOX1, but not $gp91^{phox}$ are present in freshly dissociated rat sympathetic neurons, like in vascular smooth muscle cells, which have different NAD(P)H oxidase subunits profile from phagocytic NAD(P)H oxidase (Lassegue et al., 2001). In contrast,

vascular endothelial cells (Jones et al., 1996) and fibroblasts (Pagano et al., 1997) have the same NAD(P)H oxidase subunits as phagocytes. However, the preparation of primary cultured sympathetic ganglionic neurons contains not only neurons, but also satellite glial cells as well. $O_2^{\cdot-}$ is generated in both neurons and glial cells in IMG (Dai et al., 2004b), therefore, it is possible that mRNAs of NAD(P)H oxidase subunits come from glial cells, but not neurons. In order to exclude this possibility, we examined mRNAs of NAD(P)H oxidase subunits in differentiated PC-12 cells, a homogeneous rat cell line with the sympathetic neuronal phenotype. The results showed that NAD(P)H oxidase subunits mRNAs present in differentiated PC-12 cells were the same as in sympathetic postganglionic neurons, supporting the presence of NAD(P)H oxidase in sympathetic neurons.

In sympathetic postganglionic neurons and differentiated PC-12 cells, like vascular smooth muscle cells (Griendling et al., 1994), $O_2^{\cdot-}$ was detected in the cytoplasm, suggesting an intracellular source of $O_2^{\cdot-}$ production, distinct from the extracellular $O_2^{\cdot-}$ production in phagocytes (Bastian and Hibbs, Jr., 1994). Since the lipid content of cell plasma membrane is relatively impermeable to charged $O_2^{\cdot-}$, the detected intraneuronal $O_2^{\cdot-}$ should be generated via the activation of sympathetic NAD(P)H oxidase within neurons themselves, not from glial cells or other cell types. Some of non-phagocytic cell types generate intracellular $O_2^{\cdot-}$, which may due to their unique non-phagocytic NAD(P)H oxidase subunits. One of the candidate subunits responsible for intracellular $O_2^{\cdot-}$ production might be NOX1, the homologue of $gp91^{phox}$. The $gp91^{phox}$, originally found in phagocytes

and recently cloned from vascular endothelial cells and fibroblasts, is responsible for extracellular $O_2^{\cdot-}$ production; on the other hand, NOX1, discovered in vascular smooth muscle cells (Lassegue et al., 2001), is mainly functional to produce intracellular $O_2^{\cdot-}$ (Griendling et al., 1994;Griendling et al., 2000). The intracellular sympathetic $O_2^{\cdot-}$ production may also lie on the fact of presence of NOX1.

NAD(P)H oxidase can be activated in CG.

Sympathetic NAD(P)H oxidase can be activated to generate $O_2^{\cdot-}$. One required step for NAD(P)H oxidase activation is the phosphorylation of $p47^{phox}$ by PKC, which permits $p47^{phox}$ to interact with the cytoplasmic tail of membrane-bound $p22^{phox}$ and initiate the formation of an active and membrane bound enzyme complex (Groemping et al., 2003). PMA activates PKC pathway independent of receptors stimulation (Raddassi and Murray, 2000) and the activated PKC phosphorylates $p47^{phox}$ to form an functional NAD(P)H oxidase (Swain et al., 1997). Apocynin, a selective NADPH oxidase inhibitor, impedes the assembly of NAD(P)H oxidase complex (Meyer and Schmitt, 2000). PMA induced $O_2^{\cdot-}$ production is almost completely inhibited by apocynin in rat neutrophils (Salmon et al., 1998). PMA was capable of inducing $O_2^{\cdot-}$ production in sympathetic neurons and PC-12 cells and this $O_2^{\cdot-}$ production was blocked by apocynin treatment. These findings confirm the presence of functional NAD(P)H oxidase in sympathetic neurons with the ability to generate $O_2^{\cdot-}$, like the NAD(P)H oxidase in phagocytes (Babior et al., 2002) and vascular cells (Li and Shah, 2002).

Physiological importance of increased $O_2^{\cdot-}$ production

The rationale for increased $O_2^{\cdot-}$ production in sympathetic neurons is still a mystery. Under physiological conditions, the generation of intracellular ROS in normal cells, including neurons, is under tight homeostatic control and does not alter the redox state of cells, which have large reserves of reducing agents, notably reduced glutathione, as well as biological antioxidant defense mechanisms, such as SOD, catalase, and peroxidases (Forman et al., 2002;Klein and Ackerman, 2003;Lassegue and Clempus, 2003). This reducing intracellular environment allows ROS to function as second messengers (Lassegue and Clempus, 2003). Nonphagocytic vascular cells produce low amounts of ROS that stimulate transcription factors as well as signaling cascades via the activation of kinases and inhibition of tyrosine phosphatases, in contrast to cytotoxic amounts of superoxide generated by phagocytes (Droge, 2002;Lassegue and Clempus, 2003). Similar to what is happening in vascular cells, ROS may also operate as second messengers in neurons to mediate the effects of neuroactive substances. Ang II/ROS signaling system mediates the action of Ang II to increase blood pressure (Zimmerman et al., 2002). This opens the possibility that the increased ROS may play roles in elevating blood pressure. Furthermore, there is an interesting interactive and feedforward relationship between PKC and ROS. The PKC activation induces ROS production, and ROS also can activate PKC pathway. The hydrogen peroxide activates PKC isoforms α, β and γ (Konishi et al., 1997), and the oxidative activation of PKC may enhance or facilitate the release of vasoconstrictor neurotransmitters, such as norepinephrine and ATP, from peripheral sympathetic nerves (Droge,

2002;Majewski and Iannazzo, 1998). Particularly considering a high sympathetic outflow present in hypertension (Anderson et al., 1989), such as in DOCA-salt hypertensive rats (Reid et al., 1975), ROS activated PKC may result in more vasoconstrictive neurotransmitters to be released from nerve terminals innervating blood vessels, and accordingly increase blood pressure.

Possible mechanisms for an increased NAD(P)H oxidase activity in CG in hypertension

$O_2^{\cdot-}$ levels are higher in sympathetic ganglia from DOCA-salt hypertensive rats than from Sham rats (Dai et al., 2004b), and this increase may come from the increased NAD(P)H oxidase activity. NAD(P)H oxidase activity was increased in celiac ganglia homogenates from DOCA-salt hypertensive rats. Several factors are possibly responsible for this increased NADPH oxidase activity in hypertension. SHRs exhibit no significant difference in NADPH oxidase activity at 16 weeks old, but develop a higher NAD(P)H oxidase activity when 30-week old, compared to normal rats (Zalba et al., 2000). This suggests that in this model long-term hypertension may be necessary for increased NADPH oxidase activity. Besides, nonhemodynamic factors, such as hormones or cytokines, may be responsible for an enhanced NADPH oxidase activity. Ang II treatment increases $O_2^{\cdot-}$ production through the increased NAD(P)H oxidase activity in cultured vascular smooth muscle cells (Griendling et al., 1994). In DOCA-salt hypertension, ET-1 might be one of the potential endogenous stimulating factors. There is more ET-1 mRNA and peptide in endothelial cells in DOCA hypertension and ET-1 increases the vascular NAD(P)H oxidase activity in

carotid arteries (Li et al., 2003). The elevated ET-1 may possibly increase the sympathetic NAD(P)H oxidase activity to produce greater amounts of $O_2^{\cdot-}$ in sympathetic ganglia from DOCA-salt hypertensive rats than from Sham rats. Finally, the increased NAD(P)H oxidase activity may come from the upregulated expression of NAD(P)H oxidase. In DOCA-salt hypertensive rats, $p22^{phox}$ mRNA is increased accompanied with an increased NAD(P)H oxidase activity in aorta (Zalba et al., 2000). In vivo angiotensin II treatment (7 days) in rats significantly increases NAD(P)H oxidase activity and upregulates the expression of NAD(P)H oxidase subunits, NOX1, $gp91^{phox}$, and $p22^{phox}$ (Mollnau et al., 2002). The changes in NAD(P)H oxidase mRNA and protein expression in sympathetic ganglia from DOCA-salt hypertensive rats need to be investigated.

The substrate preference of NAD(P)H oxidase

The NAD(P)H oxidase in sympathetic neurons uses both reduced β-NADH and β-NADPH as enzyme substrates, analogous to vascular NAD(P)H oxidase (Lassegue and Clempus, 2003). In contrast, the phagocytic NAD(P)H oxidase uses NADPH exclusively as an electron donor (Cross et al., 1984;Lassegue and Clempus, 2003). Besides, the sympathetic NAD(P)H oxidase generates more $O_2^{\cdot-}$ when utilizing NADPH than NADH. On the contrary, the NAD(P)H oxidase in rat thoracic aorta vascular smooth muscle cells is able to produce more $O_2^{\cdot-}$ when NADPH is used as the substrate compared to NADH (Sorescu et al., 2001). In addition, sympathetic ganglia from DOCA-salt hypertensive showed more increase in NAD(P)H oxidase activity when using NADPH as the substrate than when using NADH as the substrate. The sympathetic NAD(P)H oxidase

may have the preference to NADPH over NADH as the NAD(P)H oxidase substrate. In vascular cells, the abnormal lack of specificity of NAD(P)H oxidase might lie on the fact that vascular cells express multiple NOX family members and that NOX4, unlike gp91phox and NOX1, might preferentially use NADH (Lassegue and Clempus, 2003).

Perspectives

This study demonstrates that mRNA for NAD(P)H oxidase subunits $p47^{phox}$, $p22^{phox}$, and NOX1, but not $gp91^{phox}$ are present in sympathetic neurons and differentiated PC-12 cells. Furthermore, we identify PMA as a stimulus to increase $O_2^{\bullet-}$ levels in sympathetic postganglionic neurons and PC-12 cells, and this increase can be attenuated by pretreatment with specific NAD(P)H oxidase inhibitor apocynin. Finally, there is more $O_2^{\bullet-}$ production in sympathetic ganglia from DOCA-salt hypertensive rats than from Sham rats and NAD(P)H oxidase activity is upregulated in sympathetic ganglia from DOCA-salt hypertensive rats. We propose that $O_2^{\bullet-}$ production evoked by the active NAD(P)H oxidase may play roles in the increased sympathetic excitability and pathogenesis in DOCA-salt hypertension. We speculate that ROS in the sympathetic nervous system may be an important target for therapeutic treatment of hypertension.

CHAPTER 3C: ET-1 INDUCED $O_2^{\cdot-}$ PRODUCTION IN SYMPATHETIC NEURONS VIA NAD(P)H OXIDASE

Introduction

Many factors are potentially responsible for changes that occur in hypertension. Recent studies suggest that one of the prospective factors might be ROS. $O_2^{\cdot-}$ is one of the most important ROS and is pivotal in generating other ROS (Droge, 2002). In hypertensive children and adolescents, the systemic oxidative stress is Increased irrespective of their body mass index (BMI), by measuring oxidative stress parameters, such as the redox status of the red blood cell glutathione (Turi et al., 2003). An elevated level of vascular $O_2^{\cdot-}$ production has been shown to occur in several hypertension animal models, including DOCA-salt hypertension (Heitzer et al., 1999;Li et al., 2003;Nakane et al., 2000;Ushio-Fukai et al., 1996;Wu et al., 2001). Treatment with antioxidants reduces vascular $O_2^{\cdot-}$production as well as the blood pressure to normal levels (Beswick et al., 2001b;Dobrian et al., 2001;Somers et al., 2000a).

ROS may exert critical effects on the sympathetic nervous system and increase the sympathetic nerve activity, which will result in blood pressure increase. In the central nervous system, ROS contributes to the oxidative damage and cell death in neurodegenerative diseases, such as amyotropic lateral sclerosis and Parkinson's disease (Pong, 2003). More evidence is emerging to suggest that ROS may get involved in normal neuronal activity (Yermolaieva et al., 2000). ROS play critical roles in the central sympathetic neural control of blood pressure. The rostral ventral lateral medulla (RVLM) in

brainstem is the vasomotor center that determines the basal sympathetic nerve activity (SNA) and maintains the basal vasomotor tone (Dampney, 1994). SNA is greater in SHR, including stroke-prone SHR (SHRSP) (Judy et al., 1976;Kishi et al., 2002); and $O_2^{\cdot-}$ derived ROS signal is increased in the RVLM in SHRSP. Bilateral microinjection of superoxide dismutase (SOD) mimic tempol into the RVLM decreases blood pressure in SHRSP, but not in normotensive control; and SOD overexpression in the RVLM of SHRSP decreases blood pressure and inhibits sympathetic nerve activity (Kishi et al., 2004). The change in the redox environment of the peripheral nervous system induced by ROS may modulate neuronal activity directly. Administration of hydrogen peroxide (H_2O_2), one of the ROS, in the vicinity of sympathetic preganglionic neurons projecting to the adrenal gland results in the activation of sympathetic preganglionic neurons innervating the adrenal gland and the subsequent release of catecholamine from adrenal medulla, which in turn elevates blood pressure and heart rate (Lin et al., 2003).

ROS can be induced by a humoral factor ET-1. ET-1, a peptide originally described as a potent vasoconstrictor synthesized in endothelial cells, is also present in the sensory and sympathetic nervous system (Damon, 1999;Milner et al., 2000a) and has multiple actions on them (Cao et al., 1993;Zhou et al., 2001). The endothelin system is activated in salt-sensitive hypertension in animals and humans (Schiffrin, 2001). Pathogenesis in this hypertensive model is associated with increased ROS, especially $O_2^{\cdot-}$ (Sedeek et al., 2003;Somers et al., 2000b), one of the most important ROS and pivotal in generating other ROS (Droge,

2002). In arteries, ET-1 evokes $O_2^{\bullet-}$ production via ET_A receptors (Li et al., 2003), whereas in sympathetic ganglia, ET-1 generates $O_2^{\bullet-}$ via ET_B receptors (Dai et al., 2004b). Additionally, ET-1 binds to ET_B receptors to activate PKC (Mateo and de Artinano, 1997) and the PKC-dependent NAD(P)H oxidase activation generates $O_2^{\bullet-}$ in sympathetic ganglia (Dai et al., 2004a). However, whether there is a link connecting ET_B receptor activation with NAD(P)H oxidase activation induced $O_2^{\bullet-}$ generation, or not, is not clear.

The aims of this study are to determine whether ET-1-triggered $O_2^{\bullet-}$ generation depends upon NAD(P)H oxidase activation, and if so, to determine the specific ET receptor subtypes mediating this response. Besides NADPH oxidase, xanthine oxidase and uncoupled nitric oxide synthase are also responsible for $O_2^{\bullet-}$ generation in some cell types (Droge, 2002). As a result, we also determined if ET-1 induced $O_2^{\bullet-}$ production is also partially mediated through the other two enzymes. We finally investigated if ET-1 binding to ET_B receptors activates PKC and generates $O_2^{\bullet-}$ in sympathetic cells.

Methods

Animals

See Chapter 2 Methods.

Tissue harvest and cell culture

See Chapter 2 Methods.

Measurement of superoxide anion generation

a. Confocal microscopy imaging

See Chapter 2 Methods.

IMGs were divided in 3 groups: no treatment, incubated with ET-1 ($3x10^{-8}$mol/L) for 30 minutes, and incubated with NAD(P)H oxidase inhibitor apocynin (10^{-7}mol/L) for 45 minutes followed by ET-1 incubation for 30 minutes. Cells were divided into 3 groups: control (no treatment), treated with ET-1 as the agonist, and treated with ET-1 plus apocynin pretreatment.

b. Fluorescence plate reader

Quantification of fluorescent signal was also achieved with a Biotek FL600 fluorescence plate reader (Bio-Tek Instruments, Inc., Winooski, Vermont). Equal amounts of PC-12 cells, $2x10^5$/well, were plated on the Costar® 24-well tissue culture plate. Three sets of experiment protocol were performed.

Protocol one: Cells were divided into 3 groups: control (no treatment), treated with selective ET_B receptor agonist sarafotoxin 6c (S6c, 10^{-8}mol/L) as the agonist, and treated with S6c plus apocynin (1μM) pretreatment.

Protocol two: Cells were divided into 4 groups: 1) control (no treatment); 2) treated with ET-1 as the agonist; 3) treated with ET-1 plus apocynin (1μM) pretreatment; 4) treated with ET-1 plus xanthine oxidase inhibitor allopurinol (1μM) pretreatment, and treated with ET-1 plus uncoupled nitric oxide synthases inhibitor N-nitro-L-arginine (NOLA, 100μM) pretreatment.

Protocol three: Cells were divided into 3 groups: control (no treatment), treated with ET-1 as the agonist, and treated with ET-1 plus general PKC inhibitor RO-31-8425 (1μM) pretreatment.

Cells were incubated with apocynin for 45 minutes, followed by incubation with agonists for 30 minutes, and then loaded with DHE for 30 minutes at 37°C.

The fluorescent signal was detected using excitation filter 485±40nm and emission filter 590±35nm.

Data analysis

See Chapter 3A Methods.

Drugs

Apocynin was purchased from Sigma Chemical Co.. ET-1and S6c were obtained from Peninsula Laboratories. DHE was purchased from Molecular Probes and RO-31-8425 was purchased from LC Laboratories.

Results

Effects of ET-1 administration on $O_2^{\cdot-}$ levels in sympathetic ganglia

$O_2^{\cdot-}$ levels were evaluated in IMG (n=3-4 rats in each group). The control IMG received no ET-1. $O_2^{\cdot-}$ levels in both neurons and glia were higher in ET-1 (30μM) treated IMG (Figure 24B) compared to the control (Figure 24A). ET-1 treatment resulted in 250% and 200% increase in fluorescent intensity in neurons and glia respectively (Figure 24D). Ganglia pretreated with NAD(P)H oxidase inhibitor apocynin followed by ET-1 treatment showed no significant increase in $O_2^{\cdot-}$ fluorescence (Figure 24C) compared to the control (Figure 24A). This indicates that ET-1 induced $O_2^{\cdot-}$ generation in neurons and glial cells of prevertebral sympathetic ganglia was blocked by NAD(P)H oxidase inhibitor.

Figure 24: Superoxide levels in neurons and glial cells in rat inferior mesenteric ganglia (IMG) treated with ET-1 or ET-1 plus NAD(P)H oxidase inhibitor apocynin. $O_2^{\cdot-}$ levels, indicated by DHE fluorescence intensity in confocal images, are higher in IMG *in vitro* treated with ET-1 than in control IMG, and this ET-1 induced increase is attenuated by pretreatment with apocynin. Cells with a soma diameter of 15 to 35 μm are identified as neurons and cells with a diameter of 5 to 10 μm are identified as glial cells. Arrows indicate examples of neurons and arrowheads indicate examples of glial cells. (A) Control Sham IMG; (B) IMG *in vitro* treated with ET-1; (C) IMG *in vitro* treated with apocynin plus ET-1; (D) Comparison of mean fluorescence intensity of 68 to 157 neurons or from 288 to 496 glial cells (n=3-4 rats in each group). The significance ($P<0.05$) is indicated by * vs. control in neurons and glial cells. The calibration bar in C applies to all panels.

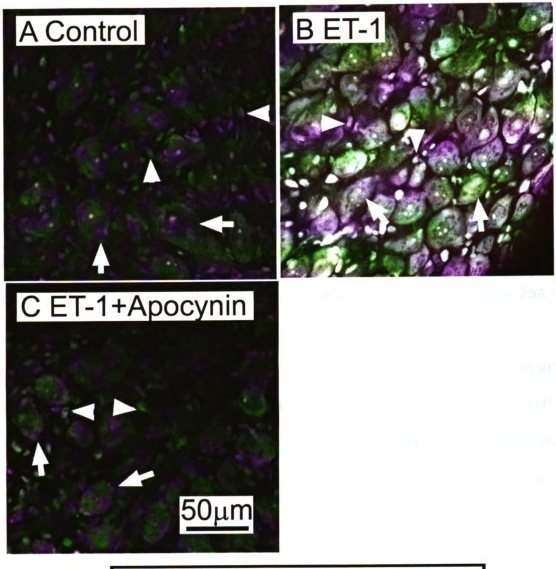
A Control
B ET-1
C ET-1+Apocynin
50μm
D
CTRL
ET-1
ET-1+ Apocynin
Fluorescence Intensity Units
250
200
150
100
50
0
*
*
n=157
n=95
n=68
n=496
n=582
n=288
Neuron
Glial cell

$O_2^{\cdot-}$ levels in dissociated celiac ganglionic neurons and PC-12 cells

To determine whether ET-1 acts on neurons directly to activate the NAD(P)H oxidase and elevate $O_2^{\cdot-}$ levels, we incubated freshly dissociated celiac ganglionic neurons from normal rats and differentiated PC-12 cells with ET-1 and measured $O_2^{\cdot-}$ levels. Representative confocal images of DHE fluorescence in treated cells are shown in Figure 25 and 26 (n=4-5 dishes of cultured cells in each group). The changes in fluorescent intensity were quantified (Figure 27). Phase-contrast images of control cells were shown in Figure 25B and 26B in parallel with the corresponding confocal images of control cells in Figure 25A and 26A.

Freshly dissociated and cultured cells included sympathetic neurons and glial cells and both of them respond to ET-1 to generate $O_2^{\cdot-}$ (Dai et al., 2004b). Because these two cell types have different diameters, they did not appear on the same confocal plane. In this study, we measured the response in cells with typical neuronal morphology, which is with soma diameters ranging from 15 to 35μm. Compared with the control (Figure 25A, 38.3 ±4.5 Arbitrary Fluorescence Units (AFUs)), the fluorescence intensity of sympathetic ganglionic neurons incubated with ET-1 was 420% greater (Figure 25C, 201 ±6.3 AFUs), indicating elevated $O_2^{\cdot-}$ levels. Pretreatment with NAD(P)H oxidase inhibitor apocynin attenuated the ET-1-induced increase in fluorescence intensity to the control level (Figure 25D, 51.3±2.0 AFUs). These experiments indicate that the NAD(P)H oxidase mediates the ET-1 induced $O_2^{\cdot-}$ production in sympathetic postganglionic neurons.

Figure 25: NAD(P)H oxidase activation by ET-1 elevates $O_2^{\cdot-}$ levels in dissociated celiac ganglia (CG) neurons *in vitro* and this increase is attenuated by pretreatment with NADPH oxidase inhibitor apocynin. Confocal fluorescent images of (A) Control group; (C) ET-1; (D) ET-1 plus apocynin. Phase-contrast microscopy images of control group (B). The calibration bar in D applies to all panels.

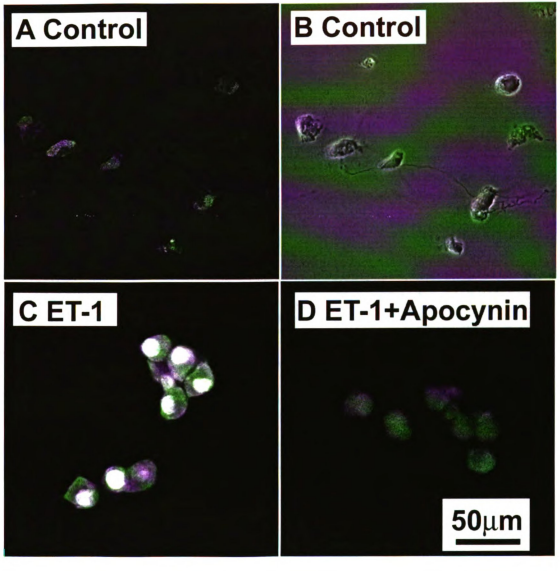
A Control
B Control
C ET-1
D ET-1+Apocynin
50μm

Figure 26: NAD(P)H oxidase activation by ET-1 elevates $O_2^{\bullet-}$ levels in differentiated PC-12 cells *in vitro* and this increase is attenuated by pretreatment with NADPH oxidase inhibitor apocynin. Confocal fluorescent images of (A) Control group; (C) ET-1; (D) ET-1 plus apocynin. Phase-contrast microscopy images of control group (B). The calibration bar in D applies to all panels.

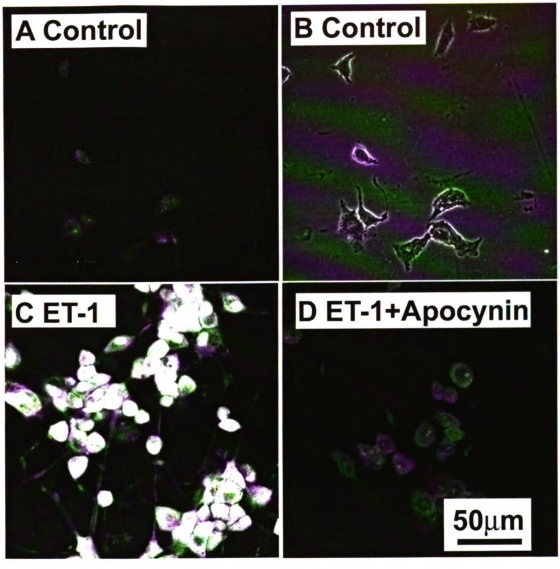
A Control
B Control
C ET-1
D ET-1+Apocynin
50μm

Figure 27: Effects of ET-1 induced NAD(P)H oxidase activation on $O_2^{\cdot-}$ levels in celiac ganglia (CG) neurons and PC-12 cells *in vitro*. Results are expressed as mean±SE. Control cells received no agonist treatment. The significance ($P<0.05$) is indicated by # vs. control in CG cells and PC-12 cells (n=4 dishes in each treatment group).

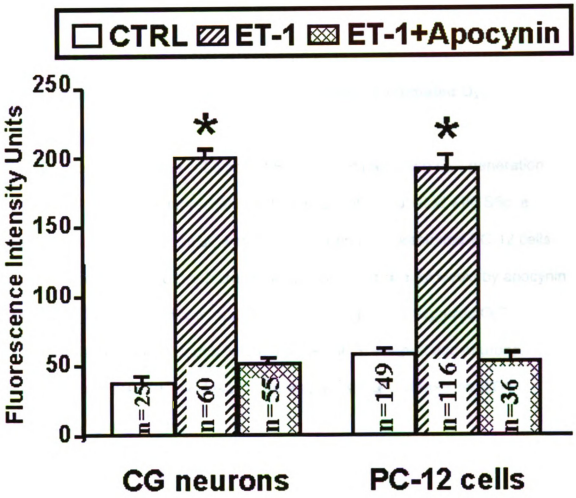
CTRL
ET-1
ET-1+Apocynin
Fluorescence Intensity Units
250
200
150
100
50
0
*
*
n=25
n=60
n=55
n=149
n=116
n=36
CG neurons
PC-12 cells

The activation of NAD(P)H oxidase on ET-1-induced $O_2^{\cdot-}$ generation was also evaluated in PC-12 cells. The fluorescence intensity of cells incubated with ET-1 was 223% greater (Figure 26C, 191.7±8.0 AFUs) than control cells (Figure 26A, 59.3±3.1 AFUs). The ET-1-induced increase in the fluorescence intensity was attenuated to control levels by pretreatment with apocynin (Figure 26D, 56.1±3.6 AFUs). These results indicate that ET-1-induced $O_2^{\cdot-}$ production in differentiated PC-12 cells is mediated by NAD(P)H oxidase.

Role of NAD(P)H oxidase on ET_B receptors mediated $O_2^{\cdot-}$ production

We determined the subtypes of ET receptor mediating $O_2^{\cdot-}$ generation triggered by ET-1. The fluorescence intensity of cells incubated with S6c, a selective ET_B receptor agonist, was 386% greater in differentiated PC-12 cells than in control cells, and this increase was reduced to control levels by apocynin (Figure 28). The data indicate that ET_B receptor activation triggered $O_2^{\cdot-}$ generation is mediated through NAD(P)H oxidase in sympathetic neurons.

Roles of NADPH oxidase, NOS, and xanthine oxidase on ET-1 induced $O_2^{\cdot-}$ production

To determine the enzymes involved in ET-1 induced $O_2^{\cdot-}$ generation in differentiated PC-12 cells, ET-1 and inhibitors of enzymes were incubated with cells and $O_2^{\cdot-}$ generation was measured. Apocynin, a selective NADPH oxidase inhibitor, significantly lessened ET-1-induced $O_2^{\cdot-}$ generation from 250% to 130% of control levels in differentiated PC-12 cells (Figure 29). In contrast, the xanthine oxidase inhibitor allopurinol and the nitric oxide synthase

Figure 28: Effects of NADPH oxidase on ET_B receptor activation mediated $O_2^{\bullet-}$ production. Treatment with apocynin (100nM) reduced ET_B receptor S6c (10nM) induced $O_2^{\bullet-}$ production to control levels in differentiated PC-12 cells. The significance ($P<0.05$) is indicated by # vs. control group and * vs. S6c group (n=6 wells, $2x10^5$ per well).

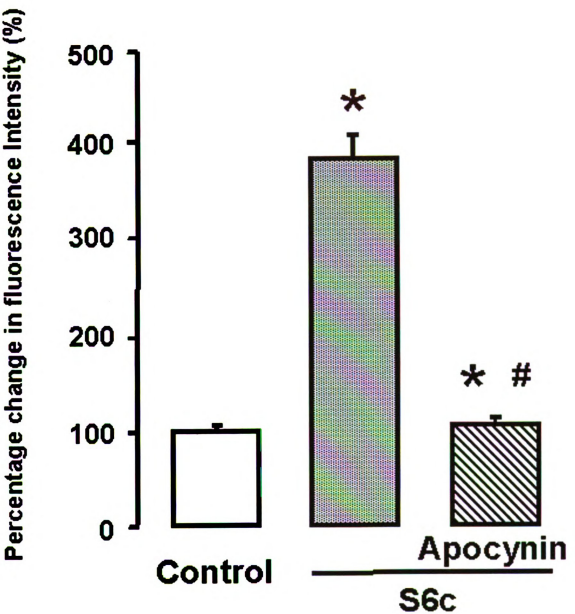
Percentage change in fluorescence Intensity (%)
500
400
300
200
100
0
*
* #
Control
Apocynin
S6c

Figure 29: Effects of NADPH oxidase on ET-1 induced $O_2^{\cdot-}$ production. Treatment with apocynin (100nM) reduces ET-1 (30nM) induced $O_2^{\cdot-}$ production to control levels in differentiated PC-12 cells. In contrast, treatment with allopurinol (1nM) and NOLA (100nM) decreases 15% and 10% of ET-1-induced $O_2^{\cdot-}$ production respectively in PC-12 cells. The significance ($P<0.05$) is indicated by # vs. control group and * vs. ET-1 group (n=6 wells, $2x10^5$ per well).

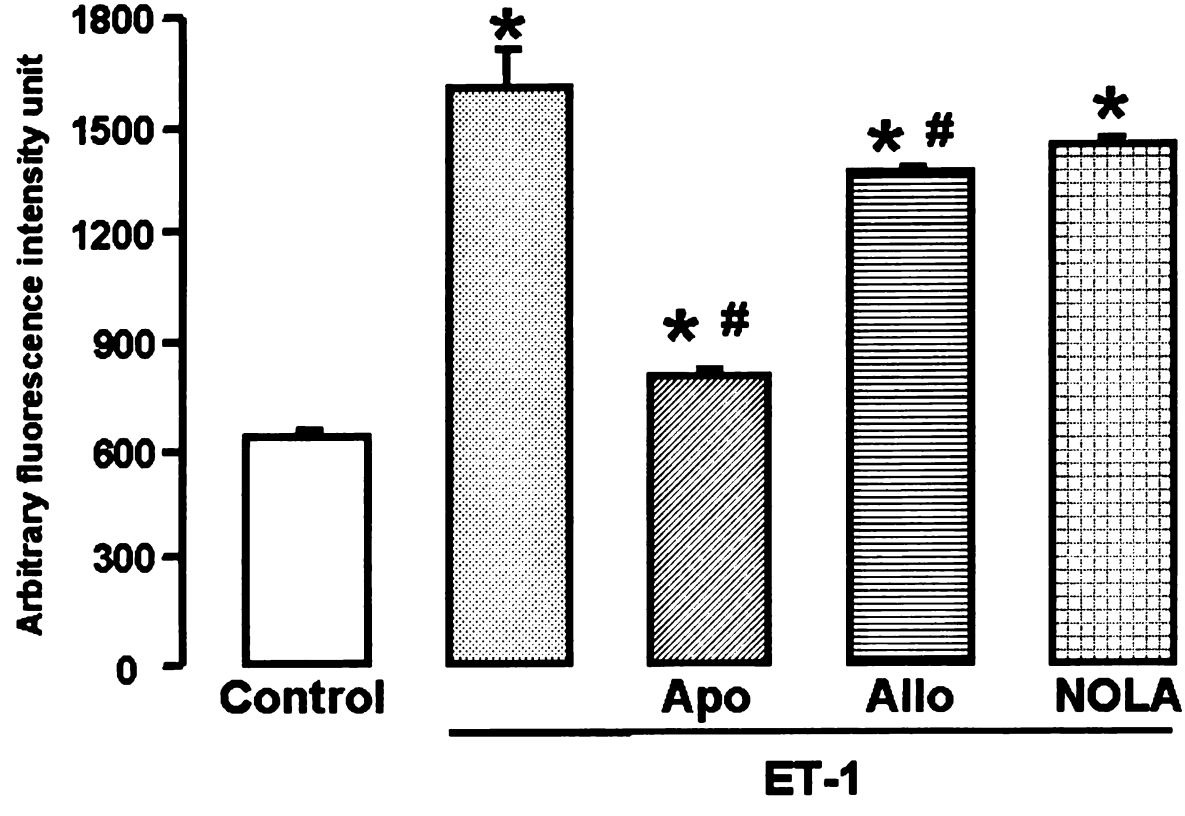
Arbitrary fluorescence intensity unit
1800
1500
1200
900
600
300
0
*
* #
* #
*
Control
Apo
Allo
NOLA
ET-1

inhibitor NOLA only reduced ET-1-induced $O_2^{\cdot-}$ generation from 250% to 215% and 225% of control levels respectively. The results indicated that the major source of $O_2^{\cdot-}$ in the sympathetic neurons is from NAD(P)H oxidase activation.

Effects of PKC inhibitor on ET-1 induced $O_2^{\cdot-}$ production in PC-12 cells

To determine if ET-1 activated PKC pathway is responsible for $O_2^{\cdot-}$ generation in sympathetic cells, we incubated differentiated PC-12 cells with ET-1 and a PKC inhibitor and measured $O_2^{\cdot-}$ levels. ET-1 treatment resulted in a 363% increase in $O_2^{\cdot-}$ generation in PC-12 cells, and this increase was reduced 65% by PKC inhibitor RO-31-8425 (Figure 30). The data indicated that a PKC-dependent pathway mediates ET-1 triggered $O_2^{\cdot-}$ generation in sympathetic neurons.

Discussion

These results provide the first evidence that exogenous ET-1 or selective ET_B receptor agonist S6c activates NADPH oxidase, evoking $O_2^{\cdot-}$ production in sympathetic postganglionic neurons and differentiated PC-12 cells. ET-1 induced $O_2^{\cdot-}$ production is mainly mediated through NADPH oxidase, but not xanthine oxidase or uncoupled nitric oxide synthase. ET-1 acts on ET_B receptors coupled to a PKC-dependent pathway, which activates NADPH oxidase to generate $O_2^{\cdot-}$.

ET-1 induced $O_2^{\cdot-}$ in sympathetic ganglia is mainly mediated through NADPH oxidase

ET-1 stimulates $O_2^{\cdot-}$ production in rat sympathetic ganglia, both of

Figure 30: Effects of PKC on ET-1 induced $O_2^{\cdot-}$ production. Treatment with PKC inhibitor RO-31-8425 (1uM) reduces ET-1 (30nM) induced $O_2^{\cdot-}$ production by 65% in differentiated PC-12 cells. The significance ($P<0.05$) is indicated by # vs. control group and * vs. ET-1 group (n=6 wells, $2x10^5$ per well).

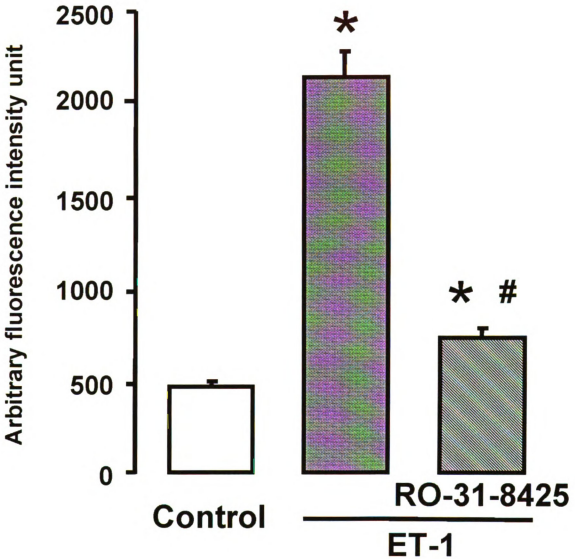
Arbitrary fluorescence intensity unit
2500
2000
1500
1000
500
0
*
* #
Control
RO-31-8425
ET-1

neurons and glial cells (Dai et al., 2004b). The mechanisms leading to ET-1 triggered $O_2^{\cdot-}$ production in sympathetic ganglia have not been demonstrated, but studies in other cell types provide some insights. The major enzymatic sources for superoxide formation are NADPH oxidase, xanthine oxidase, and uncoupled nitric oxide synthase (Droge, 2002). In vascular cells, NADPH oxidase is the major source of $O_2^{\cdot-}$ production. The key subunit of NADPH oxidase, $p47^{phox}$, is phosphorylated when agonists bind to their corresponding receptors, subsequently the membrane bound and cytosolic subunits of NADPH oxidase are assembled together to form an activated NADPH oxidase (Babior, 2004). Hormones, such as Ang II and ET-1, can activate NADPH oxidase. Angiotensin II signalling, via AT1 receptors, is upregulated in resistance arteries of hypertensive patients and rats and this is associated with hyperactivation of vascular NADPH oxidase, leading to increased generation of ROS, particularly $O_2^{\cdot-}$ and H_2O_2 (Touyz et al., 2003). In DOCA-salt hypertension, ET-1 binds to ET_A receptors to generate $O_2^{\cdot-}$ in vascular cells, which can be blocked by NAD(P)H oxidase inhibitors apocynin and diphenylene iodinium (DPI) (Li et al., 2003).

Besides vascular smooth muscle cells, endothelial cells and fibroblasts, neurons and glial cells might be other types of nonphagocytic cells which can generate $O_2^{\cdot-}$ via activation of NADPH oxidase. Our recent study shows that mRNAs of NADPH oxidase subunits are present in rat sympathetic postganglionic neurons and differentiated PC-12 cells, and activation of NADPH oxidase in these cells results in $O_2^{\cdot-}$ generation (Dai et al., 2004a). In this study, we treated sympathetic ganglia with ET-1 plus NADPH oxidase inhibitor

apocynin, a methoxy-substituted catechol, to investigate the involvement of NADPH oxidase in ET-1 induced $O_2^{\cdot-}$ generation. Apocynin impedes the assembly of $p47^{phox}$ and $p67^{phox}$ subunits within the membrane-bound NADPH oxidase complex to prevent the formation of a functional NADPH oxidase (Meyer and Schmitt, 2000). The major blocking effect that apocynin exerts on ET-1 induced $O_2^{\cdot-}$ production in sympathetic neurons and glial cells demonstrated that ET-1 induced $O_2^{\cdot-}$ production is mostly mediated through NADPH oxidase. The functional NADPH oxidase in neurons and glial cells are also reported to be present in the study of cultured cortical neurons and astrocytes, in which zinc induces and activates the NADPH oxidase to generate $O_2^{\cdot-}$ in the CNS (Noh and Koh, 2000).

Xanthine oxidase and nitric oxide synthase also partially contribute to $O_2^{\cdot-}$ generation in sympathetic neurons. The major enzymatic sources for superoxide formation are NADPH oxidase, xanthine oxidase, and uncoupled nitric oxide synthase (Elmarakby et al., 2003;Spiekermann et al., 2003). However, in vasculature, ET-1 induced $O_2^{\cdot-}$ production is mainly blocked by NADPH oxidase inhibitor, but not by inhibitors of xanthine oxidase and nitric oxide synthase (Li et al., 2003). In this study, inhibitors of xanthine oxidase or nitric oxide synthase resulted in 10% to 15% reduction in ET-1 induced $O_2^{\cdot-}$ generation in differentiated PC-12 cells. These results suggest that NADPH oxidase is the main enzyme responsible for ET-1 induced $O_2^{\cdot-}$ generation in sympathetic neurons, and xanthine oxidase and uncoupled nitric oxide synthase play a minor role. Nonphagocytic cells generate $O_2^{\cdot-}$ constitutively under basal silent state

other than agonists stimulation (Lassegue and Clempus, 2003). This opens another possibility that inhibitors of xanthine oxidase and nitric oxide synthase may merely decrease the basal $O_2^{\cdot-}$ production, but not ET-1 induced $O_2^{\cdot-}$ generation.

PKC dependent ET_B activation pathway connects to NADPH oxidase

Two subtypes of ET receptors, ET_A receptors and ET_B receptors, have been identified. In the sympathetic neurons ET-1 induced $O_2^{\cdot-}$ production is mediated through its binding to G protein–coupled ET_B receptors (Dai et al., 2004b). Whereas in vascular cells, ET-1 induced $O_2^{\cdot-}$ production is mediated through ET_A receptors (Li et al., 2003). The NADPH oxidase inhibitor apocynin blocked the specific ET_B receptor agonist induced $O_2^{\cdot-}$ generation in the sympathetic neurons and this provides direct evidence that ET_B receptors link ET-1 stimulation to NADPH oxidase activation.

The next question was which events provide a link between the action of ET-1 on ET_B receptors and NADPH oxidase activation. There are two reasons to hypothesize that the candidate factor might be PKC. First, in sympathetic neurons, the PKC activator PMA activates NADPH oxidase and evokes $O_2^{\cdot-}$ production, which is blocked by apocynin (Dai et al., 2004a). Second, ET-1 binds to ET_B receptors to activate PKC (Mateo and de Artinano, 1997). The binding of ET-1 to ET_B receptors activates phospholipase C (PLC) which hydrolyses phosphatidilinositol-4,5-biphosphate (PIP_2) into two products, IP_3 and DAG. IP_3 causes an increase in intracellular Ca^{2+} concentration and DAG activates the PKC pathway. Pharmacological experiments shows that the intracellular Ca^{2+} is

increased with ET_B receptor agonist S6c stimulation in mixed cultures of neuronal/glial cells, and several ET receptor antagonists block this S6c initiated increase (Dooley et al., 1998). In this study in differentiated PC-12 cells, the PKC inhibitor was able to significantly, but not completely, lower the level of ET-1 increased $O_2^{\cdot-}$. The incomplete blockade provided by the PKC inhibitor might be that PKC-dependent NADPH oxidase activation pathway is not the only contributor to ET-1 induced $O_2^{\cdot-}$ production in sympathetic neurons.

ET-1 has been shown to trigger $O_2^{\cdot-}$ production (Li et al., 2003). So far, there is only one study pointing out that endothelin activates PKC and consequently increases $O_2^{\cdot-}$ production, which results in post-ischemic endothelial dysfunction (Maczewski and Beresewicz, 2000). A lot of studies are investigating biological effects of Ang II, another well-studied humoral factor and peptide besides ET-1. Like ET-1, Ang II is a potent stimulus for $O_2^{\cdot-}$ generation (Griendling et al., 1994;Griendling and Ushio-Fukai, 2000). PKC inhibitors block Ang II stimulated $O_2^{\cdot-}$ production in vascular cells and renal mesangial cells (Jaimes et al., 1998;Mollnau et al., 2002), in which the Ang II-induced increase in NADPH oxidase activity is at least to some extent PKC-dependent. Considering the similarity between ET-1 and Ang II, the PKC-dependent NAD(P)H oxidase activation pathway may be also reflected in ET-1 induced $O_2^{\cdot-}$ generation. In this study, we show that ET-1 induces $O_2^{\cdot-}$ production via a PKC-dependent pathway in sympathetic neurons, similar to what has been shown in endothelial cells.

Perspectives

The present study, for the first time, demonstrates that ET-1 induced $O_2^{\cdot-}$

production is mediated through activation of NADPH oxidase in prevertebral sympathetic ganglia. Xanthine oxidase and uncoupled nitric oxide synthase also somehow contribute to ET-1 induced $O_2^{\cdot-}$ generation. Furthermore, $O_2^{\cdot-}$ generation resulted from ET_B receptors activation can also be lessened by pretreatment with NADPH oxidase inhibitor. Finally, ET-1 acts on ET_B receptors coupled to a PKC-dependent pathway, at least partially, and activates NADPH oxidase to generate $O_2^{\cdot-}$ in sympathetic neurons. We propose that $O_2^{\cdot-}$ production evoked by ET-1 may be a mechanism for increased activity of the sympathetic system in hypertension, especially in some essential hypertensive patients and hypertensive animal models with increased ET-1 production. We speculate that ROS in the sympathetic nervous system may be an important target for therapeutic treatment of hypertension.

CHAPTER 4: GENERAL CONCLUSIONS AND PERSPECTIVES

Hypertension is a devastating disease marked by elevated arterial blood pressure. It affects nearly 50 million Americans and is responsible for considerable morbidity and mortality. Blood pressure in around 60 percent of essential hypertensive patients is sensitive to salt intake (Gonzalez-Albarran et al., 1998;Luft and Weinberger, 1982;Preuss, 1997;Somova et al., 1999;Williams and Hollenberg, 1989). Elevated sympathetic activity is observed in hypertensive patients (Mancia et al., 1999), as well as the impaired neuronal uptake of norepinephrine with consequent increase in neuroeffector junctional norepinephrine levels (Esler et al., 1980;Ferrier et al., 1993). In addition, systemic oxidative stress is increased in hypertensives (Turi et al., 2003). The difficulty with treatments of essential hypertension lies in the facts of unknown pathogenesis of this disease. A number of experimental animal models of hypertension are developed to target subpopulations of hypertensives with diverse dysfunctional systems during the development of hypertension.

The DOCA-salt hypertensive rat, one of the established animal models of salt-sensitive hypertension (Iriuchijima et al., 1975;Reid et al., 1975;Takeda and Bunag, 1980), was used in this study, because this model shows several pathophysiological similarities to essential hypertension. Basal plasma norepinephrine levels (Drolet et al., 1989) and sympathetic nerve activity (Katholi et al., 1980) are significantly higher in DOCA-salt hypertensive rats than in normotensive rats, pointing to a generalized increase in sympathetic tone in DOCA-salt treated rats (de Champlain et al., 1989). Elevated vascular $O_2^{\cdot-}$

production also occurs in DOCA-salt hypertension (Li et al., 2003;Wu et al., 2001) and treatment with antioxidants reduces vascular $O_2^{\cdot-}$ production and returns blood pressure of DOCA-salt hypertensive animals to normal levels (Beswick et al., 2001b;Somers et al., 2000a). Most importantly, the levels of ET-1 mRNA and peptide production are elevated in this animal model of hypertension. This prominent characteristic makes this animal model suitable for investigating pathophysiological mechanisms in some severe hypertensives or African American hypertensives, who exhibit elevated plasma ET-1 levels (Schiffrin, 2001).

Of the many possible sites where alterations of function could contribute to high blood pressure, I chose to investigate NET in ganglionic sympathetic neurons, which function to terminate the actions of norepinephrine. Reduction in transport activity by transporter protein would be expected to elevate norepinephrine in the neuroeffector junction, cause vasoconstriction and raise blood pressure. I also chose to evaluate the oxidative stress, which might be a signal to elevate sympathetic nerve activity and thereby increase vasoconstriction and blood pressure. A series of specific aims were devised to evaluate changes of NET and $O_2^{\cdot-}$ generation in sympathetic ganglia of DOCA-salt hypertensive rats and possible roles of ET-1 actions on levels of NET mRNA, protein and function, and of $O_2^{\cdot-}$ production in sympathetic neurons.

Although norepinephrine reuptake has been shown in sympathetically innervated tissues, the presence of NET mRNA and protein has never been demonstrated in blood vessels and their innervating sympathetic and sensory

nerves before. It was important to establish the NET expression profile first. I demonstrated that NET mRNA and protein could be found in tissue extracts of mesenteric arteries, mesenteric veins, celiac ganglia and DRG. Surprisingly, both NET mRNA and protein levels are upregulated in mesenteric blood vessels and sympathetic celiac ganglia from DOCA-salt hypertensive rats compared to Sham rats (See Chapter 2). Increased NET mRNA level, along with increased tyrosine hydroxylase (TH) mRNA, is also observed in central brain regions associated with the control of arterial blood pressure, and adrenal medulla from spontaneous hypertensive rats (Reja et al., 2002). These results are opposing to my expectation that the reduced uptake of norepinephrine in hypertension is the consequence of downregulated level of NET protein expression. This may suggest the existence of enhanced activation of the noradrenergic system with global upregulation of norepinephrine synthesis and uptake in hypertension. Moreover, the upregulated level of NET may be secondary to the increased level of extracellular norepinephrine, since levels of basal plasma norepinephrine (Drolet et al., 1989) and the amount of released norepinephrine from sympathetic nerves are both increased in hypertension (Luo et al., 2003). These unexpected findings could also stem from the existence of dysfunctional NET. It must be that the increased sympathetic nerve activity causes more norepinephrine release in hypertension, and even upregulated level of NET protein could not compensate the reduced uptake caused by dysfunctional NET. Consequently, the level of neuroeffector junctional norepinephrine is increased, followed by more vasoconstriction and higher blood pressure. However, final clarification of these

issues awaits for further studies investigating the local and global homeostasis of norepinephrine, such as norepinephrine uptake, spillover and clearance, in this animal model of hypertension.

Considering the impairment of neuronal norepinephrine reuptake and increased ET-1 production in some essential hypertensive patients, I hypothesized that ET-1 regulates NET expression and function and this regulation contributes to hypertension. I investigated the effects of ET-1 on the levels of NET mRNA, protein and uptake in differentiated PC-12 cells with sympathetic neuronal phenotype and native NET expression. ET-1 produces both acute and long-term changes in NET mRNA, protein and function (see Chapter 2). ET-1 induced downregulation of NET function may possibly come from PKC activation which is a consequence of ET receptor activation. ET-1 activates PKC in cultured brain cells (Mateo and de Artinano, 1997) and in sympathetic neurons (see Chapter 3C). The cell membrane protein and function of NET undergoes acute downregulation in response to PKC activation (Apparsundaram et al., 1998a;Apparsundaram et al., 1998b;Savchenko et al., 2003). Recent studies strongly argue that only NET protein that is located in cell membrane has the potential to transport norepinephrine (Apparsundaram et al., 1998b;Hahn et al., 2003;Savchenko et al., 2003). Acute downregulation of NET function observed in this study may come from decreased insertion of NET protein in the cell membrane due to an ET-1 dependent PKC activation pathway. In the long run, impaired norepinephrine uptake due to ET receptor activation may contribute to the increased junctional norepinephrine concentration in

hypertension.

Recent studies have shown that central neural redox mechanisms are closely involved in the autonomic control of normal cardiovascular function, as well as in the pathogenesis of cardiovascular diseases, such as hypertension and heart failure (Lindley et al., 2004;Zimmerman et al., 2002;Zimmerman and Davisson, 2004). $O_2^{\cdot-}$ could be a factor causing an increase in sympathetic drive after myocardial infarction and the reduction of $O_2^{\cdot-}$ generation decreases sympathetic outflow by a decrease in neuronal activity in the paraventricular nucleus and supraoptic nucleus (Lindley et al., 2004). In addition, central administration of AngII induced increase in blood pressure and heart rate can be abolished by the treatment to reduce $O_2^{\cdot-}$ generation (Zimmerman et al., 2002). However, the effect of redox environment on peripheral sympathetic innervation to cardiovascular function and its underlying mechanisms are not completely understood.

My experiments provided the first evidence that the redox environment in peripheral sympathetic nervous system is changed in hypertension, which is demonstrated by elevated levels of $O_2^{\cdot-}$ production in sympathetic postganglionic neurons. I also identified ET-1 as a potent stimulus for the elevation of $O_2^{\cdot-}$ levels in sympathetic neurons in DOCA-salt hypertension, an effect mediated by an upregulated level of ET_B receptor (see Chapter 3A). Furthermore, I demonstrated that NAD(P)H oxidase is present in sympathetic postganglionic neurons and the PKC dependent NAD(P)H oxidase activation in sympathetic postganglionic neurons results in $O_2^{\cdot-}$ generation. Increased sympathetic $O_2^{\cdot-}$ production in

DOCA-salt hypertensive rats is a result of upregulated NAD(P)H oxidase activity (see Chapter 3B). Finally, my study demonstrates that ET-1 acts on ET_B receptors coupled to a PKC-dependent pathway, and activates NAD(P)H oxidase to generate $O_2^{\cdot-}$ in sympathetic neurons (see Chapter 3C).

The induced $O_2^{\cdot-}$ generation may possibly reduce the neuronal NO availability, increased peripheral sympathetic nerve activity and contribute to cardiovascular diseases. With the ability to quench or inactivate NO (Li et al., 2003), which is known to increase a Ca^{++}-activated K^+ current in isolated sympathetic neurons and to reduce firing rates (Browning et al., 1998), $O_2^{\cdot-}$ would eliminate the inhibitory effect of NO and result in an increased excitability of sympathetic neurons. One recent study shows that SOD injection into the pig RVLM causes sympathoinhibition to a greater extent when the animals are under conditions of chronic ROS overproduction, and these effects of SOD are blocked by a NOS inhibitor, which further supports that $O_2^{\cdot-}$ is capable of inactivating endogenous neuronal NO to prevent its inhibitory effects on central sympathetic nerve activity (Zanzinger and Czachurski, 2000). With increased ET-1 generation in hypertension, the concomitant increase in $O_2^{\cdot-}$ levels in the peripheral sympathetic nervous system, through an activated NAD(P)H oxidase pathway, may diminish the bioavailability of NO and limit the antagonistic sympathoinhibitory influences provided by NO. This result will further increase sympathetic outflow and vasoconstrictive neurotransmitter release from nerve terminals, potentiate vasoconstrictive effects of ET-1 and consequently lead to hypertension. Unraveling these peripheral redox mechanisms in hypertension will

be important studies to pursue.

Neuronal intracellular calcium ($[Ca^{2+}]_i$) may link ET-1 and $O_2^{\cdot-}$ generation and be a key component of the ET-1-redox signaling pathway in neural control of cardiovascular function. ET-1 is capable of increasing $[Ca^{2+}]_i$ in cultured brain neurons by stimulating phosphoinositol hydrolysis and production of IP_3 and diacylglycerol (Dooley et al., 1998;Mateo and de Artinano, 1997), as well as elevating $O_2^{\cdot-}$ production in sympathetic neurons (see Chapter 3). Calcium and ROS interact with each other and establish a feed-forward signaling loop. Calcium is essential for ROS production (Gordeeva et al., 2003). Elevation of $[Ca^{2+}]_i$ level is responsible for activation of ROS generating enzymes and formation of free radicals by the mitochondria respiratory chain. A large influx of $[Ca^{2+}]_i$ into neurons has been shown to increase intracellular ROS production (Jacobson and Duchen, 2002). On the other hand, ROS may stimulate an increase in $[Ca^{2+}]_i$ (Gordeeva et al., 2003). Exposure of isolated CNS neurons to H_2O_2 leads to a dose-dependent increase in $[Ca^{2+}]_i$ (Oyama et al., 1996) and ROS potentiate Ca^{2+} signaling in rat cortical brain slices and PC12 cells (Yermolaieva et al., 2000). Future studies investigating the involvement of $[Ca^{2+}]_i$ in the intracellular signaling mechanisms utilized by ET-1 and ROS in neural cardiovascular regulation are necessary.

It is not clear if the regulation of NET by ET-1 results indirectly from an increased level of ET-1 induced $O_2^{\cdot-}$ generation. NET contains two conserved cysteine residues on the large extracellular loop similar to other monoamine transporters and these cysteine residues are highly susceptible to oxidation

(Zahniser and Doolen, 2001). Uptake mediated by DAT, SERT, or GAT is inhibited by the generation of ROS (Zahniser and Doolen, 2001). $O_2^{\bullet-}$ dramatically reduces the uptake of dopamine and GABA, but not norepinephrine in the CNS (Haughey et al., 1999). This result could be explained by the existence of different secondary protein structure of NET from other transporters (Haughey et al., 1999). However, the oxidative stress produced by norepinephrine oxidization causes a reduction in norepinephrine uptake as a result of decreased norepinephrine binding sites in PC-12 cells (Mao et al., 2004). Direct effects of $O_2^{\bullet-}$, such as treatment with $O_2^{\bullet-}$ generating enzyme xanthine oxidase plus xanthine, on the levels of NET mRNA, protein and function might need future investigation.

In conclusion, ET-1 plays critical roles in sympathetic neurons, as I demonstrated in this dissertation and these findings are summarized in Figure 31. ET-1 level is increased in DOCA-salt hypertension. This increased ET-1 potentially regulates NET, reduces uptake of norepinephrine and decreases norepinephrine clearance. In addition, ET-1 also stimulates $O_2^{\bullet-}$ generation and increases sympathetic nerve activity to increase the amount of norepinephrine released from sympathetic nerve terminals. Consequently, there is an increase in the level of neuroeffector junctional norepinephrine, followed by enhanced vasoconstriction and blood pressure elevation.

The importance of NET regulation and redox mechanisms in sympathetic neural control of cardiovascular function is a relatively new concept. NET is critical in maintaining sympathetic neuroeffector norepinephrine homeostasis and

impaired NET function is implicated in cardiovascular diseases, such as essential hypertension and congestive heart failure (Eisenhofer, 2001). ROS have important effects on neurohumoral mechanisms involved in blood pressure regulation, volume homeostasis, baroreflex function and sympathetic activity (Kishi et al., 2004;Zimmerman et al., 2002). Furthermore, oxidative stress in the CNS has been shown to be associated with some forms of hypertension and heart failure (Kishi et al., 2004;Lindley et al., 2004). The findings of this study in an animal model of hypertension demonstrate that NET regulation and neuronal oxidative stress in the peripheral sympathetic nervous system may be important new targets for therapeutic treatment of human hypertension.

Figure 31: A schematic diagram depicting possible effects of ET-1 on NET and $O_2^{\bullet-}$ generation. ET-1 level is increased in DOCA-salt hypertension and this increased ET-1 potentially not only regulates NET and impairs uptake to reduce synaptic norepinephrine clearance, but also stimulates $O_2^{\bullet-}$ generation and increases sympathetic nerve activity to increase norepinephrine release from nerve terminals. Consequently, there is an increase in junctional norepinephrine concentration and increased vasoconstriction, followed by blood pressure elevation.

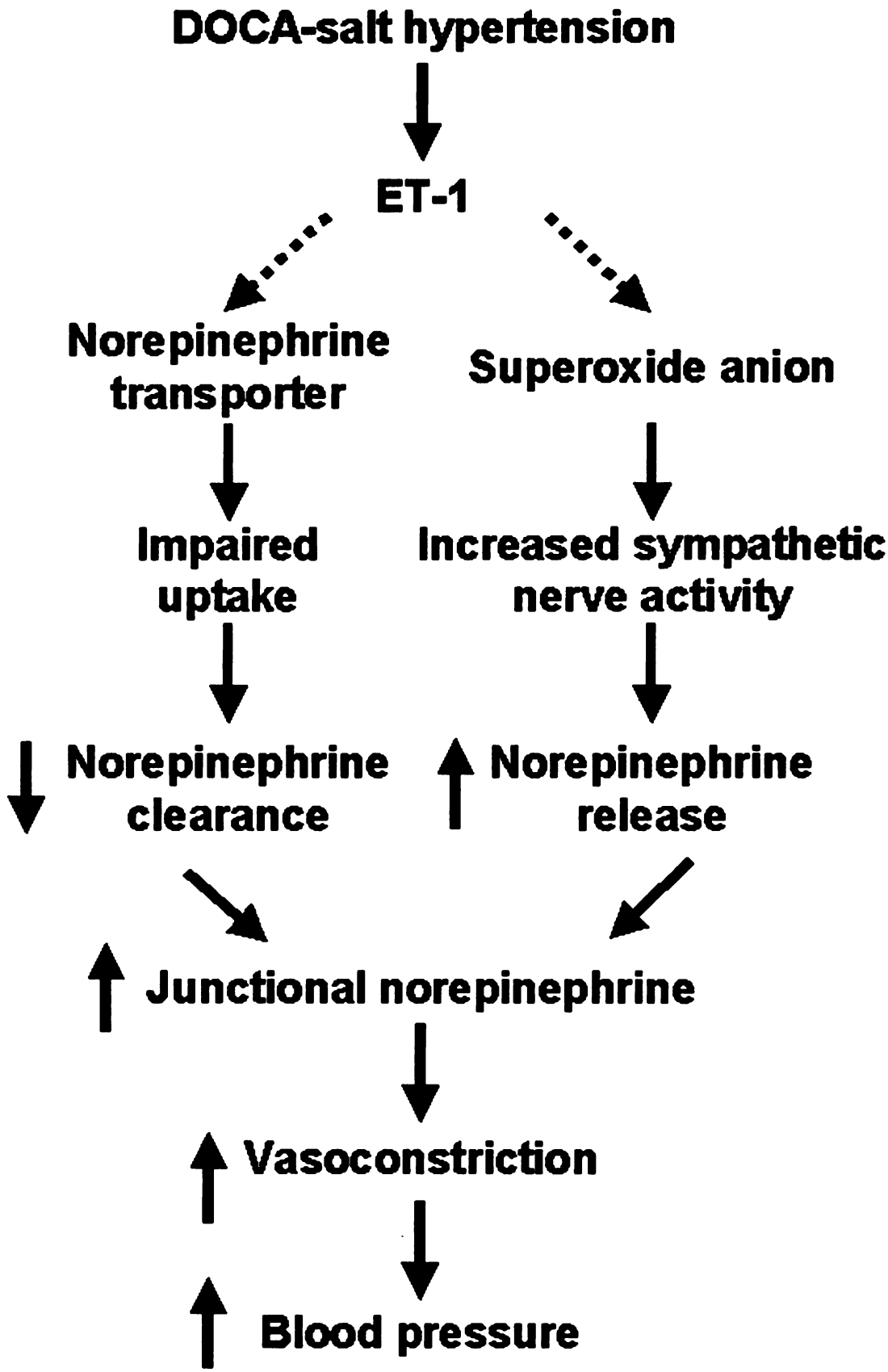
DOCA-salt hypertension
ET-1
Norepinephrine transporter
Superoxide anion
Impaired uptake
Increased sympathetic nerve activity
Norepinephrine clearance
Norepinephrine release
Junctional norepinephrine
Vasoconstriction
Blood pressure

REFERENCES

American Heart Association. 2004 Heart and Stroke Statistical Update. 2004.

Anderson EA, Sinkey CA, Lawton WJ, Mark AL (1989) Elevated sympathetic nerve activity in borderline hypertensive humans. Evidence from direct intraneural recordings. Hypertension 14: 177-183.

Apparsundaram S, Galli A, DeFelice LJ, Hartzell HC, Blakely RD (1998a) Acute regulation of norepinephrine transport: I. protein kinase C- linked muscarinic receptors influence transport capacity and transporter density in SK-N-SH cells. J Pharmacol Exp Ther 287: 733-743.

Apparsundaram S, Schroeter S, Giovanetti E, Blakely RD (1998b) Acute regulation of norepinephrine transport: II. PKC-modulated surface expression of human norepinephrine transporter proteins. J Pharmacol Exp Ther 287: 744-751.

Apparsundaram S, Sung U, Price RD, Blakely RD (2001) Trafficking-dependent and -independent pathways of neurotransmitter transporter regulation differentially involving p38 mitogen-activated protein kinase revealed in studies of insulin modulation of norepinephrine transport in SK-N-SH cells. J Pharmacol Exp Ther 299: 666-677.

Applied Biosystems. GeneAmp 5700 Sequencing Detection System: User's Manual. 1998. Foster City, CA, PE Biosystems.

Arai H, Hori S, Aramori I, Ohkubo H, Nakanishi S (1990) Cloning and expression of a cDNA encoding an endothelin receptor. Nature 348: 730-732.

Axelrod J, Whitby LG, Hertting G (1961) Effect of psychotropic drugs on the uptake of H3-norepinephrine by tissues. Science 133: 383-384.

Babior BM (1999) NADPH oxidase: an update. Blood 93: 1464-1476.

Babior BM (2004) NADPH oxidase. Curr Opin Immunol 16: 42-47.

Babior BM, Lambeth JD, Nauseef W (2002) The neutrophil NADPH oxidase. Arch Biochem Biophys 397: 342-344.

Baron R, Janig W (1991) Afferent and sympathetic neurons projecting into lumbar visceral nerves of the male rat. J Comp Neurol 314: 429-436.

Bastian NR, Hibbs JB, Jr. (1994) Assembly and regulation of NADPH oxidase and nitric oxide synthase. Curr Opin Immunol 6: 131-139.

Bauman PA, Blakely RD (2002) Determinants within the C-terminus of the human norepinephrine transporter dictate transporter trafficking, stability, and activity. Arch Biochem Biophys 404: 80-91.

Becker LB, vanden Hoek TL, Shao ZH, Li CQ, Schumacker PT (1999) Generation of superoxide in cardiomyocytes during ischemia before reperfusion. Am J Physiol 277: H2240-H2246.

Benarroch EE, Zollman PJ, Schmelzer JD, Nelson DK, Low PA (1992) Guanethidine sympathectomy increases substance P concentration in the superior sympathetic ganglion of adult rats. Brain Res 584: 305-308.

Benatti L, Fabbrini MS, Patrono C (1994) Regulation of endothelin-1 biosynthesis. Ann N Y Acad Sci 714: 109-121.

Benmansour S, Cecchi M, Morilak DA, Gerhardt GA, Javors MA, Gould GG, Frazer A (1999) Effects of chronic antidepressant treatments on serotonin transporter function, density, and mRNA level. J Neurosci 19: 10494-10501.

Benov L, Sztejnberg L, Fridovich I (1998) Critical evaluation of the use of hydroethidine as a measure of superoxide anion radical. Free Radic Biol Med 25: 826-831.

Berfield JL, Wang LC, Reith ME (1999) Which form of dopamine is the substrate for the human dopamine transporter: the cationic or the uncharged species? J Biol Chem 274: 4876-4882.

Beswick RA, Dorrance AM, Leite R, Webb RC (2001a) NADH/NADPH oxidase and enhanced superoxide production in the mineralocorticoid hypertensive rat. Hypertension 38: 1107-1111.

Beswick RA, Zhang H, Marable D, Catravas JD, Hill WD, Webb RC (2001b) Long-term antioxidant administration attenuates mineralocorticoid hypertension and renal inflammatory response. Hypertension 37: 781-786.

Bio-Rad Laboratories. Real-Time PCR: General Considerations. 2001. Bio-Rad Laboratories, Inc. Tech Note 2593.

Bio-Rad Laboratories. The iCycler iQ Real-time Detection System Resource Guide. 2002. Bio-Rad.

Blakely RD, Clark JA, Pacholczyk T, Amara SG (1991) Distinct, developmentally regulated brain mRNAs direct the synthesis of neurotransmitter transporters. J Neurochem 56: 860-871.

Bohr DF, Dominiczak AF (1991) Experimental hypertension. Hypertension 17: I39-I44.

Bonisch H, Eiden L (1998) Catecholamine reuptake and storage. Overview. Adv Pharmacol 42: 149-164.

Bonisch H, Paulus G, Martiny-Baron G, Lingen B, Coppeneur D (1991) Molecular

aspects of the neuronal noradrenaline transporter. J Neural Transm Suppl 34: 11-17.

Bonisch H, Runkel F, Roubert C, Giros B, Bruss M (1999) The human desipramine-sensitive noradrenaline transporter and the importance of defined amino acids for its function. J Auton Pharmacol 19: 327-333.

Borgman RF (1985) Dietary factors in essential hypertension. Prog Food Nutr Sci 9: 109-147.

Brandes RP, Miller FJ, Beer S, Haendeler J, Hoffmann J, Ha T, Holland SM, Gorlach A, Busse R (2002) The vascular NADPH oxidase subunit p47phox is involved in redox-mediated gene expression. Free Radic Biol Med 32: 1116-1122.

Brody MJ (1988) Central nervous system and mechanisms of hypertension. Clin Physiol Biochem 6: 230-239.

Browning KN, Zheng ZL, Kreulen DL, Travagli RA (1998) Effects of nitric oxide in cultured prevertebral sympathetic ganglion neurons. J Pharmacol Exp Ther 286: 1086-1093.

Browning KN, Zheng ZL, Kreulen DL, Travagli RA (1999) Two populations of sympathetic neurons project selectively to mesenteric artery or vein. Am J Physiol 276: H1263-H1272.

Bruss M, Hammermann R, Brimijoin S, Bonisch H (1995) Antipeptide antibodies confirm the topology of the human norepinephrine transporter. J Biol Chem 270: 9197-9201.

Bruss M, Porzgen P, Bryan-Lluka LJ, Bonisch H (1997) The rat norepinephrine transporter: molecular cloning from PC12 cells and functional expression. Brain Res Mol Brain Res 52: 257-262.

Bzoskie L, Blount L, Kashiwai K, Tseng YT, Hay WW, Jr., Padbury JF (1995) Placental norepinephrine clearance: in vivo measurement and physiological role. Am J Physiol 269: E145-E149.

Bzoskie L, Yen J, Tseng YT, Blount L, Kashiwai K, Padbury JF (1997) Human placental norepinephrine transporter mRNA: expression and correlation with fetal condition at birth. Placenta 18: 205-210.

Cai H, Harrison DG (2000) Endothelial dysfunction in cardiovascular diseases: the role of oxidant stress. Circ Res 87: 840-844.

Cao WH, Kuwaki T, Unekawa M, Ling GY, Terui N, Kumada M (1993) Action of endothelin-1 on vasomotor neurons in rat rostral ventrolateral medulla. J Cardiovasc Pharmacol 22 Suppl 8: S196-S198.

Carvalho JJ, Baruzzi RG, Howard PF, Poulter N, Alpers MP, Franco LJ, Marcopito LF, Spooner VJ, Dyer AR, Elliott P, . (1989) Blood pressure in four remote populations in the INTERSALT Study. Hypertension 14: 238-246.

Ceccatelli S, Lundberg JM, Zhang X, Aman K, Hokfelt T (1994) Immunohistochemical demonstration of nitric oxide synthase in the peripheral autonomic nervous system. Brain Res 656: 381-395.

Chappell DC, Varner SE, Nerem RM, Medford RM, Alexander RW (1998) Oscillatory shear stress stimulates adhesion molecule expression in cultured human endothelium. Circ Res 82: 532-539.

Cheng TH, Cheng PY, Shih NL, Chen IB, Wang DL, Chen JJ (2003) Involvement of reactive oxygen species in angiotensin II-induced endothelin-1 gene expression in rat cardiac fibroblasts. J Am Coll Cardiol 42: 1845-1854.

Corey JL, Davidson N, Lester HA, Brecha N, Quick MW (1994) Protein kinase C modulates the activity of a cloned gamma-aminobutyric acid transporter expressed in Xenopus oocytes via regulated subcellular redistribution of the transporter. J Biol Chem 269: 14759-14767.

Crofton JT, Share L, Shade RE, Lee-Kwon WJ, Manning M, Sawyer WH (1979) The importance of vasopressin in the development and maintenance of DOC-salt hypertension in the rat. Hypertension 1: 31-38.

Cross AR, Parkinson JF, Jones OT (1984) The superoxide-generating oxidase of leucocytes. NADPH-dependent reduction of flavin and cytochrome b in solubilized preparations. Biochem J 223: 337-344.

Cubells JF, Kim KS, Baker H, Volpe BT, Chung Y, Houpt TA, Wessel TC, Joh TH (1995) Differential in vivo regulation of mRNA encoding the norepinephrine transporter and tyrosine hydroxylase in rat adrenal medulla and locus ceruleus. J Neurochem 65: 502-509.

Dahl LK (1972) Salt and hypertension. Am J Clin Nutr 25: 231-244.

Dahl LK, HEINE M, TASSINARI L (1962) Role of genetic factors in susceptibility to experimental hypertension due to chronic excess salt ingestion. Nauchni Tr Vissh Med Inst Sofiia 194: 480-482.

Dai X, Fink GD, and Kreulen DL Elevation of superoxide anions in sympathetic neurons in DOCA-salt hypertension via activation of NADPH oxidase. FASEB J . 2004a.

Dai X, Galligan JJ, Watts SW, Fink GD, Kreulen DL (2004b) Increased O2*- production and upregulation of ETB receptors by sympathetic neurons in DOCA-salt hypertensive rats. Hypertension 43: 1048-1054.

Damon DH (1998) Postganglionic sympathetic neurons express endothelin. Am J Physiol 274: R873-R878.

Damon DH (1999) Endothelin and post-ganglionic sympathetic neurons. Clin Exp Pharmacol Physiol 26: 1000-1003.

Dampney RA (1994) Functional organization of central pathways regulating the cardiovascular system. Physiol Rev 74: 323-364.

de Champlain J (1990) Pre- and postsynaptic adrenergic dysfunctions in hypertension. J Hypertens Suppl 8: S77-S85.

de Champlain J, Cousineau D, Van Amerigen MR, Marc-Aurele J, Yamaguchi N (1977) The role of the sympathetic system in experimental and human hypertension. Postgrad Med J 53 Suppl 3: 15-30.

de Champlain J, Eid H, Drolet G, Bouvier M, Foucart S (1989) Peripheral neurogenic mechanisms in deoxycorticosterone acetate--salt hypertension in the rat. Can J Physiol Pharmacol 67: 1140-1145.

de Champlain J, Krakoff LR, AXELROD J (1966) A reduction in the accumulation of H3-norepinephrine in experimental hypertension. Life Sci 5: 2283-2291.

De Keulenaer GW, Alexander RW, Ushio-Fukai M, Ishizaka N, Griendling KK (1998) Tumour necrosis factor alpha activates a p22phox-based NADH oxidase in vascular smooth muscle. Biochem J 329 (Pt 3): 653-657.

DiBona GF, Jones SY, Kopp UC (1999) Renal mechanoreceptor dysfunction: an intermediate phenotype in spontaneously hypertensive rats. Hypertension 33: 472-475.

Dimmeler S, Zeiher AM (2000) Reactive oxygen species and vascular cell apoptosis in response to angiotensin II and pro-atherosclerotic factors. Regul Pept 90: 19-25.

Dobrian AD, Schriver SD, Prewitt RL (2001) Role of angiotensin II and free radicals in blood pressure regulation in a rat model of renal hypertension. Hypertension 38: 361-366.

Docherty JR (1998) Subtypes of functional alpha1- and alpha2-adrenoceptors. Eur J Pharmacol 361: 1-15.

Donmez G, Derici U, Erbas D, Arinsoy T, Onk A, Sindel S, Hasanoglu E (2002) The effects of losartan and enalapril therapies on the levels of nitric oxide, malondialdehyde, and glutathione in patients with essential hypertension. Jpn J Physiol 52: 435-440.

Dooley DJ, Geer JJ, Haleen SJ, Probert AW, Welch KM (1998) Assessment of endothelin receptor subtype-mediated increases of [Ca2+]i in distinct rat cell types using fluorimetric imaging. J Cardiovasc Pharmacol 31 Suppl 1: S192-S195.

Doucet J, Gonzalez W, Michel JB (1996) Endothelin antagonists in salt-dependent hypertension associated with renal insufficiency. J Cardiovasc Pharmacol 27: 643-651.

Droge W (2002) Free radicals in the physiological control of cell function. Physiol Rev 82: 47-95.

Drolet G, Bouvier M, de Champlain J (1989) Enhanced sympathoadrenal reactivity to haemorrhagic stress in DOCA-salt hypertensive rats. J Hypertens 7: 237-242.

Dubocovich ML, Langer SZ (1976) Influence of the frequency of nerve stimulation on the metabolism of 3H-norepinephrine released from the perfused cat spleen: differences observed during and after the period of stimulation. J Pharmacol Exp Ther 198: 83-101.

Dustan HP (1991) A perspective on the salt-blood pressure relation. Hypertension 17: I166-I169.

Eid H, de Champlain J (1988a) Effects of chronic dietary lithium on phosphatidylinositol pathway in heart and arteries of DOCA-salt hypertensive rats. Am J Hypertens 1: 64-66.

Eid H, de Champlain J (1988b) Increased inositol monophosphate production in cardiovascular tissues of DOCA-salt hypertensive rats. Hypertension 12: 122-128.

Eisenhofer G (1994) Plasma normetanephrine for examination of extraneuronal uptake and metabolism of noradrenaline in rats. Naunyn Schmiedebergs Arch Pharmacol 349: 259-269.

Eisenhofer G (2001) The role of neuronal and extraneuronal plasma membrane transporters in the inactivation of peripheral catecholamines. Pharmacol Ther 91: 35-62.

Elmarakby AA, Williams JM, Pollock DM (2003) Targeting sources of superoxide and increasing nitric oxide bioavailability in hypertension. Curr Opin Investig Drugs 4: 282-290.

Ely DL (1997) Overview of dietary sodium effects on and interactions with cardiovascular and neuroendocrine functions. Am J Clin Nutr 65: 594S-605S.

Endo T, Starke K, Bangerter A, Taube HD (1977) Presynaptic receptor systems

on the noradrenergic neurones of the rabbit pulmonary artery. Naunyn Schmiedebergs Arch Pharmacol 296: 229-247.

Epperson A, Hatton WJ, Callaghan B, Doherty P, Walker RL, Sanders KM, Ward SM, Horowitz B (2000) Molecular markers expressed in cultured and freshly isolated interstitial cells of Cajal. Am J Physiol Cell Physiol 279: C529-C539.

Ergul S, Parish DC, Puett D, Ergul A (1996) Racial differences in plasma endothelin-1 concentrations in individuals with essential hypertension. Hypertension 28: 652-655.

Esler M, Jackman G, Bobik A, Leonard P, Kelleher D, Skews H, Jennings G, Korner P (1981) Norepinephrine kinetics in essential hypertension. Defective neuronal uptake of norepinephrine in some patients. Hypertension 3: 149-156.

Esler M, Leonard P, Kelleher D, Jackman G, Bobik A, Skews H, Jennings G, Korner P (1980) Assessment of neuronal uptake of noradrenaline in humans: defective uptake in some patients with essential hypertension. Clin Exp Pharmacol Physiol 7: 535-539.

Ferrario CM, Tramposch A, Kawano Y, Brosnihan KB (1987) Sodium balance and the reflex regulation of baroreceptor function. Circulation 75: I141-I148.

Ferrier C, Cox H, Esler M (1993) Elevated total body noradrenaline spillover in normotensive members of hypertensive families. Clin Sci (Colch) 84: 225-230.

Foecking MK, Hofstetter H (1986) Powerful and versatile enhancer-promoter unit for mammalian expression vectors. Gene 45: 101-105.

Forman HJ, Torres M, Fukuto J (2002) Redox signaling. Mol Cell Biochem 234-235: 49-62.

Fujita K, Matsumura Y, Kita S, Miyazaki Y, Hisaki K, Takaoka M, Morimoto S (1995) Role of endothelin-1 and the ETA receptor in the maintenance of deoxycorticosterone acetate-salt-induced hypertension. Br J Pharmacol 114: 925-930.

Fukui T, Ishizaka N, Rajagopalan S, Laursen JB, Capers Q, Taylor WR, Harrison DG, de Leon H, Wilcox JN, Griendling KK (1997b) p22phox mRNA expression and NADPH oxidase activity are increased in aortas from hypertensive rats. Circ Res 80: 45-51.

Fukui T, Ishizaka N, Rajagopalan S, Laursen JB, Capers Q, Taylor WR, Harrison DG, de Leon H, Wilcox JN, Griendling KK (1997a) p22phox mRNA expression and NADPH oxidase activity are increased in aortas from hypertensive rats. Circ Res 80: 45-51.

Galli A, Blakely RD, DeFelice LJ (1996) Norepinephrine transporters have

channel modes of conduction. Proc Natl Acad Sci U S A 93: 8671-8676.

Galli A, DeFelice LJ, Duke BJ, Moore KR, Blakely RD (1995) Sodium-dependent norepinephrine-induced currents in norepinephrine- transporter-transfected HEK-293 cells blocked by cocaine and antidepressants. J Exp Biol 198 (Pt 10): 2197-2212.

Gao HM, Liu B, Zhang W, Hong JS (2003) Critical role of microglial NADPH oxidase-derived free radicals in the in vitro MPTP model of Parkinson's disease. FASEB J 17: 1954-1956.

Garty H (1986) Mechanisms of aldosterone action in tight epithelia. J Membr Biol 90: 193-205.

Gershon MD (1995) Neural crest development. Do developing enteric neurons need endothelins? Curr Biol 5: 601-604.

Giaid A, Gibson SJ, Herrero MT, Gentleman S, Legon S, Yanagisawa M, Masaki T, Ibrahim NB, Roberts GW, Rossi ML (1991) Topographical localisation of endothelin mRNA and peptide immunoreactivity in neurones of the human brain. Histochemistry 95: 303-314.

Giros B, El Mestikawy S, Bertrand L, Caron MG (1991) Cloning and functional characterization of a cocaine-sensitive dopamine transporter. FEBS Lett 295: 149-154.

Goddard J, Webb DJ (2000) Plasma endothelin concentrations in hypertension. J Cardiovasc Pharmacol 35: S25-S31.

Goldstein DS (1983) Plasma catecholamines and essential hypertension. An analytical review. Hypertension 5: 86-99.

Gonzalez-Albarran O, Ruilope LM, Villa E, Garcia RR (1998) Salt sensitivity: concept and pathogenesis. Diabetes Res Clin Pract 39 Suppl: S15-S26.

Gordeeva AV, Zvyagilskaya RA, Labas YA (2003) Cross-talk between reactive oxygen species and calcium in living cells. Biochemistry (Mosc) 68: 1077-1080.

Gradin K, Dahlof C, Persson B (1986) A low dietary sodium intake reduces neuronal noradrenaline release and the blood pressure in spontaneously hypertensive rats. Naunyn Schmiedebergs Arch Pharmacol 332: 364-369.

Greene LA, Farinelli SE, Cunningham ME, Park DS (1998) Culture and experimental use of the PC 12 rat pheochromacytoma cell line. In: Culturing Nerve Cells (Gary Banker, Kimberly Goslin, eds), Cambridge, Massachusetts: The MIT Press.

Greenway CV (1983b) Role of splanchnic venous system in overall

cardiovascular homeostasis. Fed Proc 42: 1678-1684.

Greenway CV (1983a) Role of splanchnic venous system in overall cardiovascular homeostasis. Fed Proc 42: 1678-1684.

Griendling KK, Minieri CA, Ollerenshaw JD, Alexander RW (1994) Angiotensin II stimulates NADH and NADPH oxidase activity in cultured vascular smooth muscle cells. Circ Res 74: 1141-1148.

Griendling KK, Sorescu D, Ushio-Fukai M (2000) NAD(P)H oxidase: role in cardiovascular biology and disease. Circ Res 86: 494-501.

Griendling KK, Tsuda T, Alexander RW (1989) Endothelin stimulates diacylglycerol accumulation and activates protein kinase C in cultured vascular smooth muscle cells. J Biol Chem 264: 8237-8240.

Griendling KK, Ushio-Fukai M (2000) Reactive oxygen species as mediators of angiotensin II signaling. Regul Pept 91: 21-27.

Groemping Y, Lapouge K, Smerdon SJ, Rittinger K (2003) Molecular basis of phosphorylation-induced activation of the NADPH oxidase. Cell 113: 343-355.

Guimaraes S, Moura D (2001) Vascular adrenoceptors: an update. Pharmacol Rev 53: 319-356.

Guyton AC (1991a) Cardiac output, venous return, and their regulation. In: Textbook of Medical Physiology (Guyton AC, ed), pp 221-233. Philadelphia: W. B. Saunders Company.

Guyton AC (1991b) Nervous regulation of the circulation, and rapid control of arterial pressure. In: Textbook of Medical Physiology (Guyton AC, ed), pp 194-204. Philadelphia, Pennsylvania: W.B. Saunders Company.

Hahn MK, Robertson D, Blakely RD (2003) A Mutation in the Human Norepinephrine Transporter Gene (SLC6A2) Associated with Orthostatic Intolerance Disrupts Surface Expression of Mutant and Wild-Type Transporters. J Neurosci 23: 4470-4478.

Hama H, Sakurai T, Kasuya Y, Fujiki M, Masaki T, Goto K (1992) Action of endothelin-1 on rat astrocytes through the ETB receptor. Biochem Biophys Res Commun 186: 355-362.

Harder R, Bonisch H (1985) Effects of monovalent ions on the transport of noradrenaline across the plasma membrane of neuronal cells (PC-12 cells). J Neurochem 45: 1154-1162.

Haughey HM, Brown JM, Fleckenstein AE, Hanson GR (1999) Oxygen radicals differentially affect Na+/Cl(-)-dependent transporters. Eur J Pharmacol 379: 107-

110.

Hebert C, Habimana A, Elie R, Reader TA (2001) Effects of chronic antidepressant treatments on 5-HT and NA transporters in rat brain: an autoradiographic study. Neurochem Int 38: 63-74.

Heitzer T, Wenzel U, Hink U, Krollner D, Skatchkov M, Stahl RA, MacHarzina R, Brasen JH, Meinertz T, Munzel T (1999) Increased NAD(P)H oxidase-mediated superoxide production in renovascular hypertension: evidence for an involvement of protein kinase C. Kidney Int 55: 252-260.

Higashi M, Shimokawa H, Hattori T, Hiroki J, Mukai Y, Morikawa K, Ichiki T, Takahashi S, Takeshita A (2003) Long-term inhibition of Rho-kinase suppresses angiotensin II-induced cardiovascular hypertrophy in rats in vivo: effect on endothelial NAD(P)H oxidase system. Circ Res 93: 767-775.

Hirata Y, Takagi Y, Fukuda Y, Marumo F (1989) Endothelin is a potent mitogen for rat vascular smooth muscle cells. Atherosclerosis 78: 225-228.

Hohler B, Holzapfel B, Kummer W (2000) NADPH oxidase subunits and superoxide production in porcine pulmonary artery endothelial cells. Histochem Cell Biol 114: 29-37.

Hottenstein OD, Kreulen DL (1987) Comparison of the frequency dependence of venous and arterial responses to sympathetic nerve stimulation in guinea-pigs. J Physiol (Lond) 384: 153-167.

Iriuchijima J, Mizogami S, Sokabe H (1975) Sympathetic nervous activity in renal and DOC hypertensive rats. Jpn Heart J 16: 36-43.

Itaya Y, Suzuki H, Matsukawa S, Kondo K, Saruta T (1986) Central renin-angiotensin system and the pathogenesis of DOCA-salt hypertension in rats. Am J Physiol 251: H261-H268.

Iversen L (1963) The uptake of noradrenaline by isolated perfused rat heart. Br J Pharmacol 21: 523-537.

Jackisch R, Huang HY, Rensing H, Lauth D, Allgaier C, HERTTING G (1992) Alpha 2-adrenoceptor mediated inhibition of exocytotic noradrenaline release in the absence of extracellular Ca2+. Eur J Pharmacol 226: 245-252.

Jacobson J, Duchen MR (2002) Mitochondrial oxidative stress and cell death in astrocytes--requirement for stored Ca2+ and sustained opening of the permeability transition pore. J Cell Sci 115: 1175-1188.

Jaimes EA, Galceran JM, Raij L (1998) Angiotensin II induces superoxide anion production by mesangial cells. Kidney Int 54: 775-784.

Job C, Eberwine J (2001) Localization and translation of mRNA in dendrites and axons. Nat Rev Neurosci 2: 889-898.

Johnson RJ, Fink GD, Watts SW, Galligan JJ (2002) Endothelin receptor function in mesenteric veins from deoxycorticosterone acetate salt-hypertensive rats. J Hypertens 20: 665-676.

Jones SA, O'Donnell VB, Wood JD, Broughton JP, Hughes EJ, Jones OT (1996) Expression of phagocyte NADPH oxidase components in human endothelial cells. Am J Physiol 271: H1626-H1634.

Joyce PI, Atcheson R, Marcus RJ, Heffernan AM, Rowbotham DJ, Lambert DG (2001) Interaction of local anaesthetic agents with the endogenous norepinephrine transporter in SH-SY5Y human neuroblastoma cells. Neurosci Lett 305: 161-164.

Judy WV, Watanabe AM, Henry DP, Besch HR, Jr., Murphy WR, Hockel GM (1976) Sympathetic nerve activity: role in regulation of blood pressure in the spontaenously hypertensive rat. Circ Res 38: 21-29.

Julius S, Pascual AV, London R (1971) Role of parasympathetic inhibition in the hyperkinetic type of borderline hypertension. Circulation 44: 413-418.

Kantor L, Hewlett GH, Park YH, Richardson-Burns SM, Mellon MJ, Gnegy ME (2001) Protein kinase C and intracellular calcium are required for amphetamine-mediated dopamine release via the norepinephrine transporter in undifferentiated PC12 cells. J Pharmacol Exp Ther 297: 1016-1024.

Karim F, Hainsworth R (1976) Responses of abdominal vascular capacitance to stimulation of splanchnic nerves. Am J Physiol 231(2): 434-440.

Katholi RE, Naftilan AJ, Oparil S (1980) Importance of renal sympathetic tone in the development of DOCA-salt hypertension in the rat. Hypertension 2: 266-273.

Kim SH, Won SJ, Sohn S, Kwon HJ, Lee JY, Park JH, Gwag BJ (2002) Brain-derived neurotrophic factor can act as a pronecrotic factor through transcriptional and translational activation of NADPH oxidase. J Cell Biol 159: 821-831.

Kimura S, Miura Y, Adachi M, Adachi M, Nezu M, Toriyabe S, Sugawara T, Ishizuka Y, Noshiro T, Takahashi M, . (1983) The effect of sodium depletion on plasma norepinephrine kinetics in patients with essential hypertension. Jpn Circ J 47: 1232-1241.

Kishi T, Hirooka Y, Ito K, Sakai K, Shimokawa H, Takeshita A (2002) Cardiovascular effects of overexpression of endothelial nitric oxide synthase in the rostral ventrolateral medulla in stroke-prone spontaneously hypertensive rats. Hypertension 39: 264-268.

Kishi T, Hirooka Y, Kimura Y, Ito K, Shimokawa H, Takeshita A (2004) Increased reactive oxygen species in rostral ventrolateral medulla contribute to neural mechanisms of hypertension in stroke-prone spontaneously hypertensive rats. Circulation.

Klein JA, Ackerman SL (2003) Oxidative stress, cell cycle, and neurodegeneration. J Clin Invest 111: 785-793.

Kodama M, Kanaide H, Abe S, Hirano K, Kai H, Nakamura M (1989) Endothelin-induced Ca-independent contraction of the porcine coronary artery. Biochem Biophys Res Commun 160: 1302-1308.

Kohno M, Yasunari K, Murakawa K, Yokokawa K, Horio T, Fukui T, Takeda T (1990) Plasma immunoreactive endothelin in essential hypertension. Am J Med 88: 614-618.

Konishi H, Tanaka M, Takemura Y, Matsuzaki H, Ono Y, Kikkawa U, Nishizuka Y (1997) Activation of protein kinase C by tyrosine phosphorylation in response to H2O2. Proc Natl Acad Sci U S A 94: 11233-11237.

Koseki C, Imai M, Hirata Y, Yanagisawa M, Masaki T (1989) Autoradiographic localization of [125I]-endothelin-1 binding sites in rat brain. Neurosci Res 6: 581-585.

Kreulen DL, Keef KD (1989) Electrophysiological and neuromuscular relationships in extramural blood vessels. In: Handbook of Physiology (Wood JD, ed), pp 1605-1634. Baltimore,MD: American Physiological Society.

Kreulen DL, Peters S (1986) Non-cholinergic transmission in a sympathetic ganglion of the guinea-pig elicited by colon distension. J Physiol 374: 315-334.

Krum H, Viskoper RJ, Lacourciere Y, Budde M, Charlon V (1998) The effect of an endothelin-receptor antagonist, bosentan, on blood pressure in patients with essential hypertension. Bosentan Hypertension Investigators. N Engl J Med 338: 784-790.

Kuhlman D, Ragan C, Ferrebee JW, Atchley DW, Loeb RF (1939) Toxic effects of deoxycorticosterone esters in dogs. Science 90: 496-497.

Kurihara H, Kurihara Y, Nagai R, Yazaki Y (1999) Endothelin and neural crest development. Cell Mol Biol (Noisy -le-grand) 45: 639-651.

Kuwaki T, Kurihara Y, Kurihara H, Yazaki Y, Kumada M (1995) Role of endothelin in central cardiorespiratory control: modern and classical approaches. News Physiol Sci 228-233.

Lamarre-Cliche M, Cusson J (1999) Octreotide for orthostatic hypotension. Can J Clin Pharmacol 6: 213-215.

Lambeth JD, Cheng G, Arnold RS, Edens WA (2000) Novel homologs of gp91phox. Trends Biochem Sci 25: 459-461.

Lamprecht F, Richardson JS, Williams RB, Kopin IJ (1977) 6-Hydroxydopamine destruction of central adrenergic neurones prevents or reverses developing DOCA-salt hypertension in rats. J Neural Transm 40: 149-158.

Lassegue B, Clempus RE (2003) Vascular NAD(P)H oxidases: specific features, expression, and regulation. Am J Physiol Regul Integr Comp Physiol 285: R277-R297.

Lassegue B, Sorescu D, Szocs K, Yin Q, Akers M, Zhang Y, Grant SL, Lambeth JD, Griendling KK (2001) Novel gp91(phox) homologues in vascular smooth muscle cells : nox1 mediates angiotensin II-induced superoxide formation and redox-sensitive signaling pathways. Circ Res 88: 888-894.

Laursen JB, Rajagopalan S, Galis Z, Tarpey M, Freeman BA, Harrison DG (1997) Role of superoxide in angiotensin II-induced but not catecholamine-induced hypertension. Circulation 95: 588-593.

Ledingham JM, Pelling D (1970) Haemodynamic and other studies in the renoprival hypertensive rat. J Physiol Lond 210: 233-253.

Lee CM, Javitch JA, Snyder SH (1983) Recognition sites for norepinephrine uptake: regulation by neurotransmitter. Science 220: 626-629.

Lee CY, Chiappinelli VA (1989) Sequence homology between sarafotoxins S6 and porcine endothelin. Toxicon 27: 277-279.

Li JM, Mullen AM, Yun S, Wientjes F, Brouns GY, Thrasher AJ, Shah AM (2002) Essential role of the NADPH oxidase subunit p47(phox) in endothelial cell superoxide production in response to phorbol ester and tumor necrosis factor-alpha. Circ Res 90: 143-150.

Li JM, Shah AM (2002) Intracellular localization and preassembly of the NADPH oxidase complex in cultured endothelial cells. J Biol Chem 277: 19952-19960.

Li L, Fink GD, Watts SW, Northcott CA, Galligan JJ, Pagano PJ, Chen AF (2003) Endothelin-1 Increases Vascular Superoxide via Endothelin(A)-NADPH Oxidase Pathway in Low-Renin Hypertension. Circulation 107: 1053-1058.

Lilly LS (1993) Hypertension. In: Pathophysiology of Heart Disease (Lilly L, ed), pp 208-226. Philadelphia: Lea and Febiger.

Lin HH, Chen CH, Hsieh WK, Chiu TH, Lai CC (2003) Hydrogen peroxide increases the activity of rat sympathetic preganglionic neurons in vivo and in vitro. Neuroscience 121: 641-647.

Lindley TE, Doobay MF, Sharma RV, Davisson RL (2004) Superoxide is involved in the central nervous system activation and sympathoexcitation of myocardial infarction-induced heart failure. Circ Res 94: 402-409.

Lingen B, Bruss M, Bonisch H (1994) Cloning and expression of the bovine sodium- and chloride-dependent noradrenaline transporter. FEBS Lett 342: 235-238.

Lowry OH, Rosebrough NJ, Farr AL, Randall RJ (1951) Protein measurement with the Folin phenol reagent. J Biol Chem **193**: 265-275.

Lu D, Yu K, Paddy MR, Rowland NE, Raizada MK (1996) Regulation of norepinephrine transport system by angiotensin II in neuronal cultures of normotensive and spontaneously hypertensive rat brains. Endocrinology 137: 763-772.

Luff SE, Young SB, McLachlan EM (2000) Ultrastructure of substance P-immunoreactive terminals and their relation to vascular smooth muscle cells of rat small mesenteric arteries. J Comp Neurol 416: 277-290.

Luft FC, Rankin LI, Henry DP, Weinberger MH (1982) Sodium and the effects of norepinephrine. In: The role of salt in cardiovascular hypertension (Fregly MJ, Kare MR, eds), pp 267-280. New York: Academic Press.

Luft FC, Weinberger MH (1982) Sodium intake and essential hypertension. Hypertension 4: III14-III19.

Lund-Johansen P (1994) Hemodynamics of essential hypertension. In: Textbook of hypertension pp 61-76. Oxford: Blackwell Scientific Publications.

Luo M, Fink GD, Lookingland KJ, Morris JA, Galligan JJ (2004) Impaired function of alpha2-adrenergic autoreceptors on sympathetic nerves associated with mesenteric arteries and veins in DOCA-salt hypertension. Am J Physiol Heart Circ Physiol 286: H1558-H1564.

Luo M, Hess MC, Fink GD, Olson LK, Rogers J, Kreulen DL, Dai X, Galligan JJ (2003) Differential alterations in sympathetic neurotransmission in mesenteric arteries and veins in DOCA-salt hypertensive rats. Auton Neurosci 104: 47-57.

Lysko PG, Elshourbagy NA, Pullen M, Nambi P (1995) Developmental expression of endothelin receptors in cerebellar neurons differentiating in culture. Brain Res Dev Brain Res 88: 96-101.

Maczewski M, Beresewicz A (2000) The role of endothelin, protein kinase C and free radicals in the mechanism of the post-ischemic endothelial dysfunction in guinea-pig hearts. J Mol Cell Cardiol 32: 297-310.

Majewski H, Iannazzo L (1998) Protein kinase C: a physiological mediator of

enhanced transmitter output. Prog Neurobiol 55: 463-475.

Malik KU, Nasjletti A (1976) Facilitation of adrenergic transmission by locally generated angiotensin II in rat mesenteric arteries. Circ Res 38: 26-30.

Mancia G, Grassi G, Giannattasio C, Seravalle G (1999) Sympathetic activation in the pathogenesis of hypertension and progression of organ damage. Hypertension 34: 724-728.

Mao W, Qin F, Iwai C, Vulapalli R, Keng PC, Liang CS (2004) Extracellular norepinephrine reduces neuronal uptake of norepinephrine by oxidative stress in PC12 cells. Am J Physiol Heart Circ Physiol.

Marui N, Offermann MK, Swerlick R, Kunsch C, Rosen CA, Ahmad M, Alexander RW, Medford RM (1993) Vascular cell adhesion molecule-1 (VCAM-1) gene transcription and expression are regulated through an antioxidant-sensitive mechanism in human vascular endothelial cells. J Clin Invest 92: 1866-1874.

Massachusetts Institute of Technology. Primer3. 2003.

Masson J, Sagn C, Hamon M, Mestikawy SE (1999) Neurotransmitter transporters in the central nervous system. Pharmacol Rev 51: 439-464.

Mateo AO, de Artinano AA (1997) Highlights on endothelins: A review. Pharmacol Res 36: 339-351.

Matsumura Y, Fujita K, Miyazaki Y, Takaoka M, Morimoto S (1995) Involvement of endothelin-1 in deoxycorticosterone acetate-salt-induced hypertension and cardiovascular hypertrophy. J Cardiovasc Pharmacol 26 Suppl 3: S456-S458.

Melikian HE, McDonald JK, Gu H, Rudnick G, Moore KR, Blakely RD (1994) Human norepinephrine transporter. Biosynthetic studies using a site- directed polyclonal antibody. J Biol Chem 269: 12290-12297.

Mendlowitz M (1975) Neurohumoral mechanisms in hypertension. Angiology 26: 25-30.

Meyer JW, Schmitt ME (2000) A central role for the endothelial NADPH oxidase in atherosclerosis. FEBS Lett 472: 1-4.

Millette E, de Champlain J, Lamontagne D (2003) Contribution of endogenous endothelin in the enhanced coronary constriction in DOCA-salt hypertensive rats. J Hypertens 21: 115-123.

Milner P, Loesch A, Burnstock G (2000a) Endothelin immunoreactivity and mRNA expression in sensory and sympathetic neurones following selective denervation. Int J Dev Neurosci 18: 727-734.

Milner P, Loesch A, Burnstock G (2000b) Neural endothelin in hypertension: increased expression in ganglia and nerves to cerebral arteries of the spontaneously hypertensive rat. J Vasc Res 37: 39-49.

Miyashiro K, Dichter M, Eberwine J (1994) On the nature and differential distribution of mRNAs in hippocampal neurites: implications for neuronal functioning. Proc Natl Acad Sci U S A 91: 10800-10804.

Mollnau H, Wendt M, Szocs K, Lassegue B, Schulz E, Oelze M, Li H, Bodenschatz M, August M, Kleschyov AL, Tsilimingas N, Walter U, Forstermann U, Meinertz T, Griendling KK, Munzel T (2002) Effects of angiotensin II infusion on the expression and function of NAD(P)H oxidase and components of nitric oxide/cGMP signaling. Circ Res 90: E58-E65.

Mortensen LH (1999) Endothelin and the central and peripheral nervous systems: a decade of endothelin research. Clin Exp Pharmacol Physiol 26: 980-984.

Mortensen LH, Fink GD (1990) Hemodynamic effect of human and rat endothelin administration into conscious rats. Am J Physiol 258: H362-H368.

Mortensen LH, Fink GD (1992) Salt-dependency of endothelin-induced, chronic hypertension in conscious rats. Hypertension 19: 549-554.

Mortensen LH, Pawloski CM, Kanagy NL, Fink GD (1990) Chronic hypertension produced by infusion of endothelin in rats. Hypertension 15: 729-733.

Mutafova-Yambolieva VN, Radomirov RG (1994) Modulatory effects of endothelin-1 on purinergic and adrenergic components of sympathetically-mediated contractile activity of rabbit saphenous artery. Br J Pharmacol 112: 1109-1117.

Mutafova-Yambolieva VN, Westfall DP (1998) Inhibitory and facilitatory presynaptic effects of endothelin on sympathetic cotransmission in the rat isolated tail artery. Br J Pharmacol 123: 136-142.

Nakane H, Miller FJ, Jr., Faraci FM, Toyoda K, Heistad DD (2000) Gene transfer of endothelial nitric oxide synthase reduces angiotensin II-induced endothelial dysfunction. Hypertension 35: 595-601.

Nataf V, Lecoin L, Eichmann A, Le Douarin NM (1996) Endothelin-B receptor is expressed by neural crest cells in the avian embryo. Proc Natl Acad Sci USA 93: 9645-9650.

Nelson N (1998) The family of Na+/Cl- neurotransmitter transporters. J Neurochem 71: 1785-1803.

Nilsson H, Ely D, Friberg P, Folkow B (1984) Effects of low and high Na diets on

cardiovascular dynamics in normotensive and hypertensive rats: neuroeffector characteristics of the resistance vessels. J Hypertens Suppl 2: S433-S435.

Nilsson H, Ely D, Friberg P, Karlstrom G, Folkow B (1985) Effects of high and low sodium diets on the resistance vessels and their adrenergic vasoconstrictor fibre control in normotensive (WKY) and hypertensive (SHR) rats. Acta Physiol Scand 125: 323-334.

Nishimura M, Sato K, Shimada S, Tohyama M (1999) Expression of norepinephrine and serotonin transporter mRNAs in the rat superior cervical ganglion. Brain Res Mol Brain Res 67: 82-86.

Noh KM, Koh JY (2000) Induction and activation by zinc of NADPH oxidase in cultured cortical neurons and astrocytes. J Neurosci 20: RC111.

Oparil S, Zaman MA, Calhoun DA (2003) Pathogenesis of hypertension. Ann Intern Med 139: 761-776.

Osborn JW (1997) Hormones as long-term error signals for the sympathetic nervous system: importance of a new perspective. Clin Exp Pharmacol Physiol 24: 109-115.

Oyama Y, Okazaki E, Chikahisa L, Nagano T, Sadakata C (1996) Oxidative stress-induced increase in intracellular Ca2+ and Ca(2+)-induced increase in oxidative stress: an experimental model using dissociated rat brain neurons. Jpn J Pharmacol 72: 381-385.

Pacholczyk T, Blakely RD, Amara SG (1991) Expression cloning of a cocaine- and antidepressant-sensitive human noradrenaline transporter. Nature 350: 350-354.

Paclet MH, Coleman AW, Vergnaud S, Morel F (2000) P67-phox-mediated NADPH oxidase assembly: imaging of cytochrome b558 liposomes by atomic force microscopy. Biochemistry 39: 9302-9310.

Paczkowski FA, Bonisch H, Bryan-Lluka LJ (2002) Pharmacological properties of the naturally occurring Ala(457)Pro variant of the human norepinephrine transporter. Pharmacogenetics 12: 165-173.

Paczkowski FA, Bryan-Lluka LJ, Porzgen P, Bruss M, Bonisch H (1999) Comparison of the pharmacological properties of cloned rat, human, and bovine norepinephrine transporters. J Pharmacol Exp Ther 290: 761-767.

Pagani M, Lucini D (2001) Autonomic dysregulation in essential hypertension: insight from heart rate and arterial pressure variability. Auton Neurosci 90: 76-82.

Pagano PJ, Chanock SJ, Siwik DA, Colucci WS, Clark JK (1998) Angiotensin II induces p67phox mRNA expression and NADPH oxidase superoxide generation

in rabbit aortic adventitial fibroblasts. Hypertension 32: 331-337.

Pagano PJ, Clark JK, Cifuentes-Pagano ME, Clark SM, Callis GM, Quinn MT (1997) Localization of a constitutively active, phagocyte-like NADPH oxidase in rabbit aortic adventitia: enhancement by angiotensin II. Proc Natl Acad Sci U S A 94: 14483-14488.

Pang CC (2001) Autonomic control of the venous system in health and disease: effects of drugs. Pharmacol Ther 90: 179-230.

Park DS, Morris EJ, Stefanis L, Troy CM, Shelanski ML, Geller HM, Greene LA (1998) Multiple pathways of neuronal death induced by DNA-damaging agents, NGF deprivation, and oxidative stress. J Neurosci 18: 830-840.

Patterson C, Ruef J, Madamanchi NR, Barry-Lane P, Hu Z, Horaist C, Ballinger CA, Brasier AR, Bode C, Runge MS (1999) Stimulation of a vascular smooth muscle cell NAD(P)H oxidase by thrombin. Evidence that p47(phox) may participate in forming this oxidase in vitro and in vivo. J Biol Chem 274: 19814-19822.

Perry PA, Webb RC (1988) Sensitivity and adrenoceptor affinity in the mesenteric artery of the deoxycorticosterone acetate hypertensive rat. Can J Physiol Pharmacol 66: 1095-1099.

Peter D, Jimenez J, Liu Y, Merickel A, Krantz D, Edwards RH (1996) Drug interactions with vesicular amine transport. NIDA Res Monogr 161: 176-200.

Pong K (2003) Oxidative stress in neurodegenerative diseases: therapeutic implications for superoxide dismutase mimetics. Expert Opin Biol Ther 3: 127-139.

Preuss HG (1997) Diet, genetics and hypertension. J Am Coll Nutr 16: 296-305.

Raasch W, Betge S, Dendorfer A, Bartels T, Dominiak P (2001) Angiotensin converting enzyme inhibition improves cardiac neuronal uptake of noradrenaline in spontaneously hypertensive rats. J Hypertens 19: 1827-1833.

Raddassi K, Murray JJ (2000) Ethanol increases superoxide anion production stimulated with 4beta-phorbol 12-myristate 13-acetate in human polymorphonuclear leukocytes. Involvement of protein kinase C. Eur J Biochem 267: 720-727.

Rapp JP (1982) Dahl salt-susceptible and salt-resistant rats. A review. Hypertension 4: 753-763.

Reid JL, Zivin JA, Kopin IJ (1975) Central and peripheral adrenergic mechanisms in the development of deoxycorticosterone-saline hypertension in rats. Circ Res 37: 569-579.

Reis DJ, Granata AR, Perrone MH, Talman WT (1981) Evidence that glutamic acid is the neurotransmitter of baroreceptor afferent terminating in the nucleus tractus solitarius (NTS). J Auton Nerv Syst 3: 321-334.

Reja V, Goodchild AK, Pilowsky PM (2002) Catecholamine-related gene expression correlates with blood pressures in SHR. Hypertension 40: 342-347.

Rubanyi GM, Polokoff MA (1994) Endothelins: molecular biology, biochemistry, pharmacology, physiology, and pathophysiology. Pharmacol Rev 46: 325-415.

Sachs C (1970) Noradrenaline uptake mechanisms in the mouse atrium. A biochemical and histochemical study. Acta Physiol Scand Suppl 341: 1-66.

Saito Y, Nakao K, Mukoyama M, Imura H (1990) Increased plasma endothelin level in patients with essential hypertension. N Engl J Med 322: 205.

Sakamoto A, Yanagisawa M, Sakurai T, Takuwa Y, Yanagisawa H, Masaki T (1991) Cloning and functional expression of human cDNA for the ETB endothelin receptor. Biochem Biophys Res Commun 178: 656-663.

Salmon M, Koto H, Lynch OT, Haddad EB, Lamb NJ, Quinlan GJ, Barnes PJ, Chung KF (1998) Proliferation of airway epithelium after ozone exposure: effect of apocynin and dexamethasone. Am J Respir Crit Care Med 157: 970-977.

Sampath D, Jackson GR, Werrbach-Perez K, Perez-Polo JR (1994) Effects of nerve growth factor on glutathione peroxidase and catalase in PC12 cells. J Neurochem 62: 2476-2479.

Savchenko V, Sung U, Blakely RD (2003) Cell surface trafficking of the antidepressant-sensitive norepinephrine transporter revealed with an ectodomain antibody. Mol Cell Neurosci 24: 1131-1150.

Scheibner J, Trendelenburg AU, Hein L, Starke K (2001) Stimulation frequency-noradrenaline release relationships examined in alpha2A-, alpha2B- and alpha2C-adrenoceptor-deficient mice. Naunyn Schmiedebergs Arch Pharmacol 364: 321-328.

Schenk J, McNeill JH (1992) The pathogenesis of DOCA-salt hypertension. J Pharmacol Toxicol Methods 27: 161-170.

Schiffrin EL (1999) State-of-the-Art lecture. Role of endothelin-1 in hypertension. Hypertension 34: 876-881.

Schiffrin EL (2001) Role of endothelin-1 in hypertension and vascular disease. Am J Hypertens 14: 83S-89S.

Schiffrin EL, Deng LY, Sventek P, Day R (1997) Enhanced expression of endothelin-1 gene in resistance arteries in severe human essential hypertension.

J Hypertens 15: 57-63.

Schlaich MP, Lambert E, Kaye DM, Krozowski Z, Campbell DJ, Lambert G, Hastings J, Aggarwal A, Esler MD (2004) Sympathetic augmentation in hypertension: role of nerve firing, norepinephrine reuptake, and Angiotensin neuromodulation. Hypertension 43: 169-175.

Schroeter S, Apparsundaram S, Wiley RG, Miner LH, Sesack SR, Blakely RD (2000) Immunolocalization of the cocaine- and antidepressant-sensitive l-norepinephrine transporter. J Comp Neurol 420: 211-232.

Schwartz DD (1997) Activation of alpha-2 adrenergic receptors inhibits norepinephrine release by a pertussis toxin-insensitive pathway independent of changes in cytosolic calcium in cultured rat sympathetic neurons. J Pharmacol Exp Ther 282: 248-255.

Schwartz JW, Blakely RD, DeFelice LJ (2002) Binding and transport in norepinephrine transporters: Real-time, spatially resolved analysis in single cells using a fluorescent substrate. J Biol Chem 278: 9768-9777.

Scott AJ, Woods JP (2000) Monitoring internalization of Histoplasma capsulatum by mammalian cell lines using a fluorometric microplate assay. Med Mycol 38: 15-22.

Sedeek MH, Llinas MT, Drummond H, Fortepiani L, Abram SR, Alexander BT, Reckelhoff JF, Granger JP (2003) Role of reactive oxygen species in endothelin-induced hypertension. Hypertension 42: 806-810.

Selye H, Hall CE, Rowley EM (1943) Malignant hypertension produced by treatment with deoxycorticosterone acetate and sodium chloride. Can Med Assoc J 49: 88-92.

Seshiah PN, Weber DS, Rocic P, Valppu L, Taniyama Y, Griendling KK (2002) Angiotensin II stimulation of NAD(P)H oxidase activity: upstream mediators. Circ Res 91: 406-413.

Shannon JR, Flattem NL, Jordan J, Jacob G, Black BK, Biaggioni I, Blakely RD, Robertson D (2000) Orthostatic intolerance and tachycardia associated with norepinephrine- transporter deficiency. N Engl J Med 342: 541-549.

Shawver LK, Olson SA, White MK, Weber MJ (1987) Degradation and biosynthesis of the glucose transporter protein in chicken embryo fibroblasts transformed by the src oncogene. Mol Cell Biol 7: 2112-2118.

Shi AG, Ahmad S, Kwan CY, Daniel EE (1990) Alpha-adrenoceptors in dog mesenteric vessels--subcellular distribution and number of [3H]prazosin and [3H]rauwolscine binding sites. J Cardiovasc Pharmacol 15: 515-526.

Shimamoto H, Bourreau JP, Kwan CY, Daniel EE (1992) Amplification of alpha adrenergic vasoconstriction in canine isolated mesenteric artery and vein. J Pharmacol Exp Ther 260: 1119-1127.

Shokoji T, Nishiyama A, Fujisawa Y, Hitomi H, Kiyomoto H, Takahashi N, Kimura S, Kohno M, Abe Y (2003) Renal sympathetic nerve responses to tempol in spontaneously hypertensive rats. Hypertension 41: 266-273.

Sjoblom-Widfeldt N, Nilsson H, Gustafsson H, Ely DL, Folkow B (1989) Effects of pre-junctional alpha-receptor blockade on vascular neuro-effector characteristics in rats on high sodium intake. Acta Physiol Scand 137: 437-441.

Smith AB, Cunnane TC (1998) Omega-conotoxin GVIA-resistant neurotransmitter release from postganglionic sympathetic nerves in the guinea-pig vas deferens and its modulation by presynaptic receptors. Br J Pharmacol 123: 167-172.

Smith NC, Levi R (1999) LLC-PK(1) cells stably expressing the human norepinephrine transporter: A functional model of carrier-mediated norepinephrine release in protracted myocardial ischemia. J Pharmacol Exp Ther 291: 456-463.

Somers MJ, Mavromatis K, Galis ZS, Harrison DG (2000a) Vascular superoxide production and vasomotor function in hypertension induced by deoxycorticosterone acetate-salt. Circulation 101: 1722-1728.

Somers MJ, Mavromatis K, Galis ZS, Harrison DG (2000b) Vascular superoxide production and vasomotor function in hypertension induced by deoxycorticosterone acetate-salt. Circulation 101: 1722-1728.

Somova LI, Channa ML, Khan MS (1999) An experimental rat model of salt-sensitive hypertension; biochemical and morphological parameters and sympathetic nervous system. J S Afr Vet Assoc 70: 14-17.

Sorescu D, Somers MJ, Lassegue B, Grant S, Harrison DG, Griendling KK (2001) Electron spin resonance characterization of the NAD(P)H oxidase in vascular smooth muscle cells. Free Radic Biol Med 30: 603-612.

Spiekermann S, Landmesser U, Dikalov S, Bredt M, Gamez G, Tatge H, Reepschlager N, Hornig B, Drexler H, Harrison DG (2003) Electron spin resonance characterization of vascular xanthine and NAD(P)H oxidase activity in patients with coronary artery disease: relation to endothelium-dependent vasodilation. Circulation 107: 1383-1389.

Starke K (2001) Presynaptic autoreceptors in the third decade: focus on alpha2-adrenoceptors. J Neurochem 78: 685-693.

Sullivan AM, Morton AJ (1996) Endothelins induce Fos expression in neurons

and glia in organotypic cultures of rat cerebellum. J Neurochem 67: 1409-1418.

Sullivan JM (1991) Salt sensitivity. Definition, conception, methodology, and long-term issues. Hypertension 17: I61-I68.

Sullivan JM, Ratts TE (1988) Sodium sensitivity in human subjects. Hemodynamic and hormonal correlates. Hypertension 11: 717-723.

Sumners C, Muther TF, Raizada MK (1985) Altered norepinephrine uptake in neuronal cultures from spontaneously hypertensive rat brain. Am J Physiol 248: C488-C497.

Suzuki N, Miyauchi T, Tomobe Y, Matsumoto H, Goto K, Masaki T, Fujino M (1990) Plasma concentrations of endothelin-1 in spontaneously hypertensive rats and DOCA-salt hypertensive rats. Biochem Biophys Res Commun 167: 941-947.

Sved AF (2000) Cardiovascular system. In: Fundamental Neuroscience (Zigmond MJ, Bloom FE, Landis SC, Roberts JL, Squire LR, eds), pp 1051-1062. Academic Press.

Sved AF, Schreihofer AM, Kost CK, Jr. (1997) Blood pressure regulation in baroreceptor-denervated rats. Clin Exp Pharmacol Physiol 24: 77-82.

Swain SD, Helgerson SL, Davis AR, Nelson LK, Quinn MT (1997) Analysis of activation-induced conformational changes in p47phox using tryptophan fluorescence spectroscopy. J Biol Chem 272: 29502-29510.

Szabo B, Hedler L, Schurr C, Starke K (1990) Peripheral presynaptic facilitatory effect of angiotensin II on noradrenaline release in anesthetized rabbits. J Cardiovasc Pharmacol 15: 968-975.

Szilagyi JE, Masaki Z, Brosnihan KB, Ferrario CM (1981) Neurogenic suppression of carotid sinus reflexes by vagal afferents in sodium-depleted dogs. Am J Physiol 241: H255-H262.

Tabuchi Y, Nakamaru M, Rakugi H, Nagano M, Higashimori K, Mikami H, Ogihara T (1990) Effects of endothelin on neuroeffector junction in mesenteric arteries of hypertensive rats. Hypertension 15: 739-743.

Takata Y, Kato H (1996) Adrenoceptors in SHR: alterations in binding characteristics and intracellular signal transduction pathways. Life Sci 58: 91-106.

Takeda K, Bunag RD (1980) Augmented sympathetic nerve activity and pressor responsiveness in DOCA hypertensive rats. Hypertension 2: 97-101.

Takeda K, Nakamura Y, Hayashi J, Kawasaki S, Nakata T, Oguro M, Sasaki S, Nakagawa M (1988a) Effects of salt and DOCA on hypothalamic and baroreflex

control of blood pressure. Clin Exp Hypertens A 10 Suppl 1: 289-299.

Takeda K, Nakamura Y, Okajima H, Hayashi J, Kawasaki S, Lee LC, Sasaki S, Nakagawa M (1988b) Attenuated cardiovascular and sympathetic nerve responses to aortic nerve stimulation in DOCA-salt hypertensive rats. J Hypertens 6: 559-563.

Takekoshi K, Ishii K, Shibuya S, Kawakami Y, Isobe K, Nakai T (2002) Stimulation of catecholamine biosynthesis via the protein kinase C pathway by endothelin-1 in PC12 rat pheochromocytoma cells. Biochem Pharmacol 63: 977-984.

Takeshita A, Ashihara T, Yamamoto K, Imaizumi T, Hoka S, Ito N, Nakamura M (1984) Venous responses to salt loading in hypertensive subjects. Circulation 69: 50-56.

Takimoto GS, Weiner N (1981) Effects of nitroprusside-induced hypotension on sympathetic nerve activity, tyrosine hydroxylase activity and [3H]norepinephrine uptake in rabbit vascular tissues. J Pharmacol Exp Ther 219: 420-427.

Tammariello SP, Quinn MT, Estus S (2000) NADPH oxidase contributes directly to oxidative stress and apoptosis in nerve growth factor-deprived sympathetic neurons. J Neurosci 20: RC53.

Taniyama Y, Griendling KK (2003) Reactive oxygen species in the vasculature: molecular and cellular mechanisms. Hypertension 42: 1075-1081.

Thurston H (1994) Experimental model of hypertenison. In: Textbook of hypertension (Swales JD, ed), pp 477-493. Oxford: Blackwell Science Publication.

Tobian L (1991) Salt and hypertension. Lessons from animal models that relate to human hypertension. Hypertension 17: I52-I58.

Touyz RM, Tabet F, Schiffrin EL (2003) Redox-dependent signalling by angiotensin II and vascular remodelling in hypertension. Clin Exp Pharmacol Physiol 30: 860-866.

Turi S, Friedman A, Bereczki C, Papp F, Kovacs J, Karg E, Nemeth I (2003) Oxidative stress in juvenile essential hypertension. J Hypertens 21: 145-152.

Ueno Y, Mohara O, Brosnihan KB, Ferrario CM (1988a) Characteristics of hormonal and neurogenic mechanisms of deoxycorticosterone-induced hypertension. Hypertension 11: I172-I177.

Ueno Y, Mohara O, Brosnihan KB, Ferrario CM (1988b) Characteristics of hormonal and neurogenic mechanisms of deoxycorticosterone-induced hypertension. Hypertension 11: I172-I177.

Ushio-Fukai M, Zafari AM, Fukui T, Ishizaka N, Griendling KK (1996) p22phox is a critical component of the superoxide-generating NADH/NADPH oxidase system and regulates angiotensin II-induced hypertrophy in vascular smooth muscle cells. J Biol Chem 271: 23317-23321.

Vallbo AB, Hagbarth KE (1968) Activity from skin mechanoreceptors recorded percutaneously in awake human subjects. Exp Neurol 21: 270-289.

Van Amersfoort ES, Van Strijp JA (1994) Evaluation of a flow cytometric fluorescence quenching assay of phagocytosis of sensitized sheep erythrocytes by polymorphonuclear leukocytes. Cytometry 17: 294-301.

VanNess JM, Hinojosa-Laborde C, Craig T, Haywood JR (1999) Effect of sinoaortic deafferentation on renal wrap hypertension. Hypertension 33: 476-481.

Wakayama K, Ohtsuki S, Takanaga H, Hosoya K, Terasaki T (2002) Localization of norepinephrine and serotonin transporter in mouse brain capillary endothelial cells. Neurosci Res 44: 173-180.

Wang DH, Wu W, Lookingland KJ (2001) Degeneration of capsaicin-sensitive sensory nerves leads to increased salt sensitivity through enhancement of sympathoexcitatory response. Hypertension 37: 440-443.

Wang, H., Chen, A. F., Watts, S. W., Galligan, J. J., and Fink G.D. Endothelin-1 content in arteries and veins of DOCA-salt hypertensive rats. FASEB Journal 16[4], 442. 3-20-2002.

Warren JH, Lewis W, Wraa CE, Stebbins CL (2001) Central and peripheral effects of angiotensin II on the cardiovascular response to exercise. J Cardiovasc Pharmacol 38: 693-705.

Watanabe K, Hiraki H, Hasegawa H, Tanigawa T, Emura I, Honma K, Shibuya H, Fukuda T, Suzuki T (1997) Immunohistochemical localization of endothelin-1, endothelin-3 and endothelin receptors in human pheochromocytoma and paraganglioma. Pathol Int 47: 540-546.

Watts SW, Fink GD, Northcott CA, Galligan JJ (2002) Endothelin-1-induced venous contraction is maintained inDOCA-salt hypertension; studies with receptor agonists. Br J Pharmacol 137: 69-79.

Weinshenker D, White SS, Javors MA, Palmiter RD, Szot P (2002) Regulation of norepinephrine transporter abundance by catecholamines and desipramine in vivo. Brain Res 946: 239-246.

Westfall TC, Carpentier S, Naes L, Meldrum MJ (1986) Comparison of norepinephrine release in hypertensive rats: II. Caudal artery and portal vein. Clin Exp Hypertens A 8: 221-237.

Wilkes LC, Boarder MR (1991a) Characterization of the endothelin binding site on bovine adrenomedullary chromaffin cells: comparison with vascular smooth muscle cells. Evidence for receptor heterogeneity. J Pharmacol Exp Ther 256: 628-633.

Wilkes LC, Boarder MR (1991b) Characterization of the endothelin binding site on bovine adrenomedullary chromaffin cells: comparison with vascular smooth muscle cells. Evidence for receptor heterogeneity. J Pharmacol Exp Ther 256: 628-633.

Williams GH, Hollenberg NK (1989) Sodium-sensitive essential hypertension: emerging insights into an old entity. J Am Coll Nutr 8: 490-494.

Winslow SG, Henkart PA (1991) Polyinosinic acid as a carrier in the microscale purification of total RNA. Nucleic Acids Res 19: 3251-3253.

Wu R, Millette E, Wu L, de Champlain J (2001) Enhanced superoxide anion formation in vascular tissues from spontaneously hypertensive and desoxycorticosterone acetate-salt hypertensive rats. J Hypertens 19: 741-748.

Xu F, Gainetdinov RR, Wetsel WC, Jones SR, Bohn LM, Miller GW, Wang YM, Caron MG (2000) Mice lacking the norepinephrine transporter are supersensitive to psychostimulants. Nat Neurosci 3: 465-471.

Xu H, Fink GD, Galligan JJ (2002) Nitric oxide-independent effects of tempol on sympathetic nerve activity and blood pressure in DOCA-salt rats. Am J Physiol Heart Circ Physiol 283: H885-H892.

Yamamoto J, Trippodo NC, MacPhee AA, Frohlich ED (1981) Decreased total venous capacity in Goldblatt hypertensive rats. Am J Physiol 240: H487-H492.

Yanagisawa M, Inoue A, Ishikawa T, Kasuya Y, Kimura S, Kumagaye S, Nakajima K, Watanabe TX, Sakakibara S, Goto K, . (1988a) Primary structure, synthesis, and biological activity of rat endothelin, an endothelium-derived vasoconstrictor peptide. Proc Natl Acad Sci U S A 85: 6964-6967.

Yanagisawa M, Inoue A, Takuwa Y, Mitsui Y, Kobayashi M, Masaki T (1989) The human preproendothelin-1 gene: possible regulation by endothelial phosphoinositide turnover signaling. J Cardiovasc Pharmacol 13 Suppl 5: S13-S17.

Yanagisawa M, Kurihara H, Kimura S, Tomobe Y, Kobayashi M, Mitsui Y, Yazaki Y, Goto K, Masaki T (1988c) A novel potent vasoconstrictor peptide produced by vascular endothelial cells. Nature 332: 411-415.

Yanagisawa M, Kurihara H, Kimura S, Tomobe Y, Kobayashi M, Mitsui Y, Yazaki Y, Goto K, Masaki T (1988b) A novel potent vasoconstrictor peptide produced by vascular endothelial cells. Nature 332: 411-415.

Yang ZZ, Zou AP (2003) Homocysteine enhances TIMP-1 expression and cell proliferation associated with NADH oxidase in rat mesangial cells. Kidney Int 63: 1012-1020.

Yermolaieva O, Brot N, Weissbach H, Heinemann SH, Hoshi T (2000) Reactive oxygen species and nitric oxide mediate plasticity of neuronal calcium signaling. Proc Natl Acad Sci U S A 97: 448-453.

Yoshimura M, Yamashita Y, Kan S, Niwa M, Taniyama K (1996) Localization of endothelin ETB receptors on the myenteric plexus of guinea-pig ileum and the receptor-mediated release of acetylcholine. Br J Pharmacol 118: 1171-1176.

Yoshimura R, Yanagihara N, Hara K, Nakamura J, Toyohira Y, Ueno S, Izumi F (2001) Dual phases of functional change in norepinephrine transporter in cultured bovine adrenal medullary cells by long-term treatment with clozapine. J Neurochem 77: 1018-1026.

Yu WJ, Tomlinson B, Cheng JT (2002) Regulation of endothelin-1 production in deoxycorticosterone acetate- salt-treated endothelial cells. Pharmacology 64: 169-175.

Yue TL, Nambi P, Wu HL, Feuerstein G (1991) Endothelin receptor binding and cellular signal transduction in neurohybrid NG108-15 cells. Neuroscience 44: 215-222.

Zafari AM, Ushio-Fukai M, Akers M, Yin Q, Shah A, Harrison DG, Taylor WR, Griendling KK (1998) Role of NADH/NADPH oxidase-derived H2O2 in angiotensin II-induced vascular hypertrophy. Hypertension 32: 488-495.

Zahniser NR, Doolen S (2001) Chronic and acute regulation of Na+/Cl- -dependent neurotransmitter transporters: drugs, substrates, presynaptic receptors, and signaling systems. Pharmacol Ther 92: 21-55.

Zalba G, Beaumont FJ, San Jose G, Fortuno A, Fortuno MA, Etayo JC, Diez J (2000) Vascular NADH/NADPH oxidase is involved in enhanced superoxide production in spontaneously hypertensive rats. Hypertension 35: 1055-1061.

Zanzinger J, Czachurski J (2000) Chronic oxidative stress in the RVLM modulates sympathetic control of circulation in pigs. Pflugers Arch 439: 489-494.

Zheng, Z. L., Dai, X., and Kreulen, D. L. Functional norepinephrine transporter in freshly dissociated rat celiac and dorsal root ganglionic neurons. Autonomic Neuroscinece: Basic and Clinical 106[1], 24. 6-30-2003.

Zheng ZL, Shimamura K, Anthony TL, Kreulen DL (2000) Guanethidine evokes vasodilatation in guinea pig mesenteric artery by acting on sensory nerves. Neurosci Lett 288: 231-235.

Zheng ZL, Travagli RA, Kreulen DL (1999) Patterns of innervation of sympathetic vascular neurons by peptide- containing primary sensory fibers. Brain Res 827: 113-121.

Zhou QL, Strichartz G, Davar G (2001) Endothelin-1 activates ET(A) receptors to increase intracellular calcium in model sensory neurons. nr 12: 3853-3857.

Zhu MY, Blakely RD, Apparsundaram S, Ordway GA (1998) Down-regulation of the human norepinephrine transporter in intact 293- hNET cells exposed to desipramine. J Neurochem 70: 1547-1555.

Zhu MY, Kim CH, Hwang DY, Baldessarini RJ, Kim KS (2002) Effects of desipramine treatment on norepinephrine transporter gene expression in the cultured SK-N-BE(2)M17 cells and rat brain tissue. J Neurochem 82: 146-153.

Zhu MY, Ordway GA (1997) Down-regulation of norepinephrine transporters on PC12 cells by transporter inhibitors. J Neurochem 68: 134-141.

Zhu MY, Shamburger S, Li J, Ordway GA (2000) Regulation of the human norepinephrine transporter by cocaine and amphetamine. J Pharmacol Exp Ther 295: 951-959.

Zimmerman MC, Davisson RL (2004) Redox signaling in central neural regulation of cardiovascular function. Prog Biophys Mol Biol 84: 125-149.

Zimmerman MC, Lazartigues E, Lang JA, Sinnayah P, Ahmad IM, Spitz DR, Davisson RL (2002) Superoxide mediates the actions of angiotensin II in the central nervous system. Circ Res 91: 1038-1045.

Zou AP, Li N, Cowley AW, Jr. (2001) Production and actions of superoxide in the renal medulla. Hypertension 37: 547-553.